About Sustainability in Ring-Opening Metathesis Polymerisation

Zur Erlangung des akademischen Grades eines

DOKTORS DER NATURWISSENSCHAFTEN

(Dr. rer. nat.)

von der KIT-Fakultät für Chemie und Biowissenschaften
des Karlsruher Instituts für Technologie (KIT)

genehmigte

DISSERTATION

von

M. Sc. Federico Ferrari

aus

Verbania

1. Referent: Prof. Dr. Michael A. R. Meier

2. Referent: Prof. Dr. Patrick Théato

Tag der mündlichen Prüfung: 09.02.2023

Declaration of authorship

Die vorliegende Arbeit wurde von Januar 2020 bis Februar 2023 unter Anleitung von Herrn Prof. Dr. Michael A. R. Meier und Frau Dr. Dafni Moatsou am Institut für Organische Chemie (IOC) des Karlsruher Instituts für Technologie (KIT) angefertigt.

Hiermit versichere ich, dass ich die Arbeit selbstständig angefertigt, nur die angegebenen Quellen und Hilfsmittel benutzt und mich keiner unzulässigen Hilfe Dritter bedient habe. Insbesondere habe ich wörtlich oder sinngemäß aus anderen Werken übernommene Inhalte als solche kenntlich gemacht. Die Satzung des Karlsruher Instituts für Technologie (KIT) zur Sicherung wissenschaftlicher Praxis habe ich beachtet. Des Weiteren erkläre ich, dass ich mich derzeit in keinem laufenden Promotionsverfahren befinde, und auch keine vorausgegangenen Promotionsversuche unternommen habe. Die elektronische Version der Arbeit stimmt mit der schriftlichen Version überein und die Primärdaten sind gemäß Abs. A (6) der Regeln zur Sicherung guter wissenschaftlicher Praxis des KIT beim Institut abgegeben und archiviert. Zudem versichere ich, dass die eingereichte Fassung mit der vom Promotionsausschuss gemäß Abs. 2 genehmigten Fassung der Dissertation inhaltlich übereinstimmt.

Karlsruhe, 09/02/2022

. . . .

Federico Ferrari

Abstract

Degradable polymers are macromolecules that can be broken down into their constituent unit or smaller by-products or oligomers under specific conditions.[1] Degradable polymers obtainable *via* ring-opening metathesis polymerisation (ROMP) are rare. Poly(Dihydrofuran) (Poly(DHF) represents a recent example of a ROMP-obtained degradable polymer. 2,3-Dihydrofuran, the monomer leading to poly(DHF), is a cyclic enol ether. This furan derivative was previously synthesised following different synthetic routes described in the literature, such as cyclisation of alkynyl alcohol,[2] or cycloaddition.[3] In this work, possible alternative pathways for the synthesis of 2,3-dihydrofuran are investigated to improve the sustainability of the synthetic process to poly(DHF). The dilution limit of the homopolymerisation of this monomer is investigated, and a copolymer with a norbornene derivative will be synthesised to modify the thermal proprieties of poly(DHF). In addition, the synthesis of five-membered rings heterocycles is also investigated, and ring-strain calculations on thiophene derivatives are performed. Sulfur-containing polymers are, in fact, of particular interest due to their unique optical and thermal properties. In this work, sulfur-containing norbornenes are synthesised as thioethers and sulfone and polymerised by ring-opening metathesis polymerisation (ROMP). Utilising the 3rd generation Grubbs catalyst, well-controlled reactions led to polymers with low dispersities and molecular weights up to $350\,\mathrm{kg\,mol^{-1}}$.

A diblock and a statistical copolymer bearing thioether and sulfone moieties were also successfully synthesised, while the thermal properties of all polymers were also evaluated, correlating them to the structural characteristics of the corresponding monomers. Lastly, the evaluation of Levoglucosenone-derivatives as building blocks for bio-based polymers is conducted. Bio-based polymers represent a sustainable alternative to the fossil fuel-based ones. Levoglucosenone is a suitable substrate for polymerisation reactions, as, for example, pairing this substrate with cyclopentadiene allows the formation of norbornene-like structures that can undergo ring-opening metathesis polymerisation. Such reactions, however, decrease the overall sustainability of the monomer. To obtain fully bio-based levoglucosenone-derived polymers, in this work, furan was implemented as a counterpart substrate for an electrophilic substitution reaction. Three aromatic moieties were synthesised based on the cellulose derivative levoglucosenone and bio-based furan or furan derivatives, such as methyl furan and ethyl furan. The resulting products were fully characterised and exposed to a combination of a ruthenium-based catalyst and $ZnCl_2$ to investigate their polymerisation ability.

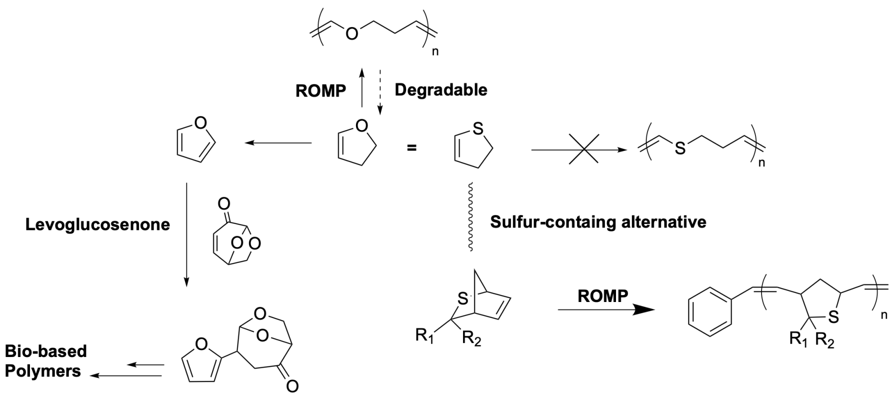

Figure 1.: Graphical abstract

Zusammenfassung

Abbaubare Polymere sind Makromoleküle, die sich unter bestimmten Bedingungen in ihre jeweiligen Einheiten, kleinere oder größere Nebenprodukte zerlegen lassen.[1] Solche abbaubaren Polymere lassen sich nur selten aus einer Ringöffnungsmetathesepoylmerisation (ROMP) erhalten. Poly(Dihydrofuran) (Poly(DHF) ist seit kurzem ein Beispiel für ein ROMP-basiertes, abbaubares Polymer. 2,3 Dihydrofuran, das benötigte Monomer, ist ein zyklischer Enolether, der in der Literatur über verschiedene Syntheserouten, wie z.B. durch Zyklisierung von Alkynylalkohol,[2] oder Cycloaddition,[3] hergestellt werden kann. In dieser Arbeit wurden mögliche alternative Routen für die Synthese von 2,3 Dihydrofuran untersucht, um letztlich die Nachhaltigkeit der Synthese von Poly(DHF) zu verbessern. Dabei wurde das Limit der Verdünnung in der Homopolymerisation erforscht und die Copolymerisation mit Norbornenderivaten erlaubte die Modifikation der thermischen Eigenschaften des Poly(DHF)s. Des Weiteren wurde in dieser Arbeit die Synthese von fünfgliedrigen Heterozyklen verfolgt, sowie Ringspannungsuntersuchungen an weiteren Heterocyclen vorgenommen. Schwefelhaltige Polymere sind aufgrund ihrer einzigartigen optischen und thermischen Eigenschaften von großem Interesse. Schwefelhaltige Norbornenderivate wurden als Thioether und Sulfone hergestellt und anschließend in einer ROMP umgesetzt. Die Verwendung des Grubbs Katalysators dritter Generation führte zu sehr kontrollierten

Reaktionen, in denen Polymere mit niedrigen Dispersitäten und Molekulargewichten von bis zu 350 kg mol^{-1} erhalten wurden. Ein Diblock und ein statistisches Copolymer mit Thioether und Sulfongruppen wurden zusätzlich erfolgreich synthetisiert. Die thermischen Eigenschaften aller Polymere wurden bestimmt und den strukturellen Charakteristika ihrer Monomereinheiten zugeordnet. In einem letzten Teil dieser Arbeit wurden Cellulose basierte Levoglucosenonderivate als Monomereinheiten für biobasierte Polymer untersucht. Biobasierte Polymere stellen eine nachhaltige Alternative zu auf fossilen Rohstoffen basierenden Polymeren dar. Levoglucosenon ist ein geeigneter Kandidat für eine Polymerisationsreaktion, z. B. kann durch die Reaktion mit Cyclopentadien ein Norbornensubstrat erhalten werden, dass in einer ROMP umgesetzt werden kann. Diese Modifikationen verringern allerdings die Nachhaltigkeit der Monomere. Daher wurde die Umsetzung von Levoglucosenon mit Furan in einer elektrophilen aromatischen Sustitution untersucht. Drei aromatische Reste wurden so hergestellt durch die Verwendung von biobasiertem Furan und seinen Derivaten (Methyl und Ethylfuran), sowie Levoglucosenon. Die erhaltenen Produkte wurde vollständig charakterisiert und ihre Polymerisationsfähigkeiten in Kombination eines Ruthenium basierendem Katalysators, sowie $ZnCl_2$ getestet.

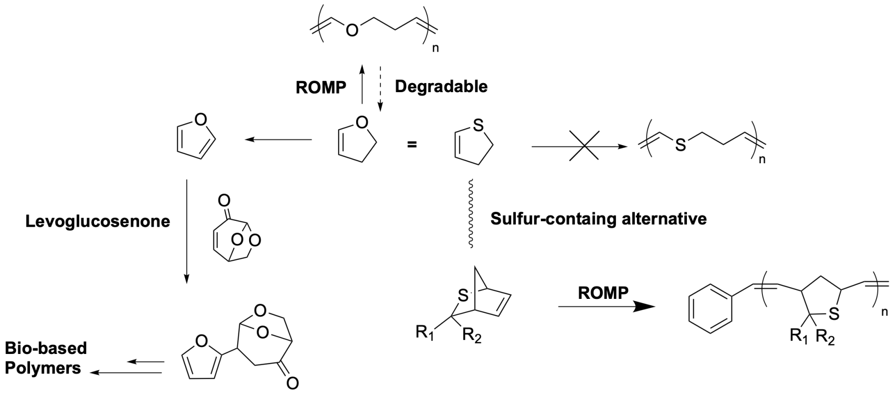

Abbildung 2.: Grafische Zusammenfassung

Acknowledgments

I want to thank my mother, Nadia, for her support during this time and everything she did to help me.

I also want to thank my grandparents, Olga and Ennio, for everything that they did for me over the years.

I thanks also my brother Fabrizio for all the help and support. Also, I want to thank Debora, Carlo, Saverio, Vito, Enrica, Edit and Greta.

Thank you, Rafael, for always being there for me and for your support, help, and kindness.

Thank you, Oscar, for everything we shared in almost ten years of friendship. I could not ask for a better best friend.

Thank you, Roberta, for all the laughs we shared, from endless days studying organic chemistry to all the evenings we shared watching "C'è Posta per Te".

Thank you Dennis, for all the time we shared in the lab and for being a great friend during my time at KIT.

Thank you, Dafni, for everything you have taught me during these years, for all the patience and all the help.

Thank you Mike, for believing in me and allowing me to join your group as a PhD candidate, for all the help, and for always being there for your group.

Thank you, Claudia, for all your help during this years.

Last but not least, I want to thank all the fantastic people I met during this experience. Thank you, AK Meier, especially Roman, Maxi, Pete, Luis, Andreas, Anja, Clara, Jonas, Celeste, Cecilia, Michi and Benny, for all the time we shared during my PhD years.

Contents

Abstract iii

Zusammenfassung v

Acknowledgments vii

1. Introduction and theoretical background 1

- 1.1. Introduction and aim of the thesis 1
- 1.2. Polymerisation techniques 3
  - 1.2.1. Radical polymerisation 4
  - 1.2.2. Molecular weight distribution 5
  - 1.2.3. Mechanism 6
  - 1.2.4. Living polymerisations 9
  - 1.2.5. ATRP 10
- 1.3. Green chemistry 11
  - 1.3.1. Principles of Green Chemistry 11
  - 1.3.2. Green Metrics 12
- 1.4. Synthetic tools 15
  - 1.4.1. The Diels-Alder reaction 15

1.4.2. Dienes and dienophile requirements in Diels-Alder reaction . . 17
1.4.3. Catalysis of the cycloaddition 18
1.4.4. Stereochemistry 19
1.5. Olefin Metathesis 21
1.5.1. Cross Metathesis 23
1.5.2. Ring-closing Metathesis 24
1.5.3. Ring opening Metathesis 25
1.6. Ring-opening metathesis polymerisation (ROMP) 25
1.6.1. Catalysis in ROMP 28
1.7. Electrophilic substitution 31

2. The use of dihydrofuran and its analogues in ring-opening metathesis polymerisation 33

2.1. Introduction 33
2.2. Synthesis pathways to poly(dihydrofuran) 35
2.2.1. Syntethic routes towards 2,5-Dihydrofuran 37
2.2.2. Environmental factors of the two synthetic pathways to obtain 2,5-DHF 39
2.2.3. Isomerisation from 2,5-DHF to 2,3-DHF 40
2.2.4. Investigation of one pot isomerisation and polymerisation of 2,5-DHF 42
2.2.5. E-Factors calculation for the synthesis process of poly(DHF) . . 45
2.3. Synthesis of copolymers containing 2,3-dihydrofuran 47
2.3.1. Copolymerisation of 2,3-DHF with **N-HexNb** 49
2.4. Investigation of DHF analogues for ROMP 53

2.5. Conclusion 56

3. Ring-Opening Metathesis Polymerisation of Thio-Norbornenes and their Sulfone-Derivatives 59

3.1. Introduction 59

3.2. The synthesis of Thionorbornenes 61

3.2.1. Polymerisation of thionorbornenes 64

3.2.2. Preparation of sulfone-based polymers 68

3.2.3. Copolymers of TNbs and sulfone-functional norbornenes . . . 69

3.2.4. Thermal properties of the polymers and their solubility 71

3.3. Conclusion 73

4. Zinc and Ruthenium Mediated Polymerisation of Levoglucosenone Derivatives 75

4.1. Introduction 75

4.2. Monomer synthesis 77

4.3. Using of furan derivatives in the electrophilic substitution reaction . . 80

4.4. Investigation of the LGO-based monomers 81

4.5. Thermal properties of polymeric materials p(**5**), p(**6**) and p(**7**) 89

4.6. Conclusions 91

5. Materials, methods, calculations and supporting images 93

5.1. Materials 93

5.2. Calculations 98

5.2.1. Computational calculations 98

5.2.2. E-factors calculations 98

5.3. Methods and supporting figures 103

5.4. Pathways to poly(dihydrofuran) 103
  5.4.1. Ring-Closing metathesis of diallyl ether 103
  5.4.2. One pot isomerisation and ROMP of 2,5-DHF 104
  5.4.3. Homopolymerisation test of 2,5-DHF 105
  5.4.4. Dilution test 106
  5.4.5. Synthesis of statistical copolymer poly(**N-HexNb**-*co*-**DHF**) . . 107
  5.4.6. Ring closing metathesis of dienes 108
5.5. Ring-Opening Metathesis Polymerisation of Thio-Norbornenes and their Sulfone-Derivatives 109
  5.5.1. Synthesis of thioketones 109
  5.5.2. Synthesis of thionorbornenes 119
  5.5.3. Synthesis of **4a** 126
  5.5.4. Polymerisations of thionorbornenes 130
  5.5.5. Thermal properties of Thionorbornenes derivated polymers. . . 140
  5.5.6. Solubility of Thionorbornenes derivated polymers 140
  5.5.7. Spectra of Poly(Norbornene) synthesised 141
5.6. Synthesis of Levoglucosenone derivatives 142
  5.6.1. Synthesis of 2-(2-Furyl)-6,8-dioxabicyclo[3.2.1]octan-4-one (**5**) . 142
  5.6.2. Synthesis of 2-(5-Methyl-2-furyl)-6,8-dioxabicyclo[3.2.1]octan-4-one (**6**) 145
  5.6.3. Synthesis of 2-(5-Ethyl-2-furyl)-6,8-dioxabicyclo[3.2.1]octan-4-one (**7**) 148
  5.6.4. Synthesis of p(**5**), p(**6**) and p(**7**) 151
  5.6.5. IR spectroscopy investigation of poly(EVE) 156
  5.6.6. Test homopolymerisation of **5** without quenching 156

5.6.7. Test homopolymerisation of EVE 158

6. Conclusion and outlook **159**

Bibliography **163**

A. Appendix **185**

A.1. Abbreviation used 185

A.2. List of pubblications 186

List of Figures

1. Graphical abstract iv

2. Grafische Zusammenfassung vi

1.1. Important steps of the mechanism of radical polymerisation. 7

1.2. Conversion vs. MW in chain growth and living polymerisation 8

1.3. Activation and Deactivation equilibrium in ATRP. 11

1.4. Reaction scheme of the Diels-Alder reaction between Furan and maleic anhydride 15

1.5. Concerted mechanism of Diels-Alder cycloaddition 16

1.6. a) Generic molecular orbital diagram for a direct electron demanding DA; b) Molecular orbital diagram of inverse electron demanding DA in the dimerisation of acrolein. 17

1.7. Example of various dienes for Diels-Alder reaction, nominally: Cyclopentadiene, Furan, *s*-cis-butadiene, 1,3-cyclohexadiene 18

1.8. Suprafacial and antarafacial interaction possibilities possibilities. 20

1.9. Schematic *exo* and *endo* energy diagram for the reaction between cyclopentadiene and maleic anhydride. 21

1.10. General representation of different organic metathesis reactions. 23

1.11. Reaction mechanism of olefin cross-metathesis (Chauvin mechanism). . 24
1.12. General mechanism of ring-opening metathesis polymerisation with chain transfer phenomena. 26
1.13. Principal Grubbs catalysts classes. 30
1.14. General mechanism of electrophilic aromatic substitution with a general electrophile (E). 31
1.15. Compared reactivity of different heterocycles and benzene. 32

2.1. Two possible synthetic routes to obtain 2,3-DHF and its subsequent polymerisation. 36
2.2. Synthetic pathway from diallyl ether to poly(DHF). 37
2.3. ^{1}H NMR spectra of poly(DHF) obtained *via* ROMP of 2,3-DHF (upper spectrum) and poly(DHF) obtained *via* one-pot isomerisation-ROMP of 2,5-DHF (bottom spectrum). 43
2.4. Kinetic results from the isomerisation of 2,5-DHF into 2,3-DHF, recorded at 65 °C, in bulk and with GII (0.02 eq) as catalyst, determined *via* ^{1}H NMR. 44
2.5. Reaction scheme of synthesis of 2,3-DHF *via* alkynol cycloisomerisation.[2] 45
2.6. SEC from the polymerisation of 2,3-DHF using different dilution rates in DCM, all the reactions were carried out at 25 °C with 0.01 eq of GII catalyst. 48
2.7. Reaction scheme of the copolymerisation of DHF with a norbornene derivative. 49
2.8. SEC chromatogram of the obtained copolymer poly(**N-HexNb**-*co*-**DHF**.). 50

2.9. ^{1}H NMR spectrum of poly(**N-HexNb**-*co*-**DHF**). 51

2.10. DSC curves of the copolymer synthesised and the analogue homopolymer of the composing monomers. 52

2.11. Synthesis route to obtain heteroatom five member rings as ROMP monomers. 54

3.1. SEC from the polymerisation of **3a** using different ruthenium-based catalysts. 64

3.2. SEC traces of the polymers obtained from the ROMP of **3a**, **3b**, **3c**, and **3d** using G3 as catalyst. and their molecular weight characteristics. . . 66

3.3. Comparison of the two routes followed to obtain the polysulfone polymers p(**4a**)i and p(**4a**)ii and their corresponding SEC. 69

3.4. SEC traces of p(**3a**-*co*-**4a** (left), and p(**3a**) and p(**3a**)-*b*-p(**4a**) (right). . . . 70

3.5. DSC curves of the polymers synthesised in this study. 71

4.1. Reaction scheme of the catalytic electrophilic substitution between LGO and furan derivatives. 77

4.2. Comparison ^{1}H NMR spectra of p(**5**) (upper spectrum) and residue of ethyl vinylether exposed to the same polymerisation conditions (bottom spectrum). 83

4.3. SEC chromatogram of test homopolymerisation of EVE 84

4.4. IR spectra of p(**5**), Levoglucosenone and the EVE test polymerisation. . 85

4.5. SEC traces of: a) p(**5**) obtained with various equivalents of $ZnCl_2$ (0.005; 0.01; 0.1; 0.5; 1.5 eq) at 25 °C, with reaction time of 24 hours and DCM as reaction solvent b) p(**5**) obtained with different equivalents of GII (0.02, 0.01, 0.002, 0.001 eq) 25 °C, concentration of the monomer equal to 5 mg/mL and DCM as reaction solvent. 86

4.6. SEC traces of polymeric materials p(**5**); p(**6**); p(**7**) obtained using the conditions reported in Table 4.8. 88

4.7. TGA traces of polymeric materials p(**5**), p(**6**) and p(**7**) under N_2 with a heating rate of 10 K/min up to 1000 °C 89

4.8. DSC traces of homopolymers p(**5**), p(**6**) and p(**7**) 90

5.1. ^{1}H NMR spectrum of 2,5-Dihydrofuran. 103

5.2. ^{1}H NMR spectrum of unsuccessful polymerisation test of 2,5-Dihydrofuran. Obtained following literature reported method for ROMP of 2,3-DHF.[11] 105

5.3. SEC chromatogram of unsuccessful polymerisation test of 2,5-Dihydrofuran. Obtained following literature reported method for ROMP of 2,3-DHF.[11] 106

5.4. ^{1}H NMR spectrum of 2,5-Dihydrothiophene. 109

5.5. ^{1}H NMR spectrum of **2a**. 111

5.6. ^{13}C NMR spectrum of **2a**. 111

5.7. ESI-MS of **2a**. 112

5.8. ^{1}H NMR spectrum of **2b**. 113

5.9. ^{13}C NMR spectrum of **2b**. 113

5.10. ESI-MS of **2b**. 114

5.11. ^{1}H NMR spectrum of **2c**. 115

5.12. ^{13}C NMR spectrum of **2c**. It is noted that the axis break indicates that the two spectral regions were collected from different measurements to improve the intensity of the C=S peak at 271 ppm. 115
5.13. ESI-MS of **2c**. 116
5.14. IR spectrum of **2d**. 116
5.15. ^{1}H NMR spectra of **2d** compared at room temperature (bottom spectra) and 100 °C (upper spectra). 117
5.16. ESI-MS of **2d**. 118
5.17. ^{1}H NMR spectrum of **3a**. 120
5.18. ^{13}C NMR spectrum of **3a**. 121
5.19. ESI-MS of **3a**. 121
5.20. ^{1}H NMR spectrum of **3c**. 122
5.21. ^{13}C NMR spectrum of **3c**. 122
5.22. ESI-MS of **3c**. 123
5.23. ^{1}H NMR spectrum of **3d** as a mixture of *endo* and *exo* isomers. 124
5.24. ^{13}C NMR spectrum of **3d**. 124
5.25. ESI-MS of **3d**. 125
5.26. ^{1}H NMR spectra of **3b** before and after removal of the solvent under reduced pressure. 126
5.27. ^{1}H NMR spectrum of **4a**. 127
5.28. ^{13}C NMR spectrum of **4a**. 128
5.29. ESI-MS of **4a**. 128
5.30. IR spectra of **4a** and **3a**. 129
5.31. SEC curves and results from the polymerisation of **3a** catalysed by G3, targeting different DPs by variation of the catalyst concentration. . . . 131

5.32. ^{1}H NMR spectrum of p(**3a**). 132

5.33. ^{1}H NMR spectrum of p(**3c**). 132

5.34. ^{1}H NMR spectrum of p(**3d**). 133

5.35. ^{1}H NMR spectrum of p(**4a**)i. 133

5.36. ^{1}H NMR spectrum of p(**4a**)ii (prior to purification). 134

5.37. IR spectra of p(**3a**), p(**4a**i) and p(**4a**ii). 134

5.38. SEC of p(**3b**) on a system equipped with columns for low molecular weight polymers. 136

5.39. ^{1}H NMR spectrum of p(**3b**). 136

5.40. ^{1}H NMR spectrum of copolymer p(**3a**-*b*-**4a**). 138

5.41. SEC traces of the p(**3a**) homopolymer and the incomplete chain extension with **4a** to obtain p(**3a**-*b*-**4a**) at room temperature. 138

5.42. ^{1}H NMR spectrum of copolymer p(**3a**-*co*-**4a)** 139

5.43. TGA of polymers synthesised in this study. The 5% weight loss line is shown for clarity. 140

5.44. ^{1}H NMR spectra of poly(norbornene) obtained *via* ROMP in the absence (upper spectrum) and the presence (lower spectrum) of 10% mol benzophenone as additive. 141

5.45. SEC traces of the polymers obtained from the ROMP of norbornene in the absence (blue curve) and the presence (red curve) of 10 mol% of benzophenone. 141

5.46. ^{1}H NMR spectrum of **5**. 143

5.47. ^{13}C-NMR spectrum of **5**. 144

5.48. COSY spectrum of **5**. 144

5.49. ESI mass spectrum of **5**. 145

5.50. ^{1}H NMR spectrum of **6**. 146
5.51. ^{13}C NMR spectrum of **6**. 147
5.52. COSY spectrum of **6**. 147
5.53. ESI mass spectrum of **6**. 148
5.54. ^{1}H NMR spectrum of **7**. 149
5.55. ^{13}C NMR spectrum of **7**. 150
5.56. COSY spectrum of **7**. 150
5.57. ESI mass spectrum of **7**. 151
5.58. ^{1}H NMR spectrum of p(**5**). 152
5.59. ^{1}H NMR spectrum of p(**6**). 153
5.60. ^{1}H NMR spectrum of p(**7**). 153
5.61. ^{1}H NMR spectrum of GII and $ZnCl_2$ in C_6D_6 (top) and GII in C_6D_6 (bottom). 154
5.62. ^{1}H NMR spectrum of crude reaction mixture of **5** after 24 hours at 55 °C with $ZnCl_2$ as catalyst. 155
5.63. IR spectra of **5**, p(**5**), p(**6**), and p(**7**), as well as 1-methyl furan and LGO, for comparison. The bands at 1735 cm^{-1} and 2870 cm^{-1} are indicated. . . 156
5.64. SEC chromatogram of test homopolymerisation of **5** without quenching 157
5.65. ^{1}H NMR spectrum of test homopolymerisation of **5** without quenching 157

List of Tables

2.1. Screening conditions for the ring-closing metathesis of diallyl ether for the formation of 2,5-DHF. 38

2.2. E-factors for the synthesis of 2,5-DHF in this chapter starting from *cis*-2-buten-1,4-diol or diallyl ether, including work-up. 39

2.3. Screening conditions for the isomerisation of 2,5-DHF to 2,3-DHF. . . . 41

2.4. Calculation of the total E-factor for the synthesis of 2,3-DHF starting from *cis*-2,buten-1,4-diol, diallyl ether, or but-3-yn-1-ol. 45

2.5. Calculation of the total E-factor for the synthesis of poly(DHF) starting from *cis*-2,buten-1,4-diol, diallyl ether, or but-3-yn-1-ol. 46

2.6. Conversion in % of various dienes in RCM using 0.01 eq of GHII, in various solvents, at 40 °C. 54

2.7. Calculated ring-strains for different five-member ring heterocycles. . . 55

3.1. Overview on synthesised thiocarbonylcompunds and thereof derived thionorbornes. 63

3.2. Molecular weight and conversion of the polymers obtained from the ROMP of **3a** using different Grubbs catalysts. 65

3.3. Characteristics molecular weight of the polymers obtained from the ROMP of **3a**, **3b**, **3c**. 67

3.4. T_g and T_d of thionorbonene derived polymers obtained. 72

4.1. Electrophilic substitution catalyst screening using LGO and furan as substrates.[1] 78

4.2. Electrophilic substitution solvent screening using LGO and furan as substrates and $ZnCl_2$ as catalyst.[1] 79

4.3. Temperature screening for the synthesis of monomer **5**.[1] 79

4.4. Reaction time and conversion in the synthesis of monomer **5** 80

4.5. M_n of p(**5**) obtained using different catalysts. All reactions were conducted at 25 °C and run for 24 hours using monomer concentration of 5 mg/mL and DCM as reaction solvent. 81

4.6. M_n of p(**5**) obtained using different quantities of $ZnCl_2$ at 25 °C, with reaction time of 24 hours, concentration of the monomer of 5 mg/mL, DCM as reaction solvent and 0.01 eq of GII. 86

4.7. M_n of p(**5**) obtained using different quantities of GII at 25 °C, with reaction time of 24 hours, concentration of the monomer of 5 mg/mL, 1.0 eq of $ZnCl_2$ and DCM as reaction solvent. 87

4.8. Molecular weights of p(**5**), p(**6**) and p(**7**) obtained at 25 °C, with reaction time of 24 hours, DCM as reaction solvent, concentration of the monomer of 5 mg/mL, 1.0 eq of $ZnCl_2$ and 0.01 eq of GII as catalysts . . 88

4.9. Decomposition and glass transitions temperatures of p(**5**), p(**6**) and p(**7**). 89

5.1. Dilution rate of 2,3-DHF in DCM. 106

5.2. Dienes quantity employed in the ring-closing metathesis 108

5.3. Reaction conditions for the synthesis of thiokethones and the thioaldehyde. 110
5.4. Reaction conditions for the synthesis of TNbs. 119
5.5. Reaction conditions for the synthesis of homopolymers. 130
5.6. Solubility of homopolymers and copolymers in common solvents. . . . 140
5.7. Quantities of reagents used for the polymerisation reactions. 152

1. Introduction and theoretical background

1.1. Introduction and aim of the thesis

Polymer materials represent an important class of chemicals, the so-called commodity plastics reached an annual production of 359 million metric tons in 2018.[4] Polyvinyl chloride (PVC),[5] polyethylene (PE),[6] polypropylene (PP)[7] and polyethylene terephthalate (PET)[5] are considered among the most used daily commodity. These polymers are implemented in several aspects of our everyday life.[8] However, these commodities present a major setback, their end of life cycle. Even if some of these materials can nowadays be recycled[9] this was not the case in the past. Accumulation of these polymers over the years in the environment leads to an environmental crisis. This is why the development of degradable polymers is a necessary step towards the future of plastic materials. Several degradable polymers are reported in the literature such as polylactic acid(PLA),[10] poly(DHF)[11] and poly(glycolic acid) (PGA).[12] Degradable polymers can be break down into their constituent monomers *via* bacterial[13] or chemical actions.[14] This allows recyclability and minimises land plastic pollution, however, the decomposition products must be investigated to prevent the release of pollutants byproducts.[15] Another major setback about plastic commodities is represented by their production. These materials are often synthesised from petroleum derivatives, using industrial processes that produce high quantity of waste and byproducts. In recent years, industrial chemical production is being re-imagined, and the principles of Green chemistry[16] are leading the redesign of industrial-scale processes to minimise their environmental footprint. Green chemistry is a branch of chemistry that studies the environmental impact of chemical processes and their footprint.[17] The principle of green chemistry[16] are a guideline on how to optimise the chemical process to improve their sustainability, taking into consideration the entire process, the nature of the starting material, their hazards and the quantity of waste produced. The development of green chemistry leads to the research of new starting materials for polymer production, for instance bio-derived molecules such as alkanoates,[18] levoglucosenone,[19] cellulose[20] and starch[21] are deeply investigated regarding their ability to yield bio-based polymers. The green metrics of polymerisation techniques overall also need to be included in the discussion. Starting from a bio-based monomer is not enough to define a process sustainable. Several polymerisation methods can be employed to obtain a polymer such as radical polymerisation,[22] cationic or anionic polymerisation, [23, 24] or ring-opening polymerisation.[25] Ring-opening metathesis polymerisation (ROMP)[26] is an interesting example of the latter. ROMP is a controlled-polymerisation technique, that can also present living character,[27] allowing great control over the polymerisation process.[28] ROMP is deeply studied as a greener alternative to other polymerisation methods, the possibility to obtain polymer at room temperature,[29] with minimal waste and byproducts[30] and in a green solvent such as dimethyl carbonate[31] or in bulk[32] possibly render these techniques more sustainable. This metathesis polymerisation can be employed to yield degradable polymers such as poly(DHF).[11] The high functional group tolerance[33] of these techniques allows the polymerisation of a vast variety of monomers such as nitrogen-containing,[34] carboxylate,[35] or sulfur-containing monomers.[36] Sulfur-containing polymers are particularly interesting due to their potential applications in optoelectronics,[37] or as conductive polymers.[38]

This work aims to improve the sustainability of current literature known polymers obtained *via* ROMP and to investigate different heteroatoms-containing polymers obtained with the aforementioned polymerisation techniques. In detail, alternative pathways to the synthesis of 2,3-dihydrofuran, the monomer of poly(DHF), will be investigated, to optimise the green metrics of the monomer synthesis. Moreover, the paring of the synthesised monomer with a norbornene derivative to obtain a copolymer will be researched, in order to observe the changes in thermal properties compared to the respective homopolymers. In addition, due to the various application of sulfur-containing polymers, the synthesis of five-membered ring heterocycles and their application in ROMP will be discussed. Using ring-opening metathesis polymerisation new sulfur-containing polymers and copolymers will be synthesised, and a pathway to the synthesis of ring-strained sulfur-contain olefins, nominally ThioNorbonene, is described. Lastly, Levoglucosenone, a derivative of cellulose will be employed with furan towards the synthesis of new bio-based monomers.

Parts of this first chapter are adapted from my master thesis.[39]

1.2. Polymerisation techniques

There are several techniques to obtain a polymer from a monomer. Depending on the monomer structure and functional groups, it is possible to choose from several possible polymerisation procedures that a monomer could undergo. The first step to define a polymerisation technique consists in identifying if the reaction will be a polyaddition,[40] or a polycondensation.[41] Polyaddition is defined by IUPAC as a polymerisation in which the growth of polymer chains proceeds by addition reactions between molecules of all degrees of polymerisation. Instead, in a polycondensation, two monomers react with each other releasing a small molecule in the process, such as water, methanol or ethanol. An example of polymer obtained by polycondensation is poly(ethyl terephthalate) (PET).[42] Another way to classify polymer reactions is by defining how the polymer chain is formed. If the chain is formed by attachment of one monomer at the time the mechanism is defined chain-growth.[43] If instead first oligomers are formed and then react together to yield a polymer chain the mechanism is called step-growth.[44] During a chain-growth polymerisation the monomer will exist trough the reaction, instead in step-growth polymerisation this will be consumed quickly at the beginning of the reaction. The mechanism of chain-growth polymerisation will be discussed in details in chapter 1.2.3. An example of chain-growth polymerisation is radical polymerisation.

1.2.1. Radical polymerisation

Radical polymerisation is one of the most widely used polymerisation processes for the industrial production of various polymers. Several monomers can undergo radical polymerisation, such as (methyl)acrylates,[45] styrene,[22] norbornene,[46] butadiene, [47] or vinyl chloride.[48] This polymerisation technique is very versatile since it can tolerate a wide range of functional groups (such as acid derivatives, hydroxyl groups, or halogen group), and a variety of reaction conditions can be employed (e.g. bulk,[49] solution,[50] emulsion,[51] suspension.[52]) However, the conventional, so called free radical process, has some limitations with respect to the degree of control that can be asserted over the macromolecular structure, in particular, the molecular weight distribution, composition, and architecture. To overcome the limitations of classical radical polymerisation, controlled or living polymerisations may instead be used. Living or controlled polymerisation is a form of chain-growth polymerisation where the ability of a growing polymer chain to terminate is virtually inexistent. In recent years, the rise of this type of radical polymerisation has provided a new set of tools for polymer chemists that allows a very precise control over the polymerisation process while retaining much of the versatility of conventional radical polymerisation.

1.2.2. Molecular weight distribution

When a polymerisation process occurs, it is rare to obtain a so-called monodisperse molecule. Often a distribution of molecular weights will be obtained.[53] During a typical uncontrolled radical polymerisation, not all the chains grow simultaneously. Therefore at the end of the process, different length chains, thus different molecular weights, will be obtained. While several means to describe molecular weight exist, three are commonly used, namely the number average molecular weight (M_n),[54] the weight average molecular weight, (M_w)[54] and z average molecular weight (M_z).[54] The mathematical definitions of are shown in equations 1.2.1; 1.2.2; 1.2.3. Where M_i is the molecular weight of the chain and N_i is the number of chains with that molecular weight.

$$M_\mathrm{n} = \frac{\sum M_\mathrm{i} N_\mathrm{i}}{\sum N_\mathrm{i}} \qquad \text{(Eq. 1.2.1)}$$

$$M_\mathrm{w} = \frac{\sum {M^2}_\mathrm{i} N_\mathrm{i}}{\sum M_\mathrm{i} N_\mathrm{i}} \qquad \text{(Eq. 1.2.2)}$$

$$M_\mathrm{z} = \frac{\sum {M^3}_\mathrm{i} N_\mathrm{i}}{\sum {M^2}_\mathrm{i} N_\mathrm{i}} \qquad \text{(Eq. 1.2.3)}$$

To define the broadness of the molecular weight distribution obtained, the dispersity (Đ) parameter was introduced (equation 1.2.4). It defines indicate the ratio between M_w and M_n and it is always bigger or equal to one.

$$Đ = \frac{M_\mathrm{w}}{M_\mathrm{n}} \qquad \text{(Eq. 1.2.4)}$$

To obtain a polymer with a narrow molecular weight distribution, controlled or living polymerisation techniques are required, such as ring-opening metathesis polymerisation (ROMP),[28] or atom transfer radical polymerisation (ATRP).[55]

1.2.3. Mechanism

Different polymerisation techniques can be classified as chain-growth polymerisations, such as anionic and cationic,[23, 24] ring-opening metathesis polymerisation (ROMP),[27] atom transfer radical polymerisation (ATRP),[56] or reversible addition-fragmentation chain transfer (RAFT) polymerisation.[57] Also, uncontrolled radical polymerisations belong in the broader family of step-growth. The chain growth polymerisation mechanism can be divided into four processes: chain initiation, propagation, chain transfer, and termination. The chain propagation and initiation steps are present in every chain-growth type polymerisation, but in living or controlled polymerisation, termination could be virtually absent.[58] The process begins with the generation of radicals, usually by the homolytic splitting of an initiator *via* light-mediated or thermal activation. The initiator-derived radicals are then added to the monomer. This represents the chain initiation step. In the chain propagation step, monomer units are sequentially added to the growing radical formed (indicated as $P_n\bullet$ in figure 1.1). Chain transfer entails the radical reacting with another molecule, for instance a solvent or the formed polymer chains, and transferring the radical, which cannot sustain the polymerisation. In the end, chain termination occurs when the propagating radicals react *via* recombination or disproportionation, in the latter the two radical species react to generate two non-radical species, by elimination or hydrogen transfer, for example.

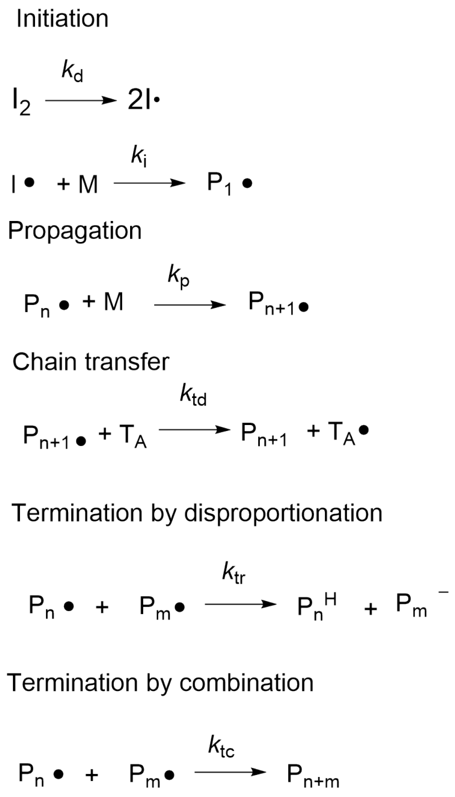
Initiation
$I_2 \xrightarrow{k_d} 2I\bullet$
$I\bullet + M \xrightarrow{k_i} P_1\bullet$
Propagation
$P_n\bullet + M \xrightarrow{k_p} P_{n+1}\bullet$
Chain transfer
$P_{n+1}\bullet + T_A \xrightarrow{k_{td}} P_{n+1} + T_A\bullet$
Termination by disproportionation
$P_n\bullet + P_m\bullet \xrightarrow{k_{tr}} P_n^H + P_m^-$
Termination by combination
$P_n\bullet + P_m\bullet \xrightarrow{k_{tc}} P_{n+m}$

Figure 1.1.: Important steps of the mechanism of radical polymerisation.

In uncontrolled chain-growth polymerisation, the molecular weight of chains increases rapidly at low monomer conversion. Instead, in living polymerisations, there is a linear correlation between the molecular weight and the monomer conversion, as shown in Figure 1.2.

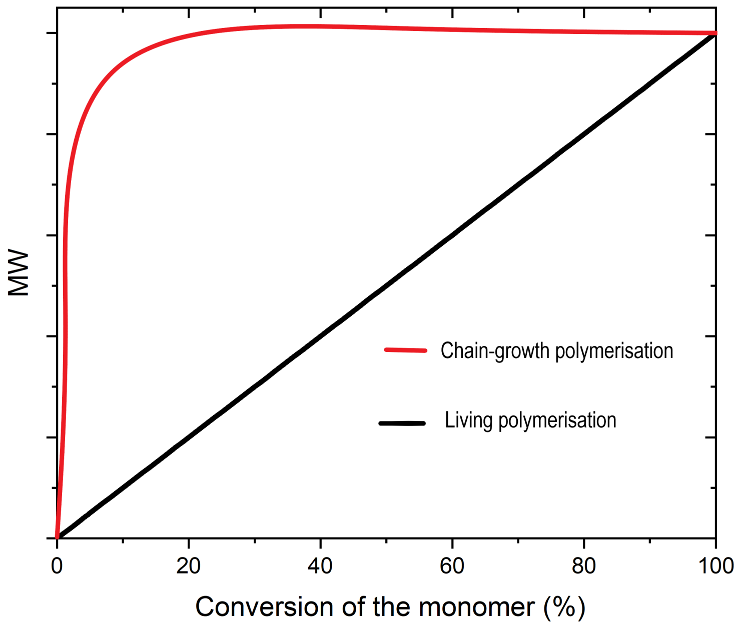

Figure 1.2.: Conversion vs. MW in chain growth and living polymerisation

The uncontrolled nature of a typical radical polymerisation results in usually broad dispersity (Đ> 1.5). Even if some factors can be optimised to reduce the ratio, such as solvent, monomer and initiator concentration, the use of controlled living radical polymerisation allows achieving more narrow molecular weight distribution.

1.2.4. Living polymerisations

In an ideal living polymerisation, all chains are initiated simultaneously, grow at the same rate, and survive the polymerisation since there is virtually no termination.[58] To confer living character on a radical polymerisation, it is necessary to suppress all processes that terminate chains in an irreversible way. Reversible-deactivation radical polymerisation (RDRP) is a class of living polymerisations that take advantage of the reversibility of deactivation and chain transfer processes, using special transfer agents so that the majority of chains are maintained in a dormant form.[59] Rapid equilibration between the active and dormant forms ensures that all chains possess an equal chance for growth and that all chains will grow at the same time, albeit intermittently. Under these conditions, the molecular weight increases linearly with conversion and the molecular weight distribution can be very narrow (e.g. $Đ$ ca. 1.1) if initiation is considerably faster than propagation. The RDRP techniques that have recently received the greatest attention are nitroxide-mediated polymerisation (NMP), atom transfer radical polymerisation (ATRP), and reversible addition-fragmentation chain transfer (RAFT) polymerisation. NMP was discovered in the early 1980s and, in recent years, has been exploited extensively for the synthesis of narrow molecular-weight distribution homopolymers and block copolymers of styrene and acrylates.[60, 61] The limit of NMP is caused by the high activation/deactivation constant presented by several nitroxide/monomer systems, such as methacrylic acid and 2,2,6,6-tetramethylpiperidin-1-yl)oxyl TEMPO, which renders the process not always controllable.

However, recent developments have made NMP applicable to a wider range of monomers.[62] Another example of RDRP is reversible addition-fragmentation chain transfer (RAFT). The RAFT process involves free-radical polymerisation in the presence of chain transfer agents, also called RAFT agents. They are usually thiocarbonyl compounds,[63] that react with the free radicals and help to afford control over the polymerisation.[64] The experimental conditions employed are those used for conventional free-radical polymerisation. The controlled character of the RAFT process is indicated by the narrow dispersity of the product and the linear molecular weight *vs.* conversion profile. The predictability of the molecular weight from the ratio of monomer consumed to transfer agent, and the ability to produce block copolymers or higher molecular weight polymers[65] by further monomer addition are the reasons why this polymerisation technique is highly popular. Another advantage of the RAFT process is that it is compatible with a wide range of monomers and is tolerant to a variety of functional groups.

1.2.5. ATRP

Atom transfer radical polymerisation (ATRP) is one of the most common RDRP polymerisations. ATRP was independently discovered by Sawamoto[66] and Matyjaszewski.[67] In this living-polymerisation, a transition metal, often copper, is used to generate radicals from a dormant species, usually alkyl halides and by this means, start the polymerisation. What makes ATRP a controlled radical polymerisation is the equilibrium between the dormant species (indicated as P_n-X in Figure 1.3) and the propagating species (shown as $P_n^{\bullet}$ in Figure 1.3).[68] The ability to influence this equilibrium leads to polymers with tailored molecular weights and narrow dispersity.[69] ATRP is a versatile technique: it can be used in a wide range of temperatures with a wide range of monomers and solvents.[70]

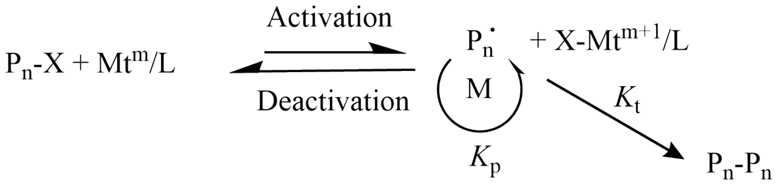

Figure 1.3.: Activation and Deactivation equilibrium in ATRP.

1.3. Green chemistry

1.3.1. Principles of Green Chemistry

The main goal of green chemistry is to make chemical products and processes less impactful for people and the environment.[17] To reach this goal, it is necessary to minimise the use and generation of hazardous substances, avoid generation of waste, and make chemistry more efficient. Implementing greener chemistry can improve several aspects of industrial manufacturing, from lower waste production to lower energy consumption. The focus of the green approach is not just human related, but also on how the chemical process affects the environment.[71]

When a chemical process is redesigned taking into account greener approaches, not only the toxicity of the product must be considered but also the sustainability of the starting materials the energy and materials needed for the synthesis and what is the shelf-life of the product and the possible end-life cycle of it.[72] Green chemistry takes into account all life-cycle stages of a chemical product. As a guide to green chemistry, Paul Anastas and John Warner developed the 12 principles of green chemistry in 1998:[16]

1. Avoidance and minimisation of waste

2. Atom economy
3. Avoidance of toxic starting materials and byproducts
4. Design of new, less toxic products
5. Use of less and safer solvents
6. Increase in energy efficiency
7. Use of renewable raw materials
8. Design of synthesis with fewer intermediates
9. Use of catalysts for more efficient synthesis
10. Design of products that can be destroyed naturally
11. Monitoring of the synthesis to prevent waste and toxic byproducts
12. Minimising the risk of accidents

These twelve principles take into consideration the entire life-cycle process of a product, and they are a useful guide to achieve the goal of sustainability.

1.3.2. Green Metrics

Once the green chemistry guidelines were established according to the twelve principles, it is necessary to develop a way to compare chemical reactions or processes and understand a way to classify the "greenness" of a reaction.[73] To be able to discuss and compare the sustainability of a synthesis, a large number of metrics have been developed. A suitable metric is characterised by the fact that it is clearly defined, easily measurable and objective.[73] One of the most used measures of the reaction's efficiency is the atom economy and it is mathematically expressed as:[74]

$$\text{Atom Economy} = \frac{\text{MW desired product}}{\text{MW all products}} 100 \qquad \text{(Eq. 1.3.1)}$$

However, this simple concept does not determine the actual yield or conversion of the reactants or other reagents used in the system. Thus, the real efficiency of the system is not calculated, AE remains a theoretical number only useful for very early stage comparisons. Thus, the reaction mass efficiency was introduced to improve the atomic efficiency formula. [74]

$$\text{Reaction Mass Efficiency (\%)} = \frac{\text{Mass of product}}{\text{Mass of al reactants}} 100 \qquad \text{(Eq. 1.3.2)}$$

In the reaction mass efficiency, the yield and stoichiometry of the reactants are taken into account. This allows to obtain the percentage of reactants that remain in the product.[74] The effective mass yield is defined as "the percentage of the mass of desired product relative to the mass of all non-benign materials used in its synthesis". [75] This metric was proposed by Hudlicky *et al.* and can be expressed mathematically as:

$$\text{Effective Mass Yield (\%)} = \frac{\text{Mass of product}}{\text{Mass of non-benign reagents}} 100 \qquad \text{(Eq. 1.3.3)}$$

This method helps to determine the yield in relation to the final mass, underlining the quantity of mass made of non-toxic substances. This metric has the limitation of not being applicable to all synthesis processes, as information on toxicity and ecotoxicity are not available for all chemicals. Also, there are some underlying risks also with non-benign substances. For example, saline solution can have specific environmental effects depending on the concentration and the waste release location.[76] To make proper sense of this metric, there must be a clear definition of how benign is defined, also related to the local environment. Also, complete information about the toxicity and ecotoxicity of all chemicals must be taken into consideration and reviewed over time. One of the most used and reported green metrics is the environmental factor (E-factor).[77] This metric was proposed by Roger Sheldon and shows the relationship between waste produced and the product of a synthesis:

$$\text{E-factor} = \frac{\text{Total waste (Kg)}}{\text{Product (Kg)}} \qquad \text{(Eq. 1.3.4)}$$

This simple metric can give a good value for the quantity of waste made for a kilogram of the product during the process.[77] On a weight basis instead of percentage, the mass intensity includes the yield, stoichiometry, the solvent, and the reagent used in the reaction, so everything that was used in the process or the single process steps (except for water).[78] The mass intensity is mathematically expressed as:

$$\text{Mass Intensity} = \frac{\text{Total mass used in all process steps/one process step (kg)}}{\text{Mass of product (kg)}} \qquad \text{(Eq. 1.3.5)}$$

These metrics can help for a better understanding and comparison of the synthesis process and allows us to keep attention to critical key factors such as waste production. Often there are still some problems related to the correct calculation of these metrics. For example, it is hard to obtain a clear definition for benign reagents, but it is an excellent way to assess the sustainability of the synthesis.

1.4. Synthetic tools

1.4.1. The Diels-Alder reaction

Cycloaddition reactions are synthetic tools where two or more unsaturated molecules react to generate a cyclic product.[79] One of the most common and used cycloaddition is the Diels-Alder reaction, this [4+2]-cycloaddition took the name from their discoverers and was first reported in 1928.[80] In this reaction, a 1,3-diene, an unsaturated conjugated molecule, reacts with a dienophile to give a six-membered ring.[81] The reaction is for instance widely used in the synthesis of natural compounds.[82] The reaction presents a high atom economy since all the atoms of the educts are incorporated into the product. This is particularly interesting from a green chemistry point of view.[83] This cycloaddition can be performed in a variety of solvents,[84] emulsion,[85] micro-emulsion,[86] or even in bulk.[87] Several Diels-Alder reactions, such the one between Furan and maleic anhydride, are favoured at room temperature,[88] other requires to be performed at higher temperature or the use of a catalyst to overcome the activation barrier.[89] Most Diels-Alder reactions are exothermic. From three π-bonds, two σ and one π-bond are formed.[90] An example for a Diels-Alder reactions is shown in Figure 1.4. The Diels-Alder reaction can either have a direct or an inverse electron-demand.[91]

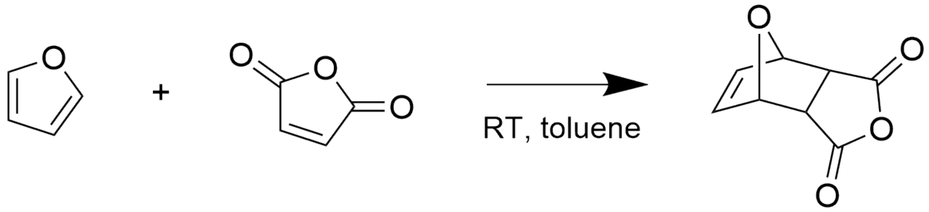

Figure 1.4.: Reaction scheme of the Diels-Alder reaction between Furan and maleic anhydride

Diels-Alder reaction is a concerted cycloaddition,[92] where three π-bonds are broken, two σ and one π formed (Figure 1.5). This always lead to the formation of a six-member ring.

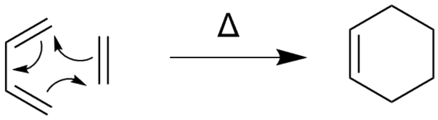

Figure 1.5.: Concerted mechanism of Diels-Alder cycloaddition

In a normal electron demand Diels-Alder reaction overlap between the highest occupied molecular orbital (HOMO) of the diene and the lowest unoccupied molecular orbital (LUMO) of the dienophile occours to allow the reaction to proceed.[93] In a reverse electron demand Diels-Alder reaction, the interaction is between the LUMO of the diene and the HOMO of the dienophile.[94] In figure 1.6 two examples for the molecular orbital diagrams of direct (a) and inverse (b) electron-demanding Diels-Alder reaction. In chapter 1.4.4 the HOMO and LUMO interaction in Diels-Alder reactions will be discuss further.

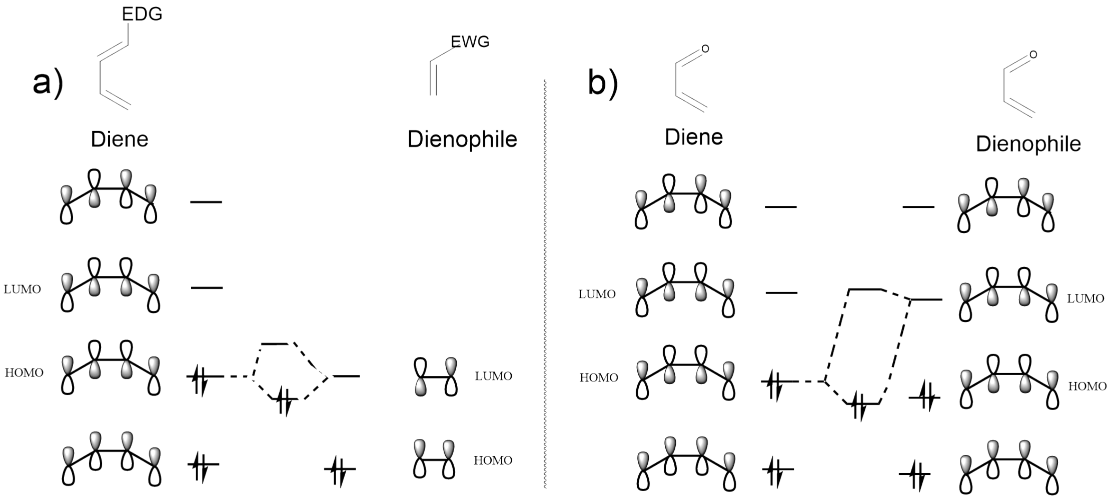

Figure 1.6.: a) Generic molecular orbital diagram for a direct electron demanding DA; b) Molecular orbital diagram of inverse electron demanding DA in the dimerisation of acrolein.

1.4.2. Dienes and dienophile requirements in Diels-Alder reaction

There are requirements that need to be fulfilled for both the diene and the dienophile to perform in a Diels-Alder reaction. For the diene, the two double bonds must be in a conjugated system.[95] This condition allows the diene's HOMO to interact with the LUMO of the dienophile. The diene has to be in *s*-cis-configuration in order to undergo a [4+2] cycloaddition.[96] Cyclic dienes, such as cyclopentadiene, are locked in *s*-cis-configuration,[97] are more reactive in comparison to acyclic dienes,[98] that can freely change their conformation at the reaction temperature.[99] Substituent influence the reactivity,[100] electron-donors will increase the reactivity of the diene in a direct electron-demanding Diels-Alder reaction.[101]

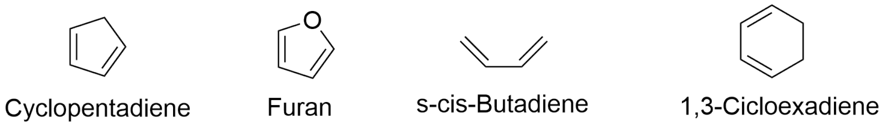

Figure 1.7.: Example of various dienes for Diels-Alder reaction, nominally: Cyclopentadiene, Furan, *s*-cis-butadiene, 1,3-cyclohexadiene

In a Diels-Alder reaction with direct electron demand, the dienophile should be electron-poor. This lowers the gap between the LUMO of the dienophile and the HOMO of the diene, making them comparable in energy, thus making the reaction possible. Electron-withdrawing groups on the dienophile help to increase the reaction rate since they have a direct correlation with the energy level of the LUMO. Instead, in an inverse electron demand Diels-Alder reaction, the dienophile should be electron-rich. To achieve this goal, a substituent with an electron-donor character should be used.[102]

1.4.3. Catalysis of the cycloaddition

Not all Diels-Alder reactions are favoured at room temperature. To lower the activation barrier, a catalyst needs to be involved. To catalyse the cycloaddition, typically, Lewis acids are used.[103] Unlike the widely known assumption that Lewis-Acids catalyse the reaction by lowering the LUMO of the dienophile to enable easier donor-acceptor interaction, recent studies indicate that the catalytic effect is induced by lowering the Pauli-repulsion of the two interacting π-orbitals and incrementing asynchronicity of the reaction.[103, 104] Organocatalysis can also be used to regulate the stereochemistry of the product obtained. This will be discussed deeply in the next chapter 1.4.4.

1.4.4. Stereochemistry

To predict the stereochemistry of a cycloaddition reaction, it is essential to understand in which way the molecular orbital of the diene and dienophile will overlap each other. The Woodward-Hoffmann rule[105] predicts the facial selectivity of the involved molecular orbital. To understand the stereochemistry involved in the Diels-Alder reaction, it is necessary to introduce two topological concepts: *antara-* and *suprafacial.* These concepts define the relationship between two simultaneous bonds forming. Applying this concept to cycloaddition reactions leads to the conclusion that if the new bonds generated in the cycloaddition are the results of overlapping from the same plane face, we are talking about *suprafacial* formation. Instead, if the overlap of the π-system came from different plane faces, the result will be a *antarafacial* formation. The molecular orbitals of the two components involved in the cycloaddition can approach each other in three different ways. The first is the supra-supra approach, where the orbitals approach each other, keeping the facial planes nearly parallel to each other. One orbital can also approach vertically to the other, while the second one maintains a suprafacial configuration. This will result in a supra-antara overlap. The last case is observed when both are antarafacial in relation to each other. Supra-supra facial overlap allows optimal overlap of the orbitals. Supra-antara approach, instead, is unfavourable because of steric hindrance, and antara-antara overlap is theoretically possible but was never observed empirically.[106] This leads to the conclusion that supra-supra facial attack is the only possibility for [4+2] cycloaddition.[107]

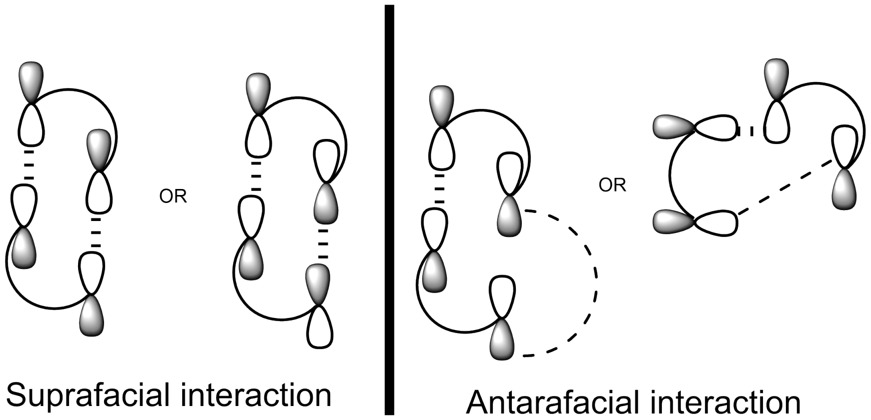

Figure 1.8.: Suprafacial and antarafacial interaction possibilities possibilities.

Hence the overlapping has been defined so the stereochemistry of the product can be analysed. The supra-supra attack can take place in two different ways: *exo* or *endo*. When the diene and the dienophiles possess a linear structure, it is often not possible to define which attack occurred. Instead, when one component is cyclic, due to the rigidity of the conformation, it is often possible to assign *exo* or *endo* configuration to the obtained molecule. When two orbitals approach in a *endo* fashion, they possess the correct symmetry to allow secondary orbital interactions,[108] lowering the activation barrier of the process, but not of the energy of the resulting product, that are higher due to steric hindrance. Instead, in the *exo* approach, secondary orbital interactions are not possible, resulting in a higher activation state but lower relative energy of the product due to the lower steric hindrance. This leads to the *endo* product being defined as the kinetic one since it is fast in formation but leads to a product higher in energy. The *exo* product instead is the thermodynamic one.[109]

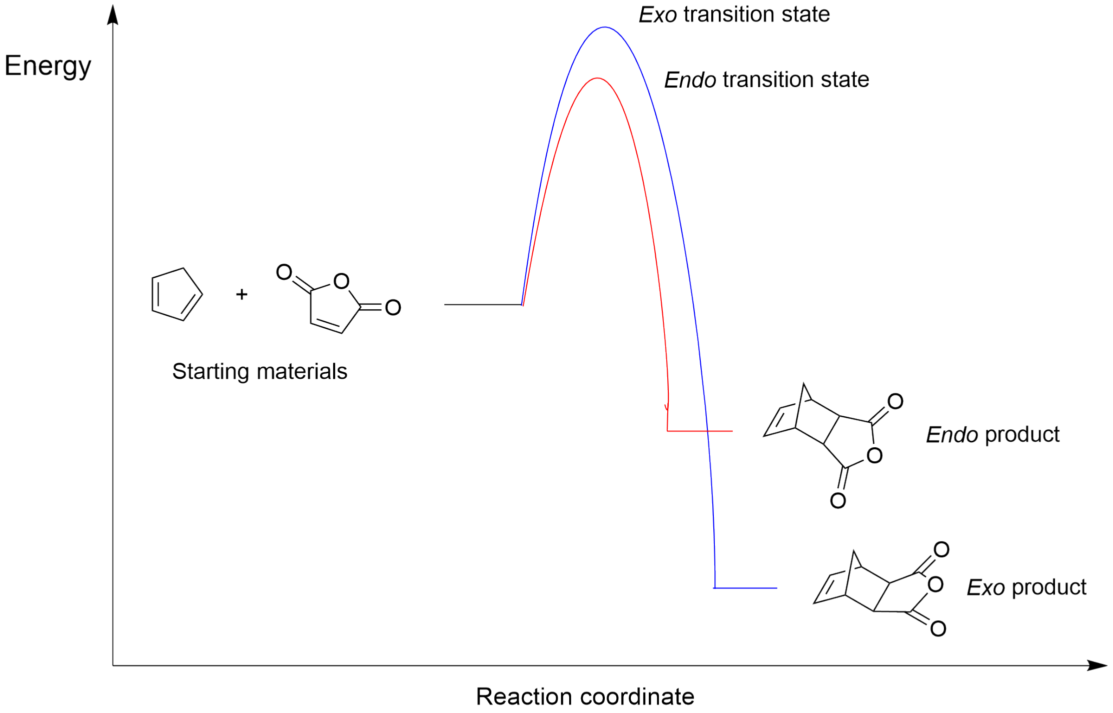

Figure 1.9.: Schematic *exo* and *endo* energy diagram for the reaction between cyclopentadiene and maleic anhydride.

Chiral organocatalysts can help to modify the activation barrier, favouring one diastereoisomer over the other.[110] However, interconversion between the two diastereoisomers is possible at high temperatures,[111] the temperature for the interconversion depends on the chemical structure of the obtained product.

1.5. Olefin Metathesis

Metathesis is a class of reactions that involves the exchange of atoms or functional groups in the substrate and the rearrangement of their matching partner to yield new compounds.[112] Olefin metathesis is a type of metathesis that involves alkenes, where the substituents of double bonds of two olefins are rearranged, forming two new olefins.[113] One of the reasons why olefin metathesis is a powerful tool for organic chemistry is the possibility to synthesise sterically hindered olefins,[114] such as tri- and tetrasubstituted olefins, which are not as easily accessible with other organic reactions.[115] Another advantage of metathesis is that there are little to no by-products produced. One of the most common by-products of olefin metathesis is ethylene. This gas can be easily removed from the reaction medium, allowing it to switch the equilibrium of the reaction. The lower amount of by-product producible from the reaction made it interesting also in green-chemistry optics.[116] Metathesis reactions can be classified based on the product obtained: Cross metathesis (CM),[117] ring-closing metathesis (RCM),[118] ring-opening metathesis (ROM),[119] ring-opening metathesis polymerisation (ROMP)[26] and acyclic diene metathesis (ADMET)[120] are the most common examples (Figure 1.10). In principle, all metathesis reactions are reversible and have to be designed to shift the equilibrium towards the desired product.[121] However, there are a few examples of ROMP and ADMET reversible reactions. One of the most prominent ones is the degradation of poly(dihydrofuran) obtained *via* ROMP.[11] Over the years, several metathesis catalysts have been developed. Grubbs, Chauvin and Schrock were awarded the Nobel prize in chemistry (2005) thanks to their contributions to this field. Grubbs and Schrock also developed two classes of metathesis catalysts, and their different iterations now represent the majority of available metathesis catalysts.[122, 123] The so-called Grubbs catalyst are a family of organometallic catalysts where the metal centre is a Ruthenium atom. This catalyst group will be discussed extensively in the subchapter 1.6.1. Schrock's catalysts type instead use Molybdenum as metal centre, this type of metathesis catalyst is able to allow the formation of sterically hindered olefins. The downside of Schrock catalysts are their poorer stability in the presence of oxygen, contrary to the Grubbs catalysts that tends to be bench stable.[124]

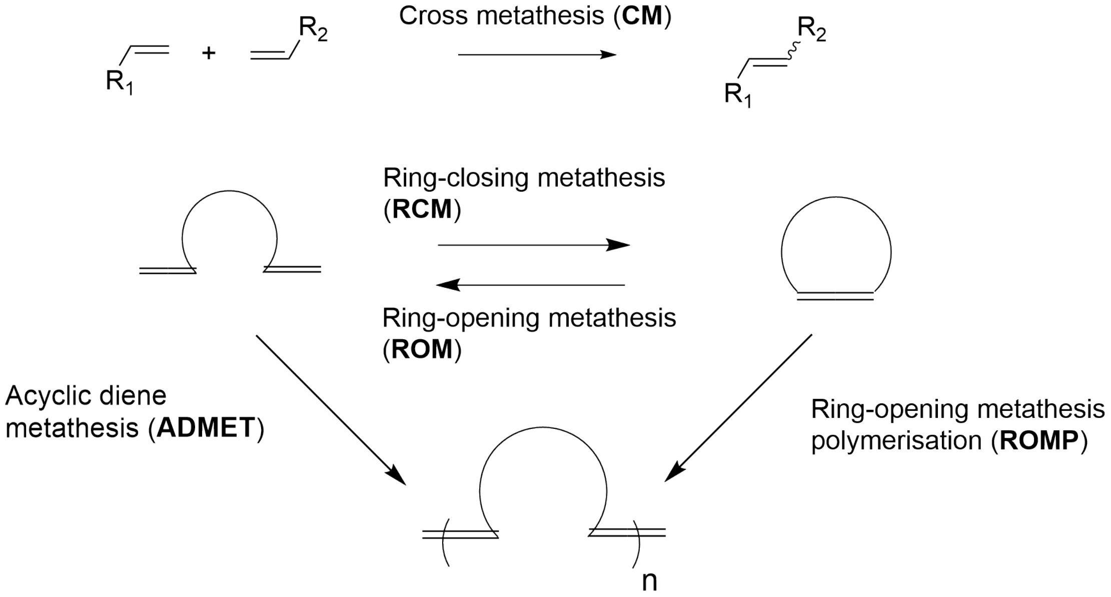
R2
R1
+
Cross metathesis (**CM**)
R2
R1
Ring-closing metathesis (**RCM**)
Ring-opening metathesis (**ROM**)
Acyclic diene metathesis (**ADMET**)
Ring-opening metathesis polymerisation (**ROMP**)
n

Figure 1.10.: General representation of different organic metathesis reactions.

1.5.1. Cross Metathesis

Cross metathesis reactions are transalkylidenations between two terminal alkenes.[117] In cross-metathesis, two olefins react with an initiating metal carbene of the catalyst and form a new olefin in a chain reaction.[125] This is called the non-pairwise or Chauvin-mechanism (Figure 1.11).[126] The first step of the mechanism is the [2+2] cycloaddition of the olefin double bond to a transition metal alkylidene. This results in the formation of a metallacyclobutane intermediate, which will then proceed *via* cycloelimination, yielding the original species or a new alkylidene and alkene. Next, the newly formed alkylidene will undergo a [2+2] cycloaddition with a new alkene. The metallacyclobutane obtained will then cycloelimininate. This results in a new alkene developed, the metathesis product, and a transition metal alkylidene that can restart the cycle. This mechanism can also be applied to the other metathesis types.[127]

One challenge of this reaction is to prevent homodimerisation,[128] the metallorganic catalysts for this reaction type are designed to minimise this phenomenon.

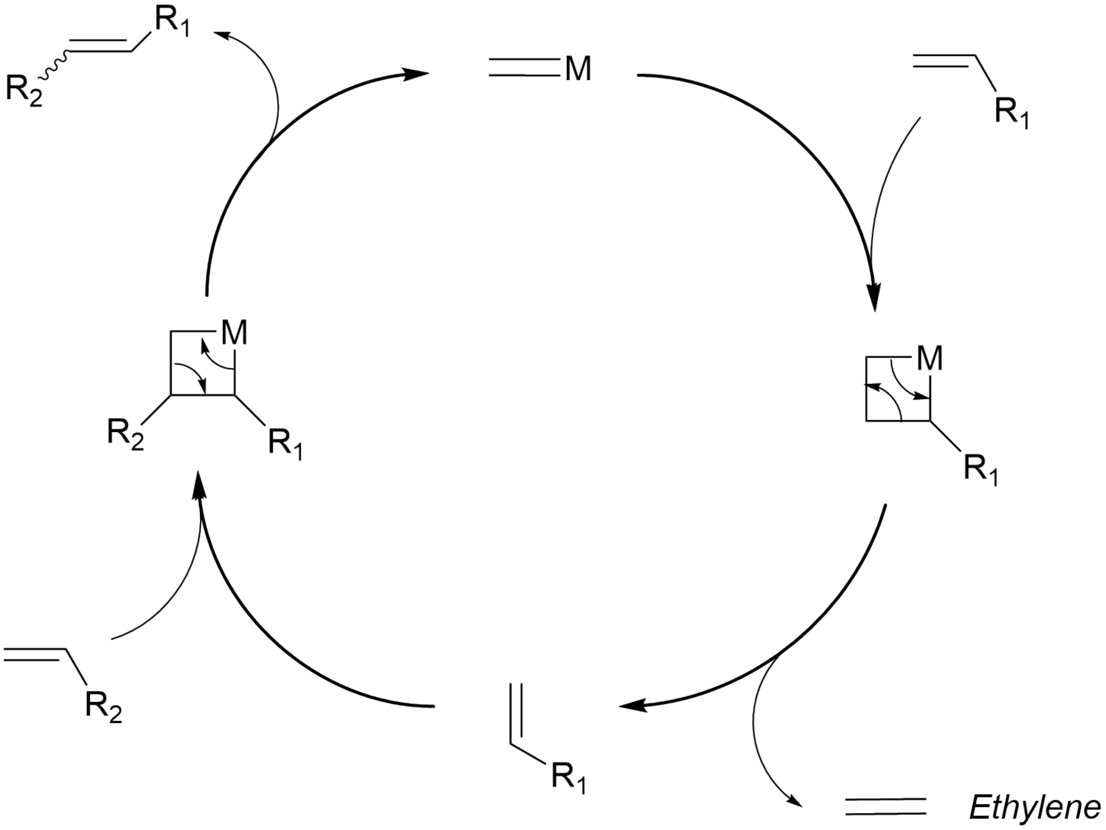

Figure 1.11.: Reaction mechanism of olefin cross-metathesis (Chauvin mechanism).

1.5.2. Ring-closing Metathesis

In ring-closing metathesis, two terminal double-bonds react in an intramolecular metathesis reaction to form two new olefins, a cyclic product and an acyclic olefin as a by-product. The mechanism is identical to the one adopted in cross-metathesis, with the only difference being that the reaction is intramolecular. Acyclic diene metathesis polymerisation (ADMET) could compete with RCM in the reaction medium. To prevent undesired reactions, the dilution of the reaction mixture must be adjusted.

1.5.3. Ring opening Metathesis

In a ring-opening metathesis, a cyclic olefin reacts with an acyclic olefin to generate an acyclic diene.[119] Often, the released ring strain is the driving force of this reaction while also being the source of minimal reversibility of the reaction. To prevent competition with ring-opening metathesis polymerisation, ring-opening metathesis reaction must be followed by cross metathesis to avoid homodimerisation and start the growing polymerisation chain subsequently.[125] This is led by the fact that the acyclic metal carbene can, in principle, react with another acyclic metal carbene and lead to polymerisation. The challenge of designing a catalyst for a ROM reaction is related to precisely achieving the intended reaction pathway to avoid the increase in ROMP reactivity.

1.6. Ring-opening metathesis polymerisation (ROMP)

Ring-opening metathesis polymerisation is a type of polymerisation that takes advantage of ring-strained cyclic olefins to yield unsaturated polymers.[26] Commonly employed ROMP monomers are norbornene,[129] norbornenes derivatives,[130] and cycloctene derivatives.[131] Norbornenes are bicyclic structures obtained by the Diels-Alder reaction of cyclopentadiene with various dienophiles,[132] the wide range of derivatives obtainable from this class of monomers gives access to a large pool of monomers. ROMP is not the only type of olefin metathesis polymerisation. Acyclic diene metathesis polymerisation represents another type of polymerisation based on metathesis.[133]

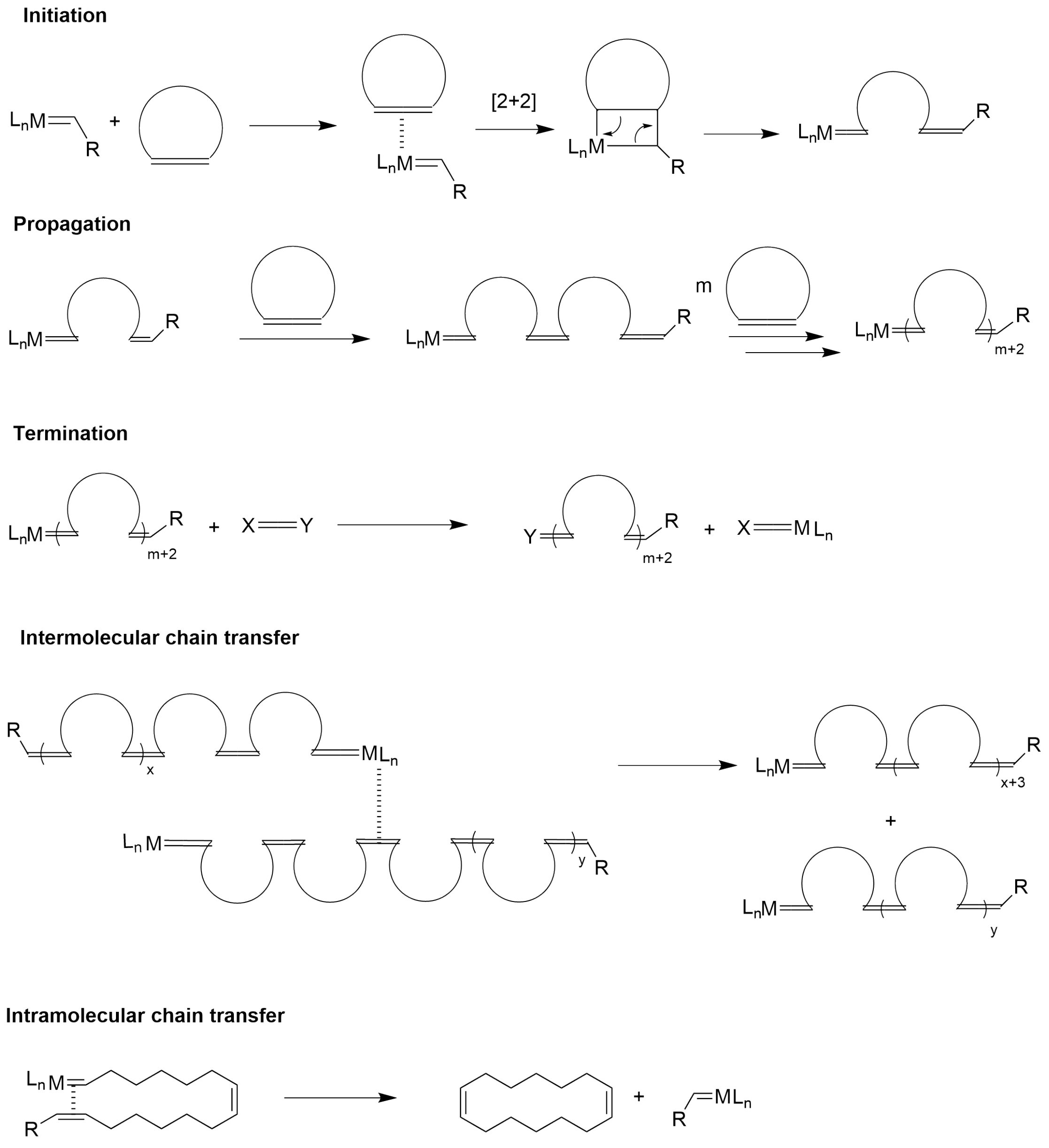
Initiation
L$_n$M
R
+
[2+2]
Propagation
m
m+2
Termination
X
Y
ML$_n$
Intermolecular chain transfer
x
x+3
y
Intramolecular chain transfer

Figure 1.12.: General mechanism of ring-opening metathesis polymerisation with chain transfer phenomena.

Even if ADMET and ROMP both belong to the metathesis family, their polymerisation mechanism is different. Ring-opening metathesis polymerisation is a chain-growth polymerisation,[134] instead, ADMET is a step-growth type polymerisation.[134] As in other chain-growth polymerisation types, the mechanism of ROMP can be divided into three different steps: Initiation, propagation and termination (Figure 1.12). In the first step, the metallorganic catalyst reacts with the monomer, generating a metallocyclobutane, *via*, [2+2] cycloaddition, similar to the mechanism of other metathesis processes. The metallocyclobutane generated then undergoes rearrangement to yield the propagating species. During this process, the cyclic strain of the olefine is released. This shifts the equilibrium of the reaction, making it irreversible with few exceptions.[11] The mechanism proceeds with the propagation step, here the propagating species, which consist of the catalyst bound to the generated linear olefin, reacts with another molecule of monomer, performing an insertion metathesis and leading to a dimer and so on. The propagation takes place until there is no further available monomer, a termination agent is added, or the catalyst is deactivated by air and/or moisture.[135] The last step of the polymerisation process is the termination. ROMP can be a living-type polymerisation,[27] termination processes are virtually nonexistent if the reaction is performed with the necessary care, which means that the polymer chain will grow until monomer units are available. To trigger termination, a quenching agent must be added to the reaction. This agent should be designed to perform irreversible metathesis with the metathesis catalyst, bonded to the propagating species, and avoid, by this means, further monomer insertion. One of the most used quenching agents is Ethyl vinyl ether (EVE).[136] Another alternative can be represented by the use of aldehydes as quenching agents.[137] Quenching agents must be added in large excess to have the certainty to terminate all growing chains. Taking into consideration a green chemistry approach, the termination with quenching agents is not optimal for the overall E-factor of the process, which lead in the last years to the development of new quenching techniques such as catalyst oxidation with basic hydrogen peroxide.[11]

Ring-opening metathesis polymerisation is also accompanied by chain transfer.[138] Both inter- and intramolecular chain-transfer could be present in the polymerisation reaction, leading to the increase of the dispersity (Đ) of the obtained polymer (Scheme 12). The possible living character of this metathesis polymerisation,[27], its high tolerance towards functional groups[33] and the high degree of control[28] allow to generate tailored polymer or copolymer with tunable properties and morphologies.[139–141] ROMP is often employed as a tool for grafting techniques, such as grafting-from,[142] grafting-to,[143] or grafting-trough,[136] leading to the generation of copolymers with a complex structure such as bottlebrush or star-shaped.[144]

1.6.1. Catalysis in ROMP

Ring-opening metathesis polymerisation requires an organometallic catalyst to be performed. The initial catalysts used for this polymerisation were based tungsten,[145] molybdenum[146] or rhenium[147] grafted on silica support or combined with Lewis's acids.[148] These heterogenous catalysis system resulted in very little control over the polymerisation. Lewis-acid-free catalysts were thus developed, allowing them to achieve higher activity and functional group tolerance. The next major advance of the field was delivered by Schrock, with molybdenum-based alkylidenes catalysts.[149] This class of catalyst bears structural similarity to the Tungesten-based alkylidene. However, Mo-based catalysts come with advantages such as allowing milder reaction conditions, allowing the study of the reaction mechanism and the ability to yield stereoregular polymers.[149] These catalysts were extremely sensitive towards air and water, so a need for easier-to-handle catalysts was apparent. Ruthenium has a lower oxophilicity, making it more stable towards many polar functional groups, but still forms carbon bonds with relative ease. Activated ruthenium chloride salts were found to catalyse the polymerisation of norbornene derivatives.[150] Even if examples of complexes of $RuCl_3$ with cyclooctadiene were reported to yield ROMP polymers,[151] the first well-defined, single-component Ru-catalyst was developed in 1992.[152] Grubbs catalysts represent the most used and important class of ROMP catalysts. The first generation of Grubbs catalyst is a ruthenium-based catalyst that uses tri-cyclohexyl phosphine as a ligand, this catalyst is moisture and air-sensitive, but it is widely tolerant toward different types of monomers and functional groups.[153] The second generation replaces one of the phosphine ligands with an N-heterocyclic carbene, leading to an increase in the catalyst's activity. Also, the bench stability of this catalyst is improved, however, the slow initiation rate leads to poor polymerisation ability.[154, 155] The third generation of the Grubbs catalyst exchange the remaining phosphine ligand for a pyridine one. This led to a great increase in the ROMP initiation rate,[156] allowing this generation to become one of the most used ROMP catalysts. Two modifications of the Grubbs second-generation catalyst were proposed by Amir Hoveyda. The phosphine ligand is exchanged with the chelating ortho-isopropoxy group, attached directly to the benzylidene unit. Two generations of the Hoveyda-Grubbs catalyst were reported. This catalyst class, even if slow in initiation,[157] is more air resistant than other Grubbs catalysts and, in some cases, can also be recycled[158] once the polymerisation reaction reaches completion (Figure 1.13).

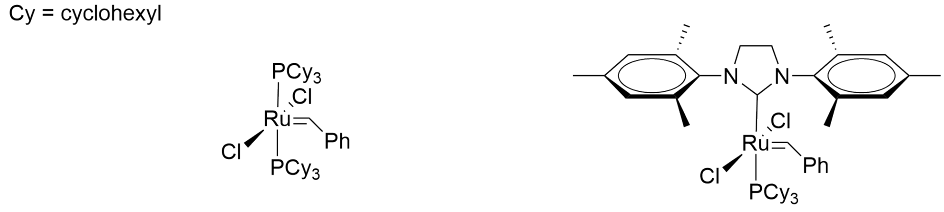
Cy = cyclohexyl
PCy3
Cl
Ru
Ph
Cl
PCy3
N
N
Cl
Ru
Ph
Cl
PCy3

Grubbs 1st generation (**GI**)

Grubbs 2nd generation (**GII**)

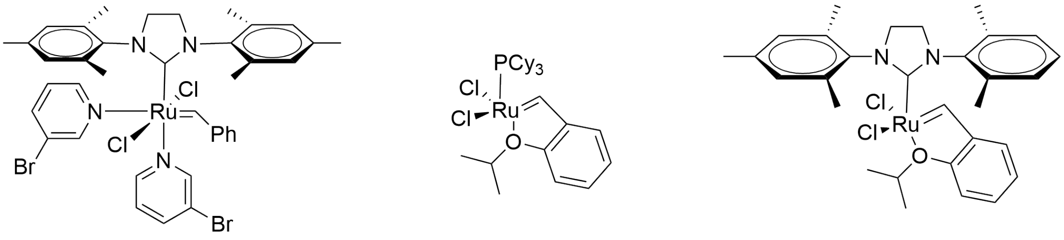
N
N
Cl
N
Ru
Ph
Cl
Br
N
Br
PCy3
Cl
Cl
Ru
O
N
N
Cl
Cl
Ru
O

Grubbs 3rd generation (**GIII**)

Hoveyda–Grubbs
first generation catalyst (**GH1**)

Hoveyda–Grubbs
second generation catalyst (**GH2**)

Figure 1.13.: Principal Grubbs catalysts classes.

1.7. Electrophilic substitution

Electrophilic substitution is a reaction class where an electrophile exchanges place with a functional group of the substrate.[159] This organic reaction can be implemented with both aromatic[160] and aliphatic moieties.[161] In the aromatic electrophilic substitution, the mechanism starts with the attack of the electrophile on the aromatic substrate. The positively charged carbocation formed, which is stabilised by resonance, will expel a proton situated in the same carbon as where the electrophilic attack happened. This will allow for reinstalling the neutrality and aromaticity of the molecule (Figure 1.14). Electrophilic aromatic substitution is widely used to obtain substituted benzene and furan derivatives.[160, 162, 163]

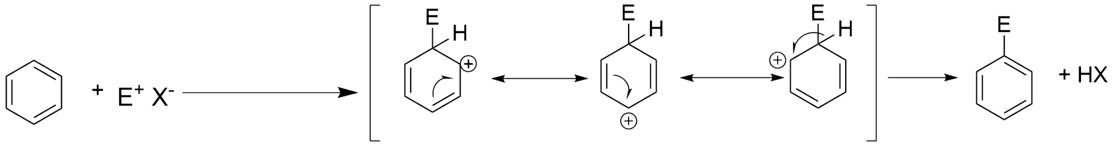

Figure 1.14.: General mechanism of electrophilic aromatic substitution with a general electrophile (E).

The ability of heteroatoms to stabilise positive charges in the carbocation intermediate allows heterocycles to possess higher reactivity than benzene in electrophilic aromatic substitution. However, heterocycles present different reactivity. When furan, thiophene and pyrrole are compared, pyrrole exhibits the highest reactivity, followed by furan and, lastly, thiophene (Figure 1.15). Nitrogen is less electronegative than oxygen, which results in a better ability to delocalise the positive charge of the carbocation, leading to higher reactivity of pyrrole over furan. Even if sulfur is less electronegative than oxygen, its $3p$ orbital overlaps less efficiently with the $2p$ orbitals of the aromatic π-system, explaining the lower reactivity of thiophene. When an electrophilic aromatic substitution occurs on an already substituted aromatic moiety, the substituent will determine the position of the electrophile attack. Electron donating group (EDG), such as amino group, will orient the electrophilic attack in *ortho* or *para*. Electron withdrawing groups, such as acid groups, will instead promote substitution in *meta* position.

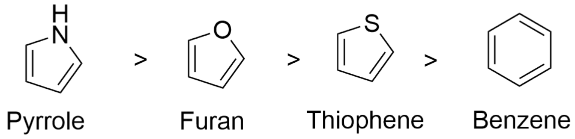

Figure 1.15.: Compared reactivity of different heterocycles and benzene.

2. The use of dihydrofuran and its analogues in ring-opening metathesis polymerisation

Part of the data in the screenings of diallyl ether RCM reported were obtained by Julia Weyandt, a bachelor student under the co-supervision of Federico Ferrari. These data are specifically indicated in the table notes. The ring strain calculations were performed by Prof. Dr. Kilbinger.

2.1. Introduction

Degradable polymers are macromolecules that can be broken down into their constituent unit or smaller by-products under specific conditions.[1] If the decomposition is performed by bacteria, the material is defined as biodegradable.[164] The decomposition can also be triggered by adding chemicals, such as acids,[165] or by temperature changes.[166] Since polymeric materials largely contribute to environmental pollution,[167] degradable polymers are not just desirable but necessary.

Degradable polymers can be synthesised following various synthetic pathways based on the type of monomer, renewable or not. In fact, renewable monomers can be polymerised *via* microbiological fermentation, leading to biodegradable polymers such as poly(hydroxy alkanoates).[18] Chemical reactions can also lead to degradable materials using renewable monomers. Poly(lactic acid) is a typical example obtained by ring-opening polymerisation (ROP).[168] However, monomers for degradable polymers can also be obtained from petrochemical resources, such as poly(caprolactone),[169] or poly(vinyl alcohol).[170]

Some degradable polymers possess limitations, such as poor mechanical properties,[171] limited control over the polymerisation,[172] or incomplete decomposition.[173] The use of controlled polymerisation techniques, such as ring-opening metathesis polymerisation (ROMP),[27] or the preparation of copolymers is herein proposed to overcome this limitation. The use of a controlled polymerisation technique allows for tailoring the molecular weight and the structure of the obtained polymer or copolymer, leading to control over the degradation and the mechanical properties.[172] Degradable polymers can be synthesised *via* olefin metathesis in a controlled way using techniques such as acyclic diene metathesis (ADMET),[174] or ring-opening metathesis polymerisation (ROMP). Degradable polymers obtained by ROMP are rare.[11] A recent example is poly(dihydrofuran)((poly(DHF)).[11]

The synthesis of poly(DHF) was first reported by Xia *et al.*[11] and it represents the first example of an enol ether polymerisable *via* ROMP. In his work, Xia reported the structure of the polymer, its thermal properties, and its degradability under acid conditions or exposure to heating, showing the versatility of this monomer and its easy recyclability. Several ways to synthesise 2,3-DHF and derivatives are reported in the literature, such as cyclisation of alkynyl alcohol,[2] oxaboration reactions or cycloaddition.[3] All these reaction pathways utilise harmful reagents and/or solvents, and overall their green metrics are rather poor. However, should the sustainability of the synthesis of 2,3-DHF be improved, its use as a monomer for ROMP will instigate the use of other heteroatom-containing five-membered rings, such as thiophene or pyrrole derivatives, as ROMP monomers.

Sulfur-containing polymers possess several interesting properties, such as high refractive index,[175] or high conductivity,[38] and they are employed in various applications, such as liquid crystals,[176] or conductive materials.[38]

In this chapter, pathways with improved green metrics towards the synthesis of poly(DHF) will be investigated. A copolymer of DHF will also be sought, aiming at improving the thermal properties. Finally, five-membered heterocycle synthesis pathways are designed, and their theoretical application in ROMP is investigated.

2.2. Synthesis pathways to poly(dihydrofuran)

The first part of the investigation started with alternative pathways to synthesising 2,3-dihydrofuran. In the literature, the reported synthesis methods possess an elevated environmental factor. The environmental factor (E-factor) is one of the most used green metrics to compare chemical processes (as discussed in chapter 1.3.2).[77] To improve the green metrics for the entire polymerisation process, the synthesis of the monomer is therefore critical to improve. Starting from allyl alcohol, a substrate that is readily obtained in a sustainable manner, *via* formic-acid mediated conversion of glycerol,[177] a by-product of biodiesel production,[178] two different routes were considered (Figure 2.1).

The first employed converting the alcohol to *cis*-2-butene-1,4-diol *via* self-metathesis.[179] This molecule then undergoes a carbonate-mediated esterification,[180] a process that takes advantage of carbonate chemistry to yield an ether more sustainably compared to traditional etherification approaches,[180] such as the Williamson ether synthesis.[181] Once the butenediol is converted to its cyclic equivalent, an isomerisation process leads to the final product.

The second synthesis pathway postulated the use of diallyl ether as an intermediate and proceeded through ring-closing metathesis and a subsequent isomerisation. diallyl ether is obtained from allyl alcohol *via* palladium catalysed haloallylation.[182] Since both reactions of allyl alcohol to yield butenediol and diallyl ether were already reported in the literature,[179, 182] this work will focus on the sequential steps of ring-closing and isomerisation.

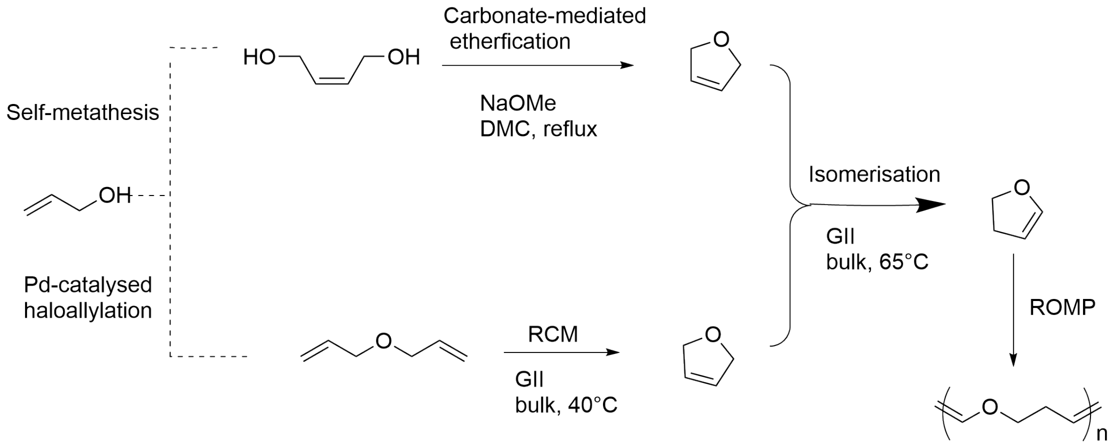
Self-metathesis
OH
Pd-catalysed haloallylation
HO
OH
Carbonate-mediated etherfication
NaOMe
DMC, reflux
O
RCM
GII
bulk, 40°C
Isomerisation
GII
bulk, 65°C
ROMP
n

Figure 2.1.: Two possible synthetic routes to obtain 2,3-DHF and its subsequent polymerisation.

2.2.1. Syntethic routes towards 2,5-Dihydrofuran

Once the synthesis pathways were chosen, the investigation started with the synthesis of 2,5-dihydrofuran. For the first approach, a method found in the literature was applied to synthesise this heterocycle.[180] This allowed to obtain 2,5-DHF with a yield of 91%.

After the first synthetic route to obtain 2,5-DHF was established, the second proposed pathway to produce 2,5-DHF, employing a ring-closing metathesis of diallyl ether, was subsequently investigated. In this pathway, the conditions for ring-closing metathesis (RCM) of diallyl ether to 2,5-dihydrofuran (Figure 2.2) were screened. Typical catalysts for RCM reactions are Grubbs-type catalysts.[183, 184] Thus, these catalysts were chosen for the screening. Grubbs catalyst can also be employed to catalyse other metathesis reactions, such as ring-opening metathesis polymerisation (ROMP) and isomerisation.[26, 185] The versatility of these catalysts could be exploited to catalyse all the reactions of this synthetic pathway, namely RCM, isomerisation and finally, ROMP, in one-pot, thus improving the green metrics of the process.

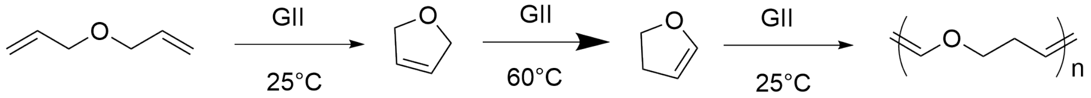

Figure 2.2.: Synthetic pathway from diallyl ether to poly(DHF).

Both GII and GHII were considered for the ring-closing metathesis of diallyl ether. The conditions screened were the solvent, the catalyst and the temperature. The catalyst loading chosen (0.01 eq) was kept constant during the screening. This loading is compatible with the loading found in the literature for ring-closing metathesis reactions.[186] The temperature range probed varied from room temperature to 65 °C. This temperature corresponds to the boiling point of the product. Two options were considered regarding the solvent for the reaction: dimethyl carbonate (DMC), a solvent with a high boiling point, relative non-toxic and with apolar character.[187] The absence of solvent was considered as an alternative. In Table 2.1, the results of the screening are shown.

Table 2.1.: Screening conditions for the ring-closing metathesis of diallyl ether for the formation of 2,5-DHF.

Catalyst	Catalyst loading (eq.)	Solvent	Temperature (℃)	Conversion (%) [1]
GII	0.01	DMC	25	0
GII	0.01	-	25	0
GHII[2]	0.01	-	25	91
GHII[2]	0.01	DMC	25	87
GII	0.01	DMC	40	92
GII	0.01	-	40	91
GHII[2]	0.01	DMC	40	91
GHII[2]	0.01	-	40	90

[1] determined *via* ^{1}H NMR spectroscopy
[2] entry obtained by Julia Weyandt

At room temperature, GII was not found active toward the ring-closing metathesis of diallyl ether, neither in DMC nor in the absence of solvent. In contrast, GHII showed a remarkable capacity for performing the ring-closing, with higher yields obtained in the absence of solvent (91%). Increasing the temperature to 40 °C, both catalysts exhibited similarly high activity with yields between 91-92%, regardless of solvent (or lack thereof). Higher temperatures were not screened since nearly complete conversion was reached already at 40 °C, while evaporation of the product practically-limited the applied temperature (literature reported boiling point 65 °C).

The results suggest that the Grubbs-Hoveyda II catalyst is more active towards the RCM of diallyl ether to 2,5-DHF, compared to GII, at room temperature. However, with the increase in temperature, a difference between the two catalysts is non-existent. The screening results also indicate that no solvent is needed to perform the RCM reaction and that a temperature of 40 °C is necessary to obtain a high yield. Interestingly, the use of Grubbs catalyst in ring-closing metathesis of diallyl ether, at a temperature higher than 25 °C promotes the isomerisation of 2,5-dihydrofuran to 2,3-dihydrofuran, the conversion of the two isomers and its consequences will be deeply discussed in chapter 2.2.3.

2.2.2. Environmental factors of the two synthetic pathways to obtain 2,5-DHF

As both synthetic pathways toward the formation of 2,3-DHF involve the synthesis of 2,5-DHF, their E-factor was calculated. For the carbonate-mediated etherification, 2.0 eq of sodium methoxide and 4.0 eq of DMC used as solvent are considered.[180] For the ring-closing metathesis, the conditions taken into consideration are the use of 0.01 eq of GHII in bulk at 25 ℃, and a follow-up purification *via* DMC-silica filtration to remove the catalyst residue. In table 2.2, the two E-factors calculated as per equations 5.2.2 and 5.2.1 are reported.

Table 2.2.: E-factors for the synthesis of 2,5-DHF in this chapter starting from *cis*-2-buten-1,4-diol or diallyl ether, including work-up.

starting material	**E-factor**
cis-2-buten-1,4-diol	8.08
diallyl ether	9.84
meso-Erythritol[188]	24.4

To compare the obtained E-factors, a literature-reported method for the synthesis of 2,5-DHF, starting from *meso*-erythritol, was included.[188] This reported synthetic pathway was chosen as a comparison, since it also employs a ruthenium-based catalyst for the synthesis. Its E-factor was calculated accordingly with the synthetic method reported in the manuscript (Equation 5.2.3).[188]

As possible to see from the Table 2.2, the conversion of *cis*-2,buten-1,4-diol to 2,5-DHF present a lower E-factor than the ring-closing metathesis of diallyl ether. Both of the proposed pathways for the formation of 2,5-DHF possess a lower E-factor compared to a literature-reported method for the synthesis of this enol ether.

2.2.3. Isomerisation from 2,5-DHF to 2,3-DHF

After the cyclic enol ether was obtained at a yield of 85%, screening of the isomerisation conditions was conducted. The investigation started with the selection of the catalyst. Several olefin isomerisation catalysts are reported in the literature, most of which are based on transition metals.[189] For this study, the second-generation Grubbs catalyst and the second-generation Grubbs-Hoveyda catalysts were selected as they are well reported to be isomerisation active.[190–192] Parsons *et al.* showed that Grubbs catalysts promoted isomerisation of heteroatom-containing olefins with yields up to 98%.[185] Crucially, Grubbs-type catalysts are well-reported to promote ROMP.[26] The possibility of combining the isomerisation and polymerisation processes in one pot would improve the green metrics and the simplicity of the synthetic pathway.

Another important parameter for the reaction is the temperature. Here, the temperature range probed varied from room temperature to 65 °C. This temperature corresponds to the boiling point of the starting material. Although isomerisation is favoured at higher temperatures,[193] a balance between the boiling point of the substrate and the reaction temperature must be found.

Two options were considered regarding the solvent for the reaction: dimethyl carbonate (DMC), a solvent with a high boiling point, relatively non-toxic and with apolar character.[187] The absence of solvent was considered as alternative. In Table 2.3, the reaction conditions tested for the isomerisation are shown.

Table 2.3.: Screening conditions for the isomerisation of 2,5-DHF to 2,3-DHF.

Catalyst	**Solvent**	**Temperature (℃)**	**Conversion (%)**[1]	**Polymerisation (%)**[1]
GII	DMC	25	0	-
GHII	DMC	25	0	-
GII	-	25	0	-
GHII[2]	-	25	5	-
GII	DMC	40	0	-
GHII[2]	DMC	40	25	-
GII	-	40	8	1
GHII[2]	-	40	31	3
GII	DMC	65	64	-
GHII[2]	DMC	65	72	-
GII	-	65	68	67
GHII[2]	-	65	72	51

[1] determined *via* ^{1}H NMR spectroscopy
[2] entry obtained by Julia Weyandt

The first isomerisation attempt employed the selected catalysts at room temperature using a catalyst loading comparable to the literature (0.01 eq).[194] This catalyst loading was kept constant during the screening to compare the results. However, neither catalyst resulted in the formation of the 2,3 isomer of DHF in DMC. Considering that the solvent might be interfering with the process, the reaction was repeated in the absence of solvent. However, no product was formed. Therefore, the reactions were repeated at a higher temperature (40 °C), albeit well below the boiling temperature of the reagents. At this temperature, some differences between the screened solvent and catalyst started to arise. GHII in DMC yielded 40% of 2,3-DHF. Instead, GII showed persistently no conversion. In the absence of solvent, however, both of the catalysts were able to promote isomerisation, with different conversions (8% for GII and 31% for GHII). The absence of solvent, however, was found to promote polymerisation as soon as the reaction was cooled down to room temperature. This was not deemed as a drawback as it is indicative that it is possible to obtain a one-pot system for isomerisation and ROMP. The yield for the obtained polymer at 40 °C, however, was poor with both catalysts, with GHII being slightly superior (Table 2.3). Further increasing the temperature to 65 °C was beneficial. In the presence of DMC, both catalysts showed comparably high yields in the formation of the 2,3 isomer (64% and 72% for GII and GHII, respectively). In bulk, a comparable scenario occurred, albeit, upon its cooling, the monomer was converted to a polymer, and the yield of the polymerisation was 67% with GII and 51% with GHII. This led to the conclusion that GHII allows higher isomerisation yield compared to GII with parity of solvent and temperature. However, taking into consideration the highly desired one-pot process, the use of GII resulted in a higher yield of the desired polymer and, consequentially, a lower E-factor. The E-factor of the entire process will be reported in the chapter 2.2.5. Temperature-wise better results are obtained with higher temperatures, and no solvent should be used to perform a one-pot isomerisation-polymerisation to obtain an overall better green metric.

2.2.4. Investigation of one pot isomerisation and polymerisation of 2,5-DHF

In order to verify the structure of the polymer obtained with the one-pot isomerisation and ROMP process above (using GII as catalyst, Table 2.3, entry 11), its ^{1}H NMR spectrum was compared to that of poly(DHF) synthesised using the method reported in the literature (Figure 2.3).[11] Indeed, the obtained spectrum exhibited all the characteristic peaks corresponding to the polymer of 2,3-DHF. However, residual 2,3-DHF as well as 2,5-DHF were observed, based on the signals at 6.18, 4.91, 4.08, and 3.86 ppm corresponding to 2,3-DHF. Signals detected at 5.89, and 4.65 ppm instead are attributed to 2,5-DHF. This finding indicates incomplete conversion of the substrate during the isomerisation step and ROMP, in accordance with the data obtained in the screening (Table 2.3).

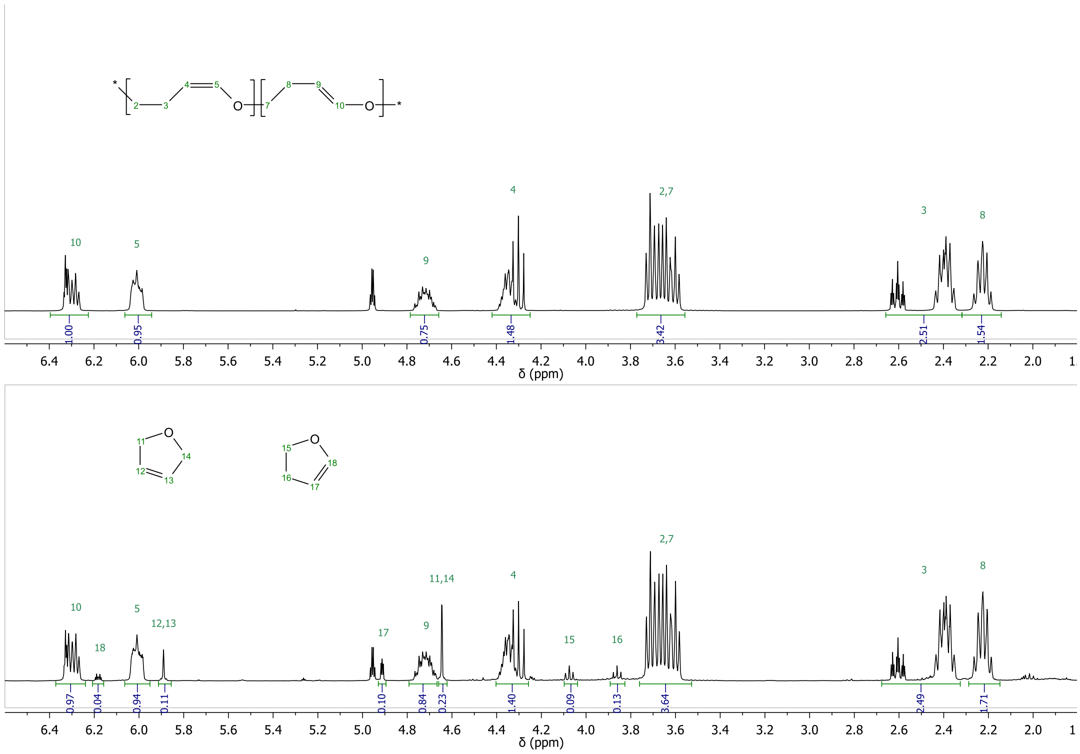

Figure 2.3.: ^{1}H NMR spectra of poly(DHF) obtained *via* ROMP of 2,3-DHF (upper spectrum) and poly(DHF) obtained *via* one-pot isomerisation-ROMP of 2,5-DHF (bottom spectrum).

Since 2,5-DHF is a cyclic olefin and, in theory, could take part in the ring-opening metathesis polymerisation of 2,3-DHF, its homopolymerisation was performed employing 0.01 eq of GII, following the literature-reported method for the polymerisation of 2,3-DHF.[11] This resulted in no observable polymerisation, both in the ^{1}H NMR spectrum (Figure 5.2) and SEC chromatogram obtained (Figure 5.3), leading to the conclusion that 2,5-DHF could not take part in the polymerisation of 2,3-DHF . It is therefore important to maximise the yield of the isomerisation to 2,3-DHF before the reaction is cooled and the polymerisation is initiated. Polymerisation of 2,3-DHF in fact is favoured at low temperatures since both entropy and enthalpy change (δS, δH) of the reaction are negative, as reported by Xia *et al.*[11]

To probe this, a partial kinetic curve of the isomerisation was obtained by initiating the isomerisation reaction at 65 °C in bulk, using GII. In Figure 2.4, the conversion versus reaction time is shown. By extrapolation and assuming the conversion continues to increase linearly, the complete conversion should be obtained after *circa* 48 hours. It is noted that the linear extrapolation does not consider the potential deactivation of the catalyst over time.[195]

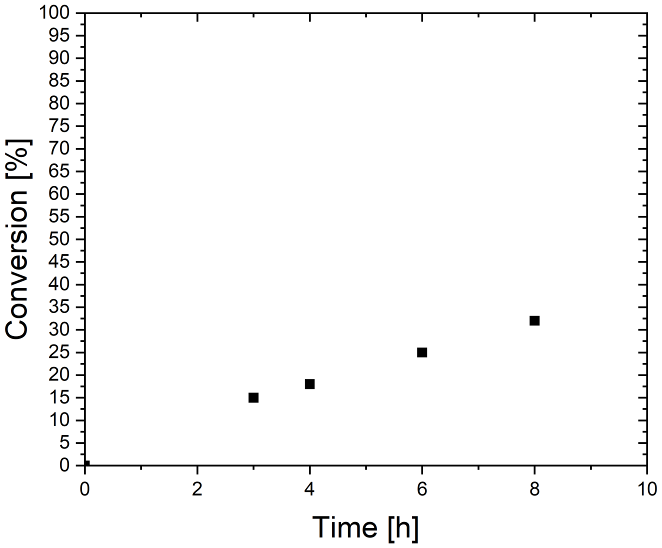

Figure 2.4.: Kinetic results from the isomerisation of 2,5-DHF into 2,3-DHF, recorded at 65 °C, in bulk and with GII (0.02 eq) as catalyst, determined *via* ^{1}H NMR.

2.2.5. E-Factors calculation for the synthesis process of poly(DHF)

In Table 2.4, E-factors for the synthesis of 2,3-DHF starting from either butenediol or diallyl ether are reported. These E-factors were calculated taking into consideration the best reaction conditions for each process (and therefore without the use of solvent), according to equations 5.2.5 and 5.2.6. The obtained E-factors are compared to the E-factor of a literature process to obtain 2,3-DHF by employing a ruthenium-based catalyst to perform an intramolecular ring-closing and isomerisation on a terminal alkynol (Figure 2.5).[2]

Table 2.4.: Calculation of the total E-factor for the synthesis of 2,3-DHF starting from *cis*-2,buten-1,4-diol, diallyl ether, or but-3-yn-1-ol.

Starting material	**E-factor**
cis-2,buten-1,4-diol	20.70
diallyl ether	13.98
but-3-yn-1-ol[2]	319.20

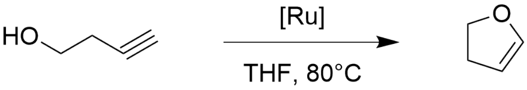

Figure 2.5.: Reaction scheme of synthesis of 2,3-DHF *via* alkynol cycloisomerisation.[2]

The E-factor was calculated based on the quantity of waste and product obtained in the synthetic method for 2,3-DHF reported in this publication,[2] according to equation 5.2.4. This method was chosen since it is another example of a ruthenium-catalysed process to obtain dihydrofuran. The obtained E-factors prove an improvement of the green metrics of the synthetic pathways proposed compared to a literature reported method to obtain 2,3-DHF. The synthetic pathways that use diallyl ether as intermediate posses the lower E-factor.

Since the synthetic pathway proposed in this work, based on the one-pot isomerisation and ROMP of 2,5-DHF, led directly to poly(DHF), to better compare the two synthetic pathways designed in this study and the alkynol cycloisomerisation process, the E-factor was recalculated, this time taking into consideration the entire synthetic process of poly(DHF) starting from *cis*-2-buten-1,4-diol, diallyl ether, or but-3-yn-1-ol (Table 2.5).

Table 2.5.: Calculation of the total E-factor for the synthesis of poly(DHF) starting from *cis*-2,buten-1,4-diol, diallyl ether, or but-3-yn-1-ol.

Starting material	**E-factor**
cis-2,buten-1,4-diol	85.0
diallyl ether	99.8
but-3-yn-1-ol[2]	521.7

For the polymerisation process, the synthetic pathway from *cis*-2-buten-1,4-diol led directly to poly(DHF), so no additional reaction and reagents were needed past the isomerisation process. However, the other two synthetic pathways (alkyne cyclisation and RCM of diallyl ether) led to the formation of the monomer 2,3-DHF. So to calculate the E-factor of the entire process, towards poly(DHF), the wastes and product generated during the polymerisation step were calculated in accordance with the synthetics method of poly(DHF) reported by Xia,[11] employing 2,3-DHF (as per equation 5.2.9 and 5.2.7). The lower E-factor is possessed by the formation of poly(DHF) starting from *cis*-2,buten-1,4-diol. The formation of poly(DHF) *via* diallyl ether instead is slightly less efficient. The E-factor of the alkynol cyclisation instead is significantly higher than both of the synthetic pathways designed in this study. This leads to the conclusion that both of the proposed paths represent a greener alternative to the reported method for the formation of poly(DHF).

2.3. Synthesis of copolymers containing 2,3-dihydrofuran

Once the alternative pathways to poly(DHF) were established and improvement of their green metrics compared to the literature shown, the focus was shifted to copolymerisation of 2,3-DHF. In the original work by Xia *et al.*[11] the use of a chain-transfer agent for the control of the polymerisation and the degradation of poly(DHF) was shown. Crucially, the polymerisation was carried out in the absence of solvent. However, some bio-based monomers are solid at room temperature, such as oxanorbornene derivatives,[196] or isosorbide,[197] the limitations of the polymerisation in solution must be understood. A solvent for the polymerisation would allow for obtaining a homogeneous solution of 2,3-DHF and the solid bio-based comonomer, which in turn allows better control over the polymerisation and faster reaction.[198] Since dichloromethane (DCM) is a widely used solvent for ROMP, it was chosen to test the homopolymerisation of 2,3-DHF.

Adapting the polymerisation previously employed, DCM was added as solvent, resulting in reactions at different concentrations, namely **PDHF0**, **PDHF14**, **PDHF7**, and **PDHF3**, with the different concentrations indicated in the number of the reaction. Typically, ROMP is performed in high dilutions, with the concentration of the monomer at *circa* 0.10 M,[199] however, since the ROMP of 2,3-DHF was well controlled in the absence of solvent, high dilutions were not deemed necessary. 2,3-Dihydrofuran was polymerised as above, using a catalyst-to-monomer ratio of 100:1, and the resulting polymers were characterised by size exclusion chromatography (SEC) (Figure 2.6).

In all cases, lowering the concentration of the polymerisation reaction led to a higher retention time of the polymer peak obtained. The comparison of the obtained chromatograms shows that the polymerisation of DHF using DCM as solvent definitely

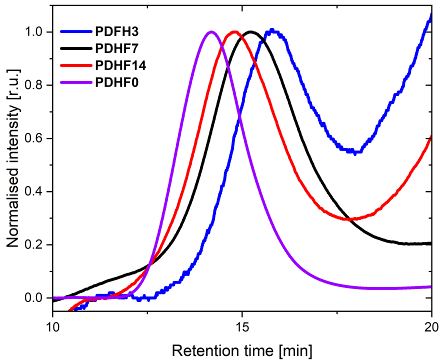

Reaction	**Concentration (M)**	M_n **(kg mol^{-1})**	**Đ**
PDHF0	-	101	1.77
PDHF14	14	71	1.38
PDHF7	7	7	2.23
PDHF3	3	3	1.20

Figure 2.6.: SEC from the polymerisation of 2,3-DHF using different dilution rates in DCM, all the reactions were carried out at 25 °C with 0.01 eq of GII catalyst.

impacts the obtained molecular weight, reducing the M_n of the obtained polymer when higher dilutions are applied. However, using a concentration of 14 M, despite a reduction in molecular weight compared to the bulk polymer, allowed obtaining a polymer closer to the result in the absence of solvent, probably the high concentration of monomer minimise chain-transfer processes involving the solvent. When the polymerisation is performed with a concentration of 7 M, the obtained molecular weight decreases drastically, leading to a polymer under 10 kg/mol. With the last concentration tested (3 M) the obtained polymer **PDHF3** exhibited a M_n of 3 kg/mol. The difference in dispersity (Đ) of the obtained polymers can be ascribed to the integration method.

The results of the dilution screening (Figure 2.6) indicate that even with a monomer concentration of 14 M, the resulting polymer possesses a lower molecular weight compared to the one obtained in bulk at parity of conditions, the presence of solvent, even in smaller quantities, allow chain-transfer processes that can lead to lower molecular weight obtained. Even if a reduction is present, this concentration leads to a polymer that is not deviating significantly from the expected molecular weight. The presence of low molecular weight shoulders in **PDHF3** and **PDHF7** suggests the presence of low molecular weight oligomers of DHF. As mentioned above, also chain-transfer processes might be favoured at a higher dilution. To investigate further the presence of chain-transfer, other solvents should be tested to understand how the nature of the solvent affects this polymerisation. Another way to avoid chain-transfer phenomena or solvent interference in the copolymerisation is the use of a liquid comonomer, this would allow to perform the polymerisation in bulk. The use of a suitable liquid comonomer for 2,5-DHF will be discussed in the next chapter (2.3.1).

2.3.1. Copolymerisation of 2,3-DHF with **N-HexNb**

According to the literature, poly(DHF) possesses a glass transition temperature (T_g) below room temperature, around −50 °C.[11] This gives the polymer a rubber-like appearance at room temperature. To create degradable polymers with tunable thermomechanical properties, copolymerisation with another monomer was necessary. Norbornene was deemed an excellent candidate to examine this as it is very reactive, and norbornene-derived polymers tend to have high T_g thanks to the rigidity of their structure. [200]

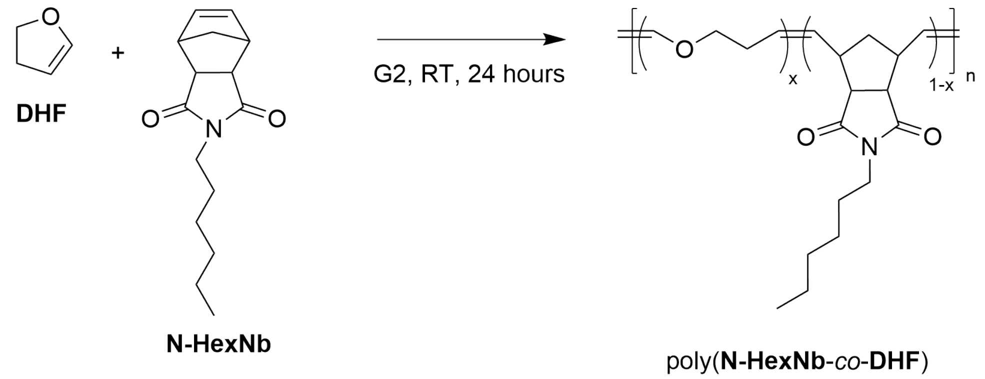

Figure 2.7.: Reaction scheme of the copolymerisation of DHF with a norbornene derivative.

[N]-hexyl-*exo*-norbornene-5,6-dicarboximide (**N-HexNb**, Figure 2.7) was chosen as a suitable co-monomer due to its liquid nature at room temperature, which allows it to be polymerised in bulk at room temperature. Even if this monomer is synthesised using a non-renewable chemical such as cyclopentadiene, it will be used to understand the possibility of copolymerisation of DHF with norbornene derivatives. In future studies, this norbornene will be replaced with more sustainable oxanorbornene derivatives.[201] To prepare the copolymer, the two monomers were mixed at a molar ratio of 1:10 (DHF:N-HexNb) at room temperature, and subsequently, GII (0.001 eq) was added to catalyse the process. The polymer obtained after 24 hours was analysed by SEC and found to possess a M_n of 483 kg/mol and a dispersity of 2.23 (Figure 2.8). The result was lower than the targeted molecular weight 1500 kg/mol. However, the obtained M_n could be underestimated due to the SEC column separation limit. As outlook for the next copolymerisation reaction, the catalyst loading should be increased to lower the obtained molecular weight.

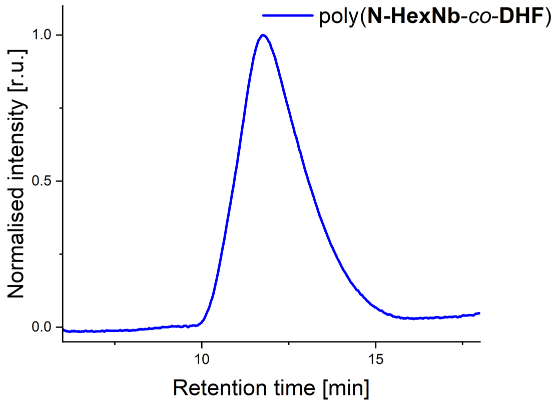

M_n (kg/mol)	**Đ**
483	2.23

Figure 2.8.: SEC chromatogram of the obtained copolymer poly(**N-HexNb**-*co*-**DHF**.).

A ^{1}H NMR spectrum of the obtained copolymer was recorded (Figure 2.9) showing an equimolar composition of the two monomers in the copolymer structure, interestingly. The difference in monomer ratio compared to the loading is ascribed to the lower reactivity of DHF.

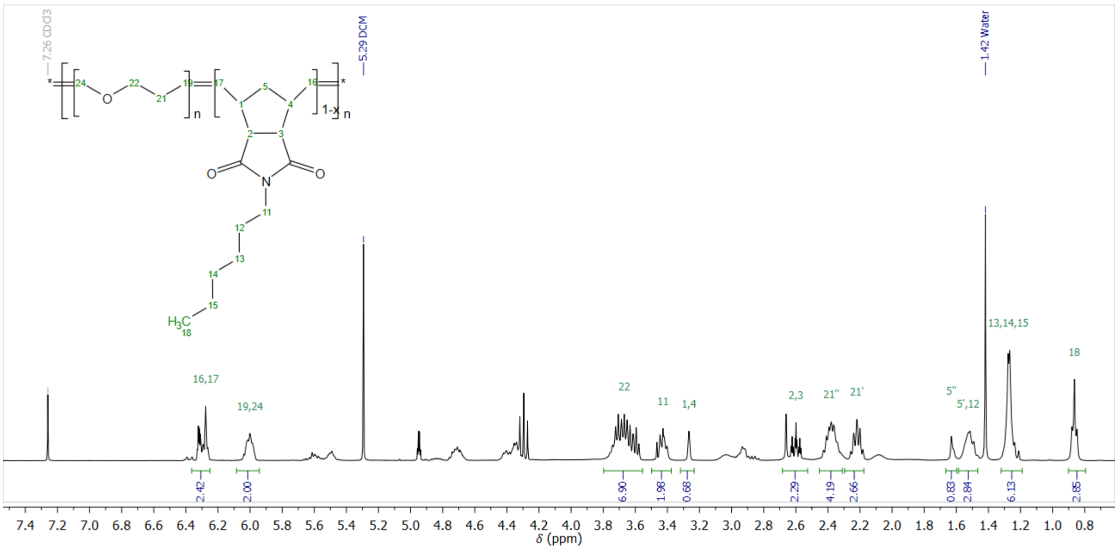

Figure 2.9.: ^{1}H NMR spectrum of poly(**N-HexNb**-*co*-**DHF**).

The obtained yield of the copolymer was 32%. The higher molecular weight obtained, the uniformity of the polymer distribution and the NMR spectrum indicate that the copolymerisation effort was successful and that DHF and norbornenes can be used as comonomers. The thermal properties of the polymer were subsequently investigated *via* DSC to determine the glass transition temperature (T_g) of the obtained copolymer and compare it with poly(DHF). Also, the number of thermal transitions detected is correlated with the morphology of the copolymer, helping to determine if the copolymer present a statistical or block nature

The polymer was found to exhibit a glass transition temperature at −23 °C, which is higher than that of the homopolymer of DHF (Figure 2.10). The presence of one

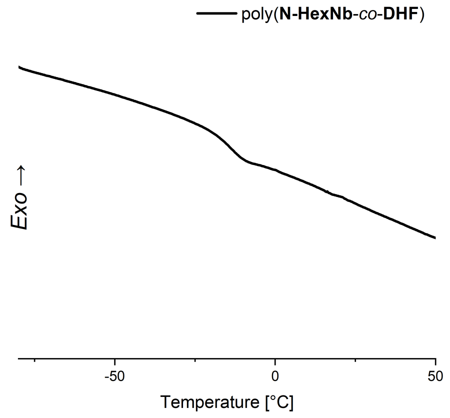

Polymer	T_{g} (°C)
poly(DHF)	-50[1]
p(**N-HexNb**-*co*-**DHF**)	-23

[1] Literature reported.[11]

Figure 2.10.: DSC curves of the copolymer synthesised and the analogue homopolymer of the composing monomers.

glass transition temperature seems to indicate that the copolymer obtained presents a statistical nature. The increase of T_g shows that norbornene structure can be exploited to tailor the thermal properties of DHF copolymers. Different copolymerisation ratios between the monomers will be tested in the future to understand how the ratio between the components influences the thermal properties.

The polymer obtained was found to possess high molecular weight and shows the possibility of co-polymerising DHF with other liquid monomers, such as norbornene derivatives. If the results of this study will be replicated with the use of oxanorbornene derivatives, this could lead to sustainable copolymers based on DHF. Furthermore, the increase of the glass transition temperature compared to poly(DHF) shows the incorporation of the **N-HexNb** monomer into the polymeric structure and supports the possibility of thus tuning the thermal properties of the copolymer by adjusting the composition.

2.4. Investigation of DHF analogues for ROMP

Unsurprisingly, 2,3-dihydrofuran was shown to be an effective monomer for ring-opening metathesis polymerisation. Poly(DHF) has been shown to be degradable *via* acid attack or using second generation Grubbs catalyst in the presence of heating.[11] The complete depolymerisation of the substrate leads back to the cyclic monomer that can be re-employed in a new polymerisation.[11] This was also qualitatively observed in the course of this work whereby exposing the synthesised poly(DHF) to GII or a chain-transfer agent such as cis-stilbene changed the appearance of the sample, from solid to liquid. In this work, other cyclic heteroatom analogues, such as dihydrothiophene and dihydropyrrole, were considered as interesting possible ROMP monomers that would result in degradable polymers (Figure 2.11), with interesting properties such as high conductivity[38] or high refractive index.[175]

A general synthesis pathway was followed to obtain the cyclic heteroatom monomers (Figure 2.11). This route is based on the synthetic strategy discussed in chapter 2.2.1. Starting from their corresponding commercially available diallyl ether equivalents, ring-closing metathesis and a subsequent isomerisation was performed to obtain the desired products. Grubbs-Hoveyda II was the only catalyst tested as it exhibits higher functional group tolerance and high activity in ring-closing metathesis.[202, 203]

In table 2.6, the results of the synthetic pathway for each heterocycle proposed are reported. To obtain the heterocycles, ring-closing metathesis with Grubbs-Hoyeveda II as a catalyst was employed. All the reactions used 0.01 eq of catalyst, and the reaction was carried out using different solvents such as DMC, DCM and the absence of solvent. The temperature used for the RCM reactions was 40 °C, and the conditions employed were chosen to compare the results to the RCM of diallyl ether, deeply investigated in

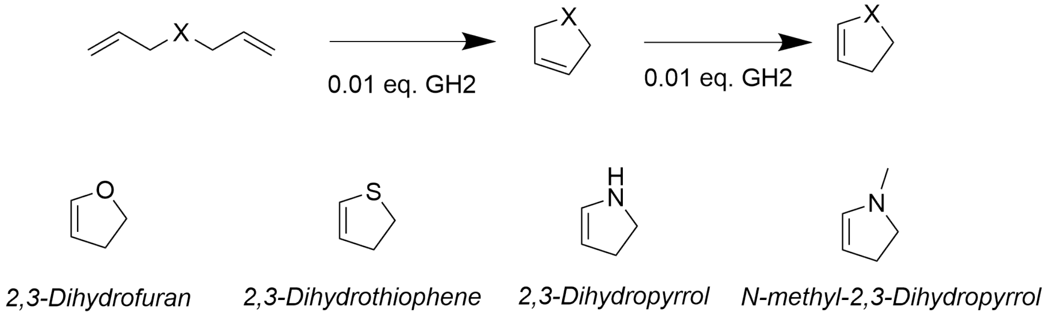

Figure 2.11.: Synthesis route to obtain heteroatom five member rings as ROMP monomers.

chapter 2.2.1. Both diallyl ether and diallyl sulfide were able to undergo ring-closing metathesis, with nearly complete conversion, in DMC and bulk (Table 2.6). However, the nitrogen derivatives chosen were not able to ring-close (Table 2.6). This was attributed to the interaction between the nitrogen and the metal centre of the catalyst.[204]

Table 2.6.: Conversion in % of various dienes in RCM using 0.01 eq of GHII, in various solvents, at 40 °C.

Substrate	**DCM**	**DMC**	**in bulk**	**Isomerisation yield(%)**
diallyl ether	94	92	99	31
diallyl sulfide	99	99	99	0
diallylamine	0	0	0	-
N-methyldiallylamine	0	0	0	-

Subsequently, the isomerisation of 2,5-dihydrothiophene to 2,3-dihydrothiophene was sought. The condition screened for the isomerisation of 2,3-DHF (chapter 2.2.3) were also applied for dihydrothiophene, GHII 0.01 eq as catalyst, DMC or absence of solvent and 65 °C. Unfortunately, the isomerisation of 2,5-dihydrothiophene to 2,3-dihydrothiophene was unsuccessful at the given reaction conditions (Table 2.6). The lack of isomerisation is probably due to the interaction of the thiophene derivative with the catalyst.[205] To prevent interaction, another metal-based catalyst should be tried, such as Palladium based ones.[189] To examine the further potential of the designed monomers in ROMP, a theoretical study on whether they possess sufficient ring strain to be implemented in ROMP was carried out. The calculations were performed using Gaussian 09's thermochemistry method: CBS-QB3.[206] 2,3-Dihydrothiophene was found to present lower ring strain compared to both the 2,3- and the 2,5-dihydrofuran isomers (Table 2.7). Even if ring strain is not the only factor determining whether a monomer is suitable for ROMP, the low ring strain from 2,3-dihydrothiophene led to the conclusion that dihydrothiophene is probably not a suitable monomer for ring-opening metathesis polymerisation. To obtain sulfur-containing polymers, other strategies need to be examined, such as norbornene-like sulfur-bearing structures (Chapter 3).

Table 2.7.: Calculated ring-strains for different five-member ring heterocycles.

Structure	**Name**	**Ring-strain (Kcal/mol)**[1]
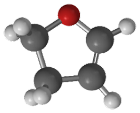	2,3-Dihydrofuran	7.64
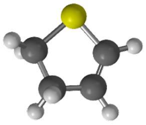	2,3-Dihydrothiophene	1.98
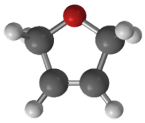	2,5-Dihydrofuran	4.24
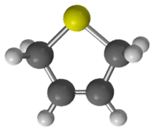	2,5-Dihydrothiopene	4.86

[1] Calculated using Gaussian 09's thermochemistry method: CBS-QB3.[206]

2.5. Conclusion

In this section, two novel pathways for the production of poly(DHF) were designed and investigated. Starting from linear substrates, their cyclisation and isomerisation into the monomer were investigated. Two synthetic pathways from the synthesis of 2,5-Dihydrofuran were proposed, starting from diallyl ether or butendiol. A screening to optimise the ring-closing metathesis of diallyl ether was performed, leading to the conclusion that the better way to achieve RCM on this substrate is to use Grubbs-Hoveyda II in bulk. The conditions for the isomerisation of 2,5-dihydrofuran to 2,3-dihydrofuran were also screened. Temperature, catalyst and solvent were all parameters examined. The use of Grubbs-Hoveyda second generation at 65 °Cin DMC led to the highest isomerisation yield. However, when no solvent is used, the possibility of subsequent polymerisation of the isomerisation product arises. This allows the one-pot isomerisation and ROMP of 2,5-DHF into poly(DHF). The obtained poly(DHF) was compared to poly(DHF) synthesised from 2,3-DHF to prove its structure. In the case of a one-pot reaction, the best conditions that need to be adopted are GII at 65°Cwithout solvent. Furthermore, the possibility of synthesising poly(DHF) in one pot, starting from 2,5-DHF, allows for improving the green metric of this synthetic pathway. Finally, a partial isomerisation kinetic, using GH2 and DMC at 65°C, was recorded, and *via* extrapolation the total time of the isomerisation determined. Environmental factors for different processes to synthesise poly(DHF) were calculated, comparing the proposed synthetic pathways with a literature-reported one. The obtained E-factors show an improvement in the sustainability of the proposed synthesis for poly(DHF) compared to the literature. The dilution limit in the homopolymerisation of dihydrofuran was also investigated, leading to understanding how the solvent chosen influences the polymerisation. Using a monomer concentration lower than 14 M dramatically affects the molecular weight of the polymer obtained. Once the limit is established, it could lead to interesting results in the copolymerisation application, allowing the pairing of DHF with other monomers that present a solid state at room temperature. A statistical copolymer of DHF was also synthesised and thermally characterised, revealing an increase in the transition glass temperature compared to poly(DHF). Lastly, Five-membered ring heterocycles as an equivalent of DHF in ROMP were studied, and the ring-closing and isomerisation cycle developed for DHF was applied to other heteroatoms containing dienes. The poor results obtained showed that diallyl sulfide could be ring-closed, but neither could this molecule be isomerised to the hypothesised monomer using Grubbs catalyst to promote isomerisation. However, ring-strain values for oxygen and sulfur-contain heterocycles were calculated, showing that dihydrothiophenes possess lower ring-strain than their oxygen counterparts.

3. Ring-Opening Metathesis Polymerisation of Thio-Norbornenes and their Sulfone-Derivatives

Monomer ***3a*** *and polymer p(****3a****) were synthesised by Kieron Laqua, a bachelor student under the co-supervision of Federico Ferrari and Dr. Roman Nickisch. The molecules prepared by the student are clearly indicated in the methods section (Chapter 5). The author conducted the planning of the synthetic pathway, the final evaluation of the results and the purification of the compounds aforementioned.*

3.1. Introduction

Thioketones and thioaldehydes are the sulfur equivalent of ketones and aldehydes. Among the various methods reported in the literature to prepare thioketones,[207] the most common is the use of Lawesson's reagent,[208] a thiation reagent possessing a four-membered, which dissociates to create a reactive dithiophosphine ylide that is the reactive species for the thiation.[209] Thioketones are known to exhibit a small gap between the lowest unoccupied molecular orbital (LUMO) and the highest occupied molecular orbital (HOMO).[210] Taking advantage of this low energy gap, these substrates are used in Diels-Alder reactions with various dienes, such as cyclopentadiene.[211] The Diels-Alder reaction is a type of cycloaddition reaction between a conjugated diene and an alkene (dienophile) to form unsaturated six-membered rings.[212–214] The use of cyclopentadiene as diene allows the formation of norbornene-like structures that contain a sulfur atom in the ring.

Norbornenes are bicyclic alkene structures,[215] capable of undergoing polymerisation, typically ring-opening metathesis polymerisation (ROMP),[129] while vinyl polymerisations are also reported.[216–219] While both types of polymerisation are frequently used for their high efficiencies and relative control,[69, 220] the mechanism employed and the resulting polymer structure, and thus the material properties, are largely different. In the vinyl-type polymerisation, the polynorbornene backbone is saturated with the bicyclic monomer structure kept intact. As a consequence, these polymers are characterised by high chemical resistance, optical transparency, and high dielectric constants.[221] On the other side, polynorbornenes obtained *via* ROMP retain double bonds in the backbone,[222] and they are typically obtained using transition metal complex catalysts, such as Grubbs catalysts.[223] Using this technique allows not only structural control over the polymer obtained, but also presents high tolerance towards several functional groups.[33] Polymers with targeted properties, e.g. thermal and optical,[200, 224] are readily synthesised and find use in various applications, e.g. for ions transport,[33] bioactive materials,[225] and metallopolymers.[226]

Sulfur-containing polymers, such as sulfur-based poly(amides),[227] poly(benzimidazoles),[228] poly(urethanes),[229] polyesters[230] have attracted a lot of interest in the literature,[231] as they exhibit interesting properties owed to the sulfur. For example, sulfur-containing polymers are reported to be optically active,[232] conductive,[38] liquid crystalline,[176] and thermally stable,[233] making them interesting for applications such as batteries [234] or displays.[37]

In this work, we present the synthesis of a range of sulfur-containing polymers from monomers obtained from the Diels-Alder reaction of various thioketones and thioaldehydes. The polymerisation is carried out using typical ROMP conditions and the materials obtained are characterised molecularly and thermally.

3.2. The synthesis of Thionorbornenes

Starting from commercially available ketones and aldehydes (**1a**, **1b**, **1c**, **1d**), their corresponding thioketones (**2a**, **2b**, **2c** and thioaldehyde **2d**) were synthesised using Lawesson's reagent under reflux in dry toluene (**Table 3.1**). These starting materials were chosen for their aromatic (**1a**, **1b**, **1d**) character, while the adamantanone moiety (**1c**) was chosen in order to obtain an aliphatic thioketone. In fact, aliphatic thioketones are known to be unstable,[235] especially if they are able to tautomerise, undergoing rapid oligomerisation or degradation in the presence of moisture.[236] However, bulky aliphatic groups, such as adamantanone, provide stability similar to that of aromatic moieties.[237]

Products **2a**, **2b**, and **2c** were obtained in high yields and purities. Unsurprisingly, **2d** was not isolated as its oligomeric form was instead obtained. The spectral data obtained match those in the literature,[238] while a ^{1}H NMR spectrum at 100 °C (Figure 5.15) indicates that the oligomeric adduct created tends to disassemble at higher temperature releasing the unimeric form of **2d**.

The thiocarbonyl compounds obtained **2a**, **2b**, **2c**, **2d** were subsequently reacted with an excess of freshly distilled cyclopentadiene in a thio-Diels-Alder (TDA) reaction at room temperature without the addition of a catalyst (Table 3.1) to obtain the corresponding thionorbornene (TNb). The successful synthesis of the corresponding thionorbornenes, namely 2,2-diphenyl-2-thio-norbornene (**3a**), xanthone-2-thionorbornene (**3b**), adamantane-2-thio-norbornene (**3c**), and 3-phenyl-2-thionorbornene (**3d**) was confirmed by spectroscopic means (Chapter 5, Figure 5.20 – 5.23). For TNb **3a**, the purity (determinated *via* ^{1}H NMR) was found persistently low (90%, Figure 5.17), despite extensive purification, as benzophenone was consistently present in the material and was attributed to the thiobenzophenone partly decomposing during workup. Xanthone-2-thio-norbornene **3b** was also found to decompose under moderate heat and reduced pressure (Figure 5.26). Nevertheless, as the target compound was formed, a one-pot approach of simultaneous thio-Diels-Alder reaction and subsequent ROMP was investigated. To achieve this, a modified TDA reaction protocol was employed in which a large excess of cyclopentadiene (50 eq.) was used in the absence of solvent. Subsequently, dichloromethane and the ruthenium catalyst were introduced in the reaction mixture to initiate polymerisation. Thionorbornene **3c** required a longer reaction time, 72 hours, to achieve an acceptable conversion (higher than 80%) in the TDA reaction. This is probably due to the bulky nature of the thiokethone (**2c**), leading to poor reactivity of the substrate towards the TDA reaction. However, the obtained thionorbornene **3c** was obtained in high purity and yield (Table 3.1). For the thionorbornene **3d**, toluene instead of dichloromethane was used as solvent and the reaction was conducted at 110 °C. This was deemed necessary to allow the formation of the free thioaldehyde species that acts as the dienophile in the Diels-Alder reaction from the oligomeric form of **2d**, as mentioned above. In all cases, the thionorbornenes were obtained in reasonable yields and purities (Table 3.1).

Table 3.1.: Overview on synthesised thiocarbonylcompunds and thereof derived thionorbornes.

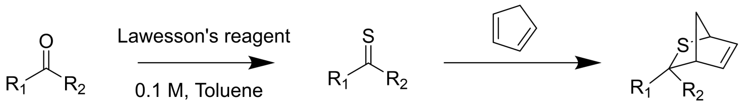

Ketone	Thioketone	Purity (%)[1]	Yield (%)	Thionorbornene	Purity (%)[1]	Yield (%)
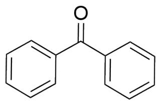 **1a**	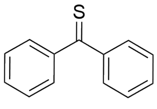 **2a**	91	87	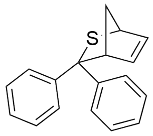 **3a**	90	80
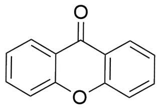 **1b**	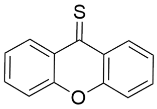 **2b**	99	91	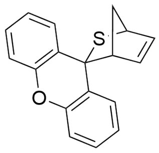 **3b**	-	50[2]
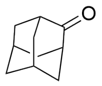 **1c**	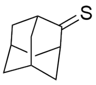 **2c**	99	86	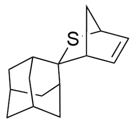 **3c**	99	80
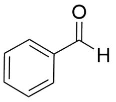 **1d**	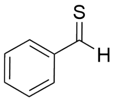 **2d**	99	80	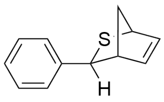 **3d**	99	72[3]

[1] determined *via* ^{1}H NMR spectroscopy

[2] conversion from the first step of the *in situ* Diels-Alder and subsequent ROMP

[3] combined yield of *endo* and *exo* product

In a subsequent step, TNb (**3a**) was oxidised to the sulfone derivative using *meta*-chloroperbenzoic acid (mCPBA) allowing the conversion of the thioether to the more polar sulfone group.[239]

3.2.1. Polymerisation of thionorbornenes

In order to identify the suitability of TNbs for ROMP reactions, the homopolymerisation of **3a** employing different ruthenium-based catalysts was investigated. In all cases, the reaction was carried out at room temperature for one hour using degassed dichloromethane as solvent. The targeted degree of polymerisation (DP) was 100 and the polymers obtained after quenching with ethyl vinyl ether were characterised by size exclusion chromatography (SEC) (Figure 3.1).

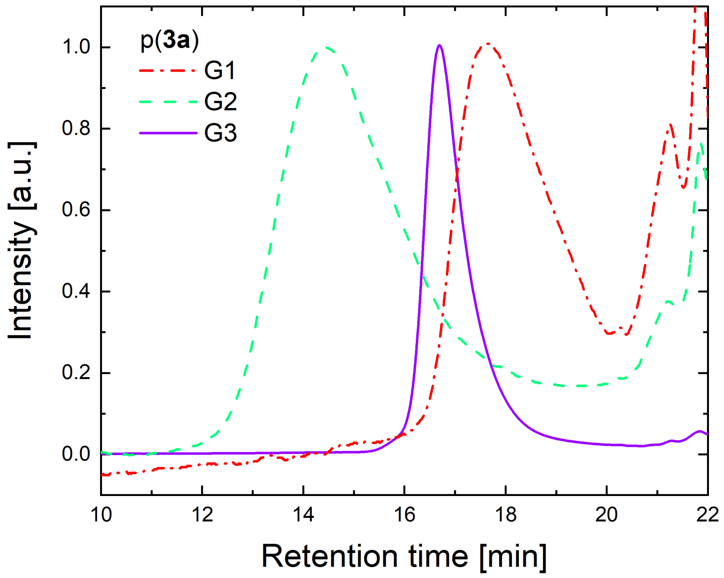

Figure 3.1.: SEC from the polymerisation of **3a** using different ruthenium-based catalysts.

First (G1), second (G2), and third generation (G3) Grubbs catalysts were used and in all cases a polymer was obtained with high molecular weight and reasonably low dispersities (Table 3.2). Broadening of the main polymer peak was observed when G1 was used and was attributed to the sulfur interfering with the ROMP by coordination with the ruthenium.[240] As G3 gave a uniform distribution, it was chosen for subsequent reactions in this study. It is noted that the monomer concentration in the reaction mixture was not found to hinder the polymerisation as introduction of 20–1,000 equivalents of **3a** (with respect to G3) yielded polymers with narrow molecular weight distributions and M_ns that matched the anticipated ones (Figure 5.31). This observation further confirmed the suitability of G3 to control the polymerisation.

Table 3.2.: Molecular weight and conversion of the polymers obtained from the ROMP of **3a** using different Grubbs catalysts.

Catalyst	**Conversion (%)**[1]	M_n **(kg mol^{-1})**	$Đ$
G1	96	7.1	1.38
G2	99	59	2.23
G3	>99	16	1.20

[1] determined *via* ^{1}H NMR spectroscopy

The obtained monomers **3a**, **3b**, **3c**, and **3d** were subsequently used in ROMP reactions catalysed by G3 to obtain the corresponding homopolymers p(**3a**), p(**3b**), p(**3c**), and p(**3d**) (Figure 3.2). In all cases a targeted DP of 100 was implemented and dichloromethane was used as solvent. The reaction time was one hour nearly complete conversion of the starting material was observed (>99%) (Table 3.3).

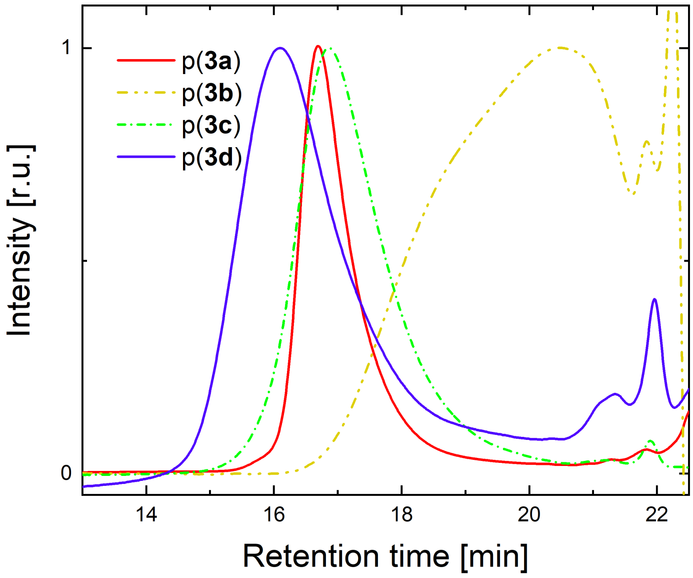

Figure 3.2.: SEC traces of the polymers obtained from the ROMP of **3a**, **3b**, **3c**, and **3d** using G3 as catalyst. and their molecular weight characteristics.

Although impurities were present in all monomers used, they were not found to hinder the polymerisation. Particularly concerning the polymerisation of **3a**, where substantial amounts of benzophenone were present as impurity from the monomer synthesis, a test ROMP reaction using norbornene as the monomer and benzophenone as an additive (10 mol%) was carried out, using the same conditions as above, to establish that these impurities do not affect the resulting polymer. Indeed, no hindrance in the ROMP was observed (Figure 5.44–5.45); therefore, the ROMP of thionorbornenes is well represented in the obtained data. In all cases, a uniform distribution was obtained in the corresponding SEC data (Figure 3.2, Table 3.3) with the M_n between 13–19 kg mol^{-1}, except for p(**3b**), for which a low molecular weight with a bimodal distribution was obtained (Figure 5.38). As previously mentioned, **3b** was generated *in situ*, and the polymerisation conducted in one pot, therefore the resulting polymer is a copolymer of the monomer and dicyclopentadiene present in the Diels-Alder reaction mixture (Figure 5.39). As such, the copolymer is likely branched and therefore the SEC data obtained reflect this architecture. Nonetheless, these results further support the versatility of thionorbornenes as ROMP monomers with the reactions proceeding in a rather controlled manner and resulting in well-defined homopolymers.

Table 3.3.: Characteristics molecular weight of the polymers obtained from the ROMP of **3a**, **3b**, **3c**.

Polymer	**Conversion (%)**[1]	M_n **(kg mol^{-1})**	**Đ**
p(**3a**)	99	16	1.20
p(**3b**)	99	2	3.43
p(**3b**)[2]	99	2.5	3.63
p(**3c**)	92	13	1.43
p(**3d**)	99	19	1.40
p(**4a**)i	95	9	1.40

[1] determined *via* ^{1}H NMR spectroscopy

[2] Data from SEC with resolution in the low M_n range

3.2.2. Preparation of sulfone-based polymers

Thioethers are known to readily oxidise to their corresponding sulfone.[241–243] Therefore, the oxidation of the thioether of the TNbs was sought to endow polymers with sulfone moieties. Two routes were thus investigated (Figure 3.3), namely the oxidation of the TNb monomer **3a** to obtain the sulfone monomer **4a** followed by the ROMP of the latter (route i), as well as the post-polymerisation oxidation of p(**3a**) (route ii).

For the first route, the chemoselective oxidation of **3a** was achieved using mCPBA at low temperatures yielding **4a** (Figure 5.27–5.30). As monomer **3a** was of rather low purity (90%), **4a** was also obtained in a similarly low purity. However, subsequent polymerisation with G3 resulted in polymer p**(4a)**i, with a M_n of 12 kg mol^{-1} and a $Đ$ of 1.50 (Figure 3.3), indicating the good polymerisability of the oxidised monomer. For the second route and the post-polymerisation modification of homopolymer p(**3a**), the same conditions applied for the synthesis of monomer **4a** were employed. This however did not yield complete oxidation, as determined by spectroscopic means (Figure 5.36–5.37), as sulfoxide species were also observed. While route ii was less successful towards the synthesis of a sulfoxide-containing polymer, the dispersity obtained was comparable to that of the parent polymer p(**3a**), and thus better defined than that of p(**4a**)i. It is noted that due to solubility issues, the sulfone-functional polymers were analysed on an SEC using dimethylacetamide (DMAc) as eluent and therefore the M_n values are not directly comparable to those of the sulfur-functional polymers.

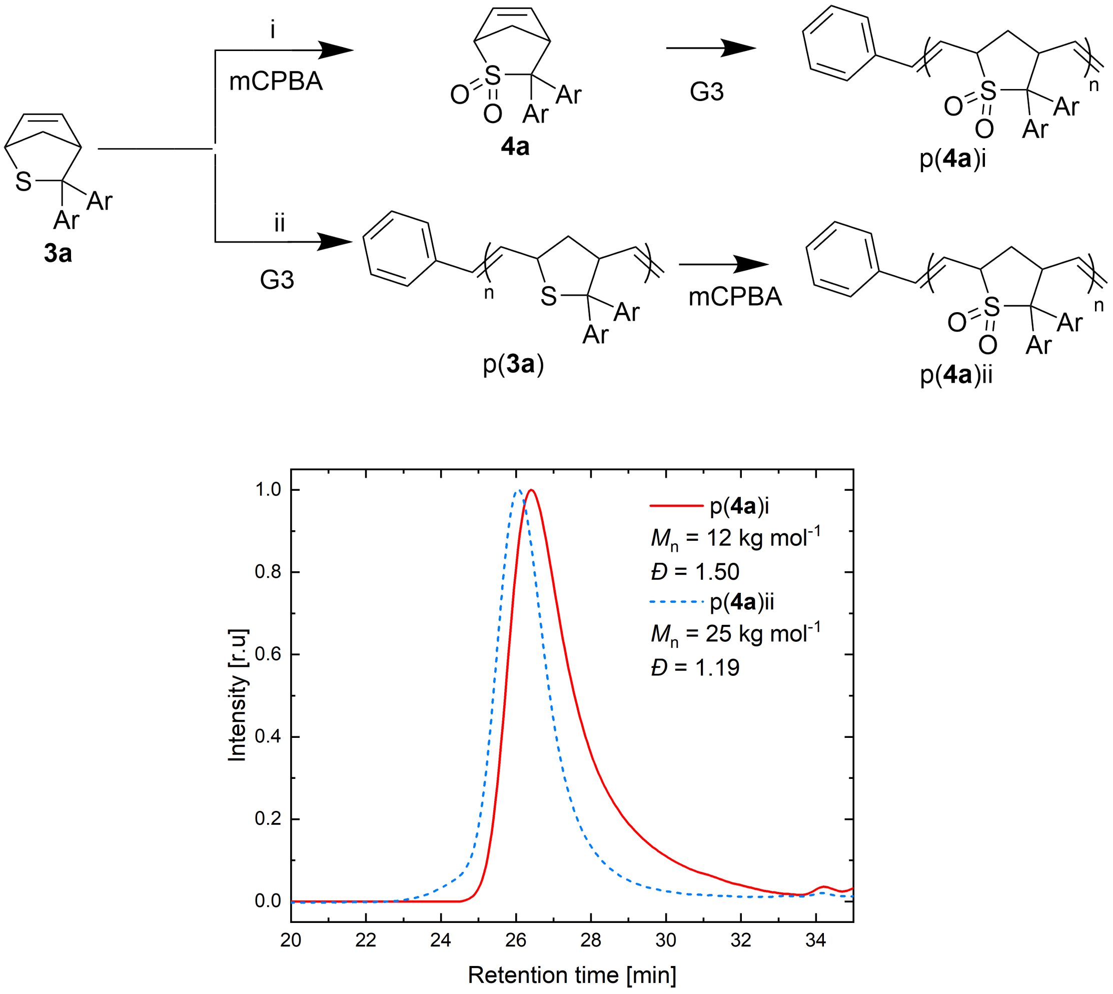

Figure 3.3.: Comparison of the two routes followed to obtain the polysulfone polymers p(**4a**)i and p(**4a**)ii and their corresponding SEC.

3.2.3. Copolymers of TNbs and sulfone-functional norbornenes

Given its good polymerisability, the sulfone-functional monomer (**4a**) was also employed in a direct copolymerisation with the parent TNb **3a** aiming to obtain a statistical copolymer p(**3a**-*co*-**4a**), while the corresponding block copolymer p(**3a**-*b*-**4a**) was also synthesised by sequential polymerisation of the two monomers. It is noted that the block copolymer required the ROMP to be carried out at -15 °C to prevent side reactions that would prevent further chain-extension (Figure 5.41).

In both cases, a uniform distribution was obtained by SEC (Figure 3.4), indicating good control of the ROMP. Crucially, the trace obtained from the chain extension of p(**3a**) with **4a** (namely the block copolymer p(**3a**-*b*-**4a**)) was shifted to lower retention times compared to the parent homopolymer p(**3a**), indicating the successful increase of the M_n of the polymer from 10 $\mathrm{kg\,mol^{-1}}$ to 19 $\mathrm{kg\,mol^{-1}}$, while the *Đ* remained virtually unchanged (from 1.22 to 1.23). The statistical copolymer p(**3a**-*co*-**4a**) yielded a broader trace with an M_n of 14 $\mathrm{kg\,mol^{-1}}$ and a *Đ* of 1.35.

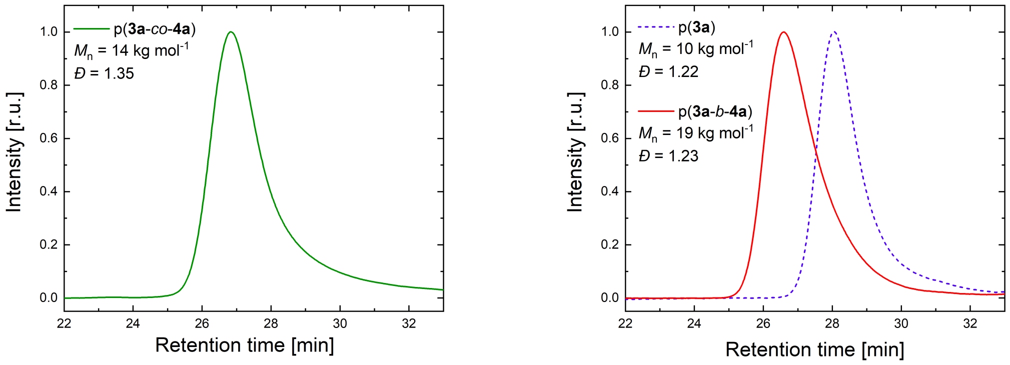

Figure 3.4.: SEC traces of p(**3a**-*co*-**4a** (left), and p(**3a**) and p(**3a**)-*b*-p(**4a**) (right).

Interestingly, we observed that p(**3a**), unlike p(**4a**), was soluble in THF and insoluble in HFIP (Table S5.6). Unsurprisingly, both the diblock and the statistical copolymers of the corresponding monomers were soluble in both solvents, pointing to the viability of these materials as compatibilisers.

3.2.4. Thermal properties of the polymers and their solubility

All homopolymers (p(**3a**), p(**3b**), p(**3c**), p(**3d**, p(**4a**)i) and the two copolymers (p(**3a**)-*b*-p(**4a**) and (p(**3a**)-*co*-p(**4a**)) were analysed using thermogravimetric analysis (TGA) and differential scanning calorimetry (DSC) to evaluate their decomposition (T_d) and glass transition (T_g) temperatures, respectively. In all cases, the polymers were found stable to temperatures up to 150 °C (Figure 3.5), except for p(**3b**) whose T_d was found at 112 °C. This observation is consistent with the lack of thermal stability observed for the corresponding monomer.

With the exception of p(**3b**), a weak thermal transition ascribed to a glass transition was observed for all homopolymers when examined by DSC (Figure 3.5). This was in the range of 130–160 ℃ for polymers p(**3a**), p(**3d**), and p(**4a**)i, while for p(**3c**) it was at *ca.* 65 ℃.

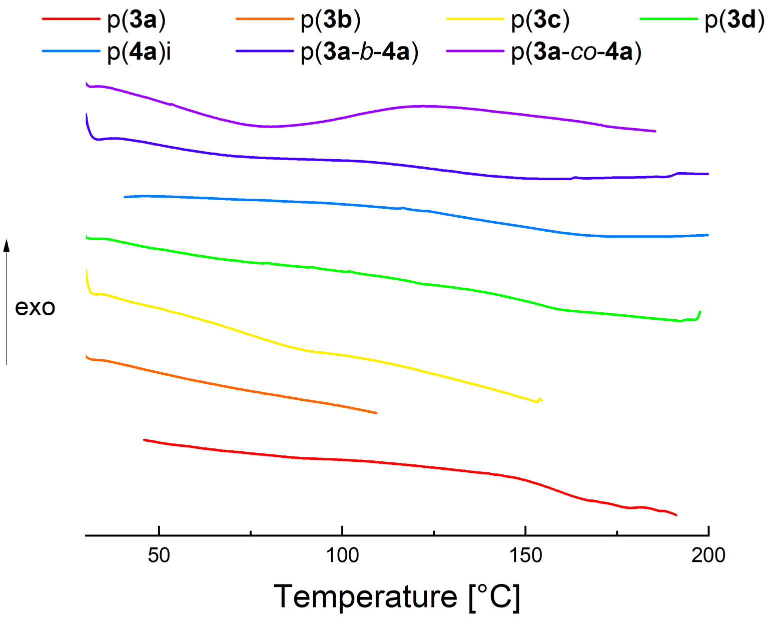

Figure 3.5.: DSC curves of the polymers synthesised in this study.

Interestingly, the T_g of p(**3c**) (Table 3.4), which bears an aliphatic side group in the repeat unit, was significantly lower than those of p(**3a**) and p(**3d**), which bear aromatic side groups. Therefore, it will be interesting in the future to investigate the thermal properties of more sulfur-containing polynorbornenes and correlate these to the structure of their repeat units.

Table 3.4.: T_g and T_d of thionorbonene derived polymers obtained.

Polymer	T_g (°C)	T_d (°C)
p(**3a**)	160	192
p(**3b**)	n.d.	110
p(**3c**)	65	155
p(**3d**)	150	237
p(**4a**)i	140[1]	226
p(**3a**-*b*-**4a**)	55, 130	241
p(**3a**-*co*-**4a**)	n.d.	187

[1] determined during the second heating cycle

Two transitions were observed for the block copolymer p(**3a**-*b*-**4a**) at 55 and 130 °C (Table 3.4), which, surprisingly, are lower than the thermal transitions of the corresponding homopolymers (p(**3a**) and p(**4a**)i). It is hypothesised that the first thermal transition is an artefact owed to the first heating cycle of the measurement being used for the evaluation of the data (a consequence of the low T_d of the polymers). Finally, the curve obtained from the statistical copolymer p(**3a**-*co*-**4a**) seemingly indicates two transitions at *ca.* 50 and 160 °C (Table 3.4), although the considerable baseline drift and the overlap of the second transition with the T_d render this observation inconclusive. Further analysis of the thermomechanical properties of these copolymers as well as their corresponding homopolymers is needed.

3.3. Conclusion

In this chapter, four thionorbornenes were synthesised and their polymerisability by ring-opening metathesis polymerisation was investigated. Utilising G3 as catalyst yielded homopolymers with well-defined molecular weights and low dispersities. Furthermore, a sulfone-functional norbornene was prepared by oxidation and its polymerisation was successfully shown. A sulfone-functional polymer was also obtained by post-polymerisation oxidation of a polythionorbornene, albeit the reaction was incomplete. The high control of the ROMP of the herein prepared monomers was further demonstrated by chain-extension of a polythionorbornene with the sulfone-functional norbornene. The resulting block copolymer exhibited properties similar to the corresponding homopolymers. The thermal properties of the herein synthesised polymers were investigated finding a correlation between the structure of the repeat units.

4. Zinc and Ruthenium Mediated Polymerisation of Levoglucosenone Derivatives

LGO derivatives ***5****,* ***6****,* ***7****, polymeric material p(****5****), and parts of the screening data were obtained by Luca Heusser, a bachelor student under the co-supervision of Federico Ferrari. The molecules prepared by the student are clearly indicated in the methods section (Chapter 5), the screening data obtained instead are indicated in the footnotes. The author conducted the planning of the synthetic pathways and the final evaluation of the results.*

4.1. Introduction

Bio-based polymers and bio-derived polymers represent an important class of materials.[244] Such polymers are, for instance, derived from natural substrates such as cellulose,[20] lactic acid,[245] succinic acid,[246] hydroxy alkanoates,[247] or furan dicarboxylate.[248] While a lot of research is invested in determining the effect of structural characteristics of polymers on their macroscopic properties, research is still mainly concerned with fossil fuel–derived polymers.[249]Such polymers have proliferated in domestic and industrial products,[250, 251] however, they are rarely biodegradable and often not recyclable, which is a significant ecological burden, since they tend to accumulate in the environment.[252] Moreover, since crude oil is a finite resource, the need to exploit renewable starting materials in order to sustain the long-term production of polymer-based materials is critical.[253]

Levoglucosenone (LGO) is obtained from the catalytic pyrolysis of cellulose.[254] It is also an intermediate in the production of cyrene, a "green" solvent showing promise in the field of polymer chemistry.[255] In recent years, LGO has been widely used to prepare renewably resourced polymers, mainly by employing it in a series of Diels-Alder reactions.[256, 257] LGO is also used as an electrophile in electrophilic substitution reactions using substrates such as furan.[258] Such reactions involve the substitution of an electrophilic group inside a compound and typically involve moieties such as benzene and furan.[163, 259, 260] LGO was first used as an electrophile by Shafizadeh *et al.*,[261] who also highlighted that the reactivity of LGO varies when a dienophile is employed: in the presence of cyclopentadiene, the corresponding Diels-Alder product is formed, whereas in the presence of furan, an electrophilic substitution takes place. While furan is often used in Diels-Alder reactions,[262–264] the presence of oxygen in the heterocycle renders it electron deficient, making it less efficient in such reactions compared, for instance, to cyclopentadiene.[265]

In 2020, Gardiner *et al.*, [266] published the ring-opening metathesis polymerisation (ROMP) of a norbornene-like structure derived from levoglucosenone. The polymers obtained in this study were shown to exhibit high thermal stability, up to 140 °C, and chirotopical properties that varied between the polymer and monomer state. LGO has been used in other ROMP processes to obtain olefinic (co)polymers.[19, 267, 268] This type of polymerisation is used for its high efficiencies and relative control. [220]Polymers obtained *via* ROMP retain double bonds in the backbone,[222] and they are typically obtained using transition metals complex catalyst such as Grubbs Catalyst. [223]

Another key compound readily obtained from cellulose is furan,[269] while some substituted alkyl derivatives are also obtained from biomass, making them excellent substrates for sustainable polymer synthesis.[270, 271] Furan is often used in electrophilic substitution reactions such as the Friedel-Craft acylation, [272] nitration,[273] or bromination.[274] In fact, furan exhibits higher reactivity in electrophilic aromatic substitution than benzene.[275] Furan derivatives are also broadly used in polymer synthesis.[276–278] As comonomer or functional group, furan allows tailoring the properties of the polymeric materials e.g. by increasing the toughness,[279] or improving the fire retarding properties.[280]

In this work, we report the synthesis of polymeric materials obtained by exposing LGO derivatives to typical polymerisation catalysts, the role of LGO therein was investigated together with the thermal properties of the obtained materials.

4.2. Monomer synthesis

To prepare LGO derivatives, furan was chosen as a renewable aromatic structure for a electrophilic substitution. However, in order to overcome its poor reactivity and improve the reaction yield, a catalyst screening was first performed (Figure 4.1).

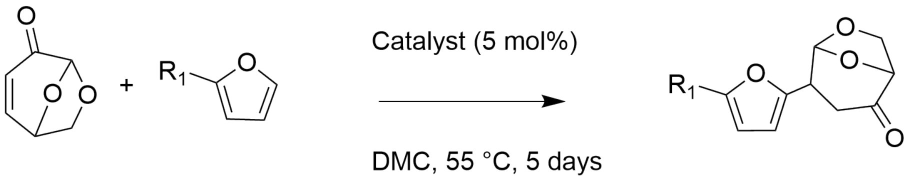

5: R_1= -H
6: R_1 = -Me
7: R_1 = -Et

Figure 4.1.: Reaction scheme of the catalytic electrophilic substitution between LGO and furan derivatives.

For this study, typical Lewis acids were screened to promote the electrophilic aromatic substitution between furan and LGO, as they are well known to catalyse such reactions [281–283]. The catalyst loading was selected to be 0.05 eq for all the experiments, as it is widely used in the literature to assess the positive contribution of a catalyst. All catalysts were tested using 24 hours of reaction time and room temperature to easily compare their effectiveness.

Table 4.1.: Electrophilic substitution catalyst screening using LGO and furan as substrates.[1]

Catalyst[2]	**Conversion (%)**[3,4]
$AlCl_3$	0
$TiCl_4$	3
$Yb(FOD)_3$	0
ZnI_2	11
$ZnCl_2$	15
$HfCl_4$	10

[1] in all cases, the solvent was DCM-d2 and the reaction was carried out at 25 °C for 24 hours. The concentration of LGO was 2.5 M, [2]0.05 eq compared to LGO, [3]determined *via* ^1H NMR spectroscopy,[4] All the conversion data in this table were obtained by Luca Heusser.

The results summarised in Table 4.1 indicate that zinc (II) chloride was the highest yielding catalyst for this particular reaction. Therefore, $ZnCl_2$ was used for further optimisations.

As the effect of solvent on the yield of the reaction is likely high, we chose to screen only a few solvents that are obtained from renewable resources, albeit our list is not exhaustive (Table 4.2). Deuterated dichloromethane was also employed to allow following the reaction *via* NMR spectroscopy.

Table 4.2.: Electrophilic substitution solvent screening using LGO and furan as substrates and $ZnCl_2$ as catalyst.[1]

Solvent	**Conversion (%)**[2]
DMC[3]	18
MeTHF[3]	3
Furan[3]	7
DCM-d2[3]	15

[1] in all cases, the reaction was carried out at 25 °C for 24 hours using 0.05 eq. $ZnCl_2$ as catalyst and concentration of LGO 2.5 M, [2]determined *via* ^{1}H NMR spectroscopy. , [3] Entry obtained by Luca Heusser

Although the difference in yield in different solvents was marginal, DMC was chosen for further optimisations as it has a high boiling point and is non-hazardous and considered renewable. After the catalyst and solvent were selected, the temperature was screened, leading to 31 % of conversion at 55 °C after 24 hours (4.3). Finally, the reaction time was optimised, leading to a conversion of 60% after 5 days of reaction time (Table 4.4).

Table 4.3.: Temperature screening for the synthesis of monomer **5**.[1]

Temperature (℃)	**Conversion (%)**[2]
25	15
35	21
55[3]	31

[1] in all cases, the reaction was carried out for 24 hours using 0.05 eq. $ZnCl_2$ as catalyst and concentration of LGO 2.5 M in DMC, [2]determined *via* ^{1}H NMR spectroscopy. [3] Entry obtained by Luca Heusser.

Table 4.4.: Reaction time and conversion in the synthesis of monomer **5**

Reaction time (days)	Conversion (%)[1]
1	31
2	52
3	63
4	71
5	75

[1] in all cases, the reaction was carried out at 55 °C using 0.05 eq. $ZnCl_2$ as catalyst and concentration of LGO 2.5 M in DMC, [2] determined *via* ^1H NMR spectroscopy.

The obtained product (**5**) was purified *via* column chromatography, although other purification techniques such as recrystallisation and distillation were considered. However, the liquid nature of the product and its high boiling point made these two purification methods unsuitable. Regarding the regio selectivity of the reaction toward **5**, the NMR reaction monitoring showed the formation of just one adduct, the 2,5-substituted furan, at the given reaction temperature (Figure 5.62).

4.3. Using of furan derivatives in the electrophilic substitution reaction

After the reaction conditions were optimised for the synthesis of product **5**, different furan derivatives were tested to obtain a set of monomers. 2-Methylfuran and 2-ethylfuran were thus tested (Figure 4.1), which are also potentially renewable, as discussed in the introduction. The reactions with methyl- and ethylfuran were successful and resulted in products **6** and **7** in good yield (58.2% and 70.5%, respectively).

4.4. Investigation of the LGO-based monomers

In an attempt to involve the **5** in subsequent reactions, it was exposed to a mixture of a ruthenium-based Grubbs type catalyst (Grubbs second generation, M204) and $ZnCl_2$, after quenching with ethyl vinylether (EVE), a polymer-like material was obtained. Size exclusion chromatography of the material yielded a uniform peak with a molecular weight (M_n) of $24\,\mathrm{kg\,mol^{-1}}$ and a dispersity (Đ) of 1.62 (Figure 4.5**b**, entry p(**5**_100)) Crucially, employing the two catalysts independently did not result in the formation of a polymer (Table 4.5).

Table 4.5.: M_n of p(**5**) obtained using different catalysts. All reactions were conducted at 25 °C and run for 24 hours using monomer concentration of 5 mg/mL and DCM as reaction solvent.

Catalyst	**Quantity**	**M_n (kg/mol)**	**Đ**
GII	0.01 eq	0.2	1
$ZnCl_2$	1.00 eq	0.2	1
GII and $ZnCl_2$	0.01 and 1.00 eq	24	1.53

To understand the behaviour of the catalysts in more detail, a ^{1}H NMR of the GII catalyst in deuterated benzene, before and after addition of $ZnCl_2$, was recorded (Figure 5.61). No change in the benzylidene area (19.64 ppm) of the Grubbs catalyst was observed. This is an indication that the addition of zinc chloride does not affect the structure of the Grubbs catalyst. When analysing the obtained polymer by ^{1}H NMR spectroscopy (Figure 5.58), the absence of peaks in the vinyl region (ca. 5-6 ppm) was noted. Initially, this indicated the absence of unreacted monomer and thus complete conversion. However, it also pointed to the fact that the obtained polymer featured no unsaturated bonds in the backbone. Moreover, the presence of peaks the aliphatic region suggested that **5** was polymerised in a vinyl-like fashion. It is, however, noted that other characteristic protons, such as that of the LGO acetal were absent. It is worth noting that, as no monomer was detected at the end of the reactions, all analyses were carried out after simple removal of the catalysts by filtration through DMT-functionalised silica.[284] The ^{1}H NMR spectrum of the obtained polymer material is similar to the literature-reported spectrum of poly(EVE).[285] This indicated that the material obtained corresponds to a polymer derived from the quenching agent. However, since EVE was added in large excess compared to **5**, the sensitivity of the NMR instrument does not allow to detect traces of the levoglucosenone-derived part of the molecule. In an attempt to analyse further the polymer structure, an IR spectrum was recorded (Figure 4.4).

A broad peak corresponding to the C=O vibration (1690 cm^{-1}) as well as an intense peak corresponding to C-H vibrations typical for levoglucosenone (2900 cm^{-1}) were observed (4.4), indicating that LGO was present in the product.

Subsequently, two test reactions were carried out to test the ability of **5** and EVE to polymerise employing the aforementioned polymerisation conditions but avoiding quenching of the catalyst. The reaction mixture obtained by the testing of **5** was analysed *via* ^{1}H NMR (Figure 5.65) and SEC (Figure 5.64), after 24 hours. The spectrum and chromatogram show no polymer was formed, supporting the hypothesis that EVE was the main component of the previous polymerisation.

EVE was subsequently exposed to the polymerisation conditions employed above, in the absence of **5**. The ^{1}H NMR spectrum (Figure 4.2) shows the rise of new peaks at 2.86, 2.58, 1.93 and 1.57 ppm. Furthermore, the broadness of the peaks at 3.50 and 1.18 ppm, and the low intensity of the vinyl peak, at 6.72 ppm, seems to indicate that polymerisation has taken place.

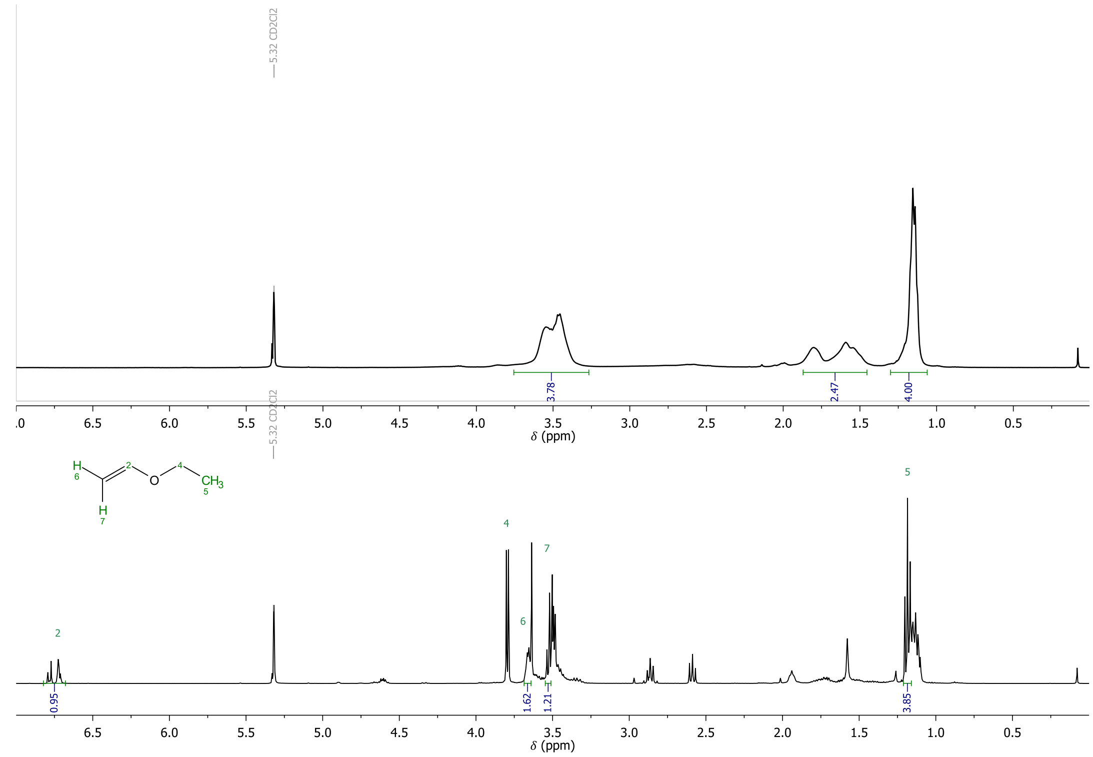

Figure 4.2.: Comparison ^{1}H NMR spectra of p(**5**) (upper spectrum) and residue of ethyl vinylether exposed to the same polymerisation conditions (bottom spectrum).

However, the SEC chromatogram (Figure 4.3) does not show any polymer peak. This led to the conclusion that the conditions applied for the polymerisation of EVE are generating oligomers with a low molecular weight that are not detected by SEC. The absence of a polymer peak can also be attributed to interactions with the SEC column, however this possibility is unlikely since p(**5**) is detectable by the same system.

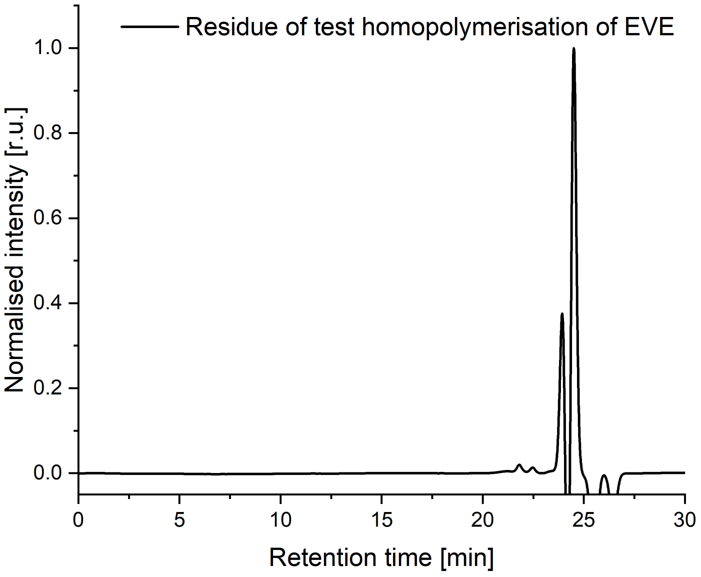

Figure 4.3.: SEC chromatogram of test homopolymerisation of EVE

The fact that EVE cannot be polymerised at the tested conditions to yield a polymer with comparable molecular weight to p(**5**) is another indication that both **5** and EVE take part in the polymerisation process. An IR spectrum of the product of the homopolymerisation test of EVE was compared with the LGO and p(**5**) spectra (Figure 4.4). The peak at 2970 cm^{-1} corresponds to C-H stretching of EVE, while the peak at 2900 cm^{-1} corresponds to C-H stretching of LGO. Furthermore, the broadening of the peak 1720 cm^{-1} in the spectrum of p(**5**), compared to EVE residue, is attributed to the presence of LGO C=O vibration peak at 1690 cm^{-1}. The presence of peaks that can be attributed to both LGO and EVE in p(**5**) spectrum indicates that the resulting polymeric material exhibits functional groups of both molecules. Therefore, this is another indication that the aforementioned molecules (LGO and EVE) are part of the obtained polymeric material.

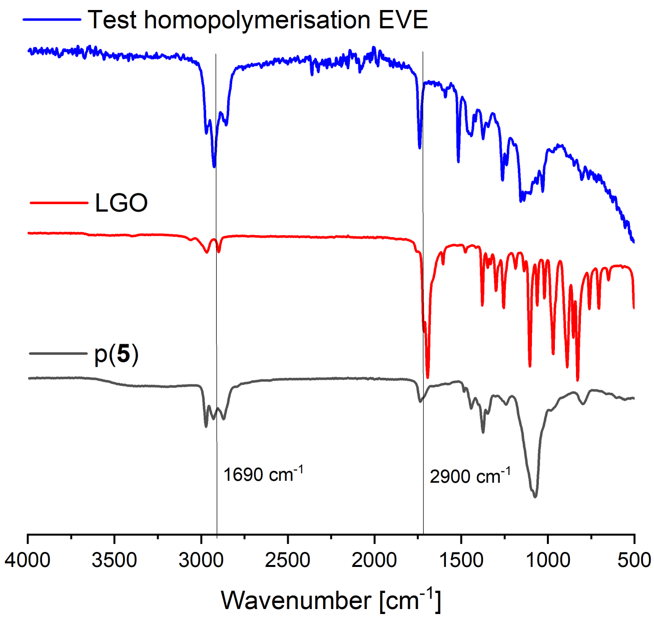

Figure 4.4.: IR spectra of p(**5**), Levoglucosenone and the EVE test polymerisation.

More investigations are needed, such as the synthesis of a low molecular weight material with an equimolar composition of EVE and LGO and its subsequent analysis. However, from obtained NMR and IR spectroscopic data, EVE seems to be the main component of the polymeric material, with LGO participating in the polymerisation reaction.

The effect of the ratio between GII and $ZnCl_2$ on the polymerisation was subsequently investigated. All investigations were conducted using the polymerisation of **5**, and subsequent quenching with EVE, as a model reaction. First, different equivalents of $ZnCl_2$ were employed. During this process, the equivalents of GII were kept constant (see Table 4.6).

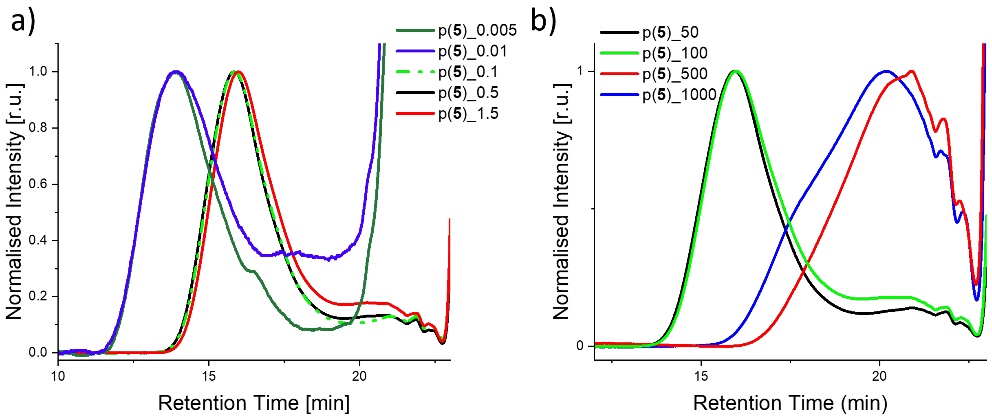

Figure 4.5.: SEC traces of: a) p(**5**) obtained with various equivalents of $ZnCl_2$ (0.005; 0.01; 0.1; 0.5; 1.5 eq) at 25 °C, with reaction time of 24 hours and DCM as reaction solvent b) p(**5**) obtained with different equivalents of GII (0.02, 0.01, 0.002, 0.001 eq) 25 °C, concentration of the monomer equal to 5 mg/mL and DCM as reaction solvent.

Table 4.6.: M_n of p(**5**) obtained using different quantities of $ZnCl_2$ at 25 °C, with reaction time of 24 hours, concentration of the monomer of 5 mg/mL, DCM as reaction solvent and 0.01 eq of GII.

Name	**Equivalents of $ZnCl_2$**	**M_n (kg/mol)**	**Đ**
p(**5**)_0.005	0.005	96	2.31
p(**5**)_0.01	0.01	129	1.72
p(**5**)_0.5	0.5	28	1.66
p(**5**)_1.0	1.0	28	1.66
p(**5**)_1.5	1.5	26	1.64

As visible from the corresponding SEC data in Figure 4.5, when the molar quantity of $ZnCl_2$ is higher than the quantity of GII, the obtained molecular weight remains constant. However when the quantity of $ZnCl_2$ is lower than 0.01 eq (with respect to the LGO derivative **5**), the conversion drops significantly (from 90% to just 2%). Moreover, using 0.01 eq results in complete conversion of the LGO derivative, thus in subsequent syntheses 1.0 eq. of $ZnCl_2$ with respect to the LGO derivative (**5**) were used. When the quantity of $ZnCl_2$ is lower than the equivalent amount of GII, a lower M_n and higher dispersity ($Đ$) are obtained. Reducing the quantity of $ZnCl_2$ led also to the increase of the low molecular shoulder of the polymer peak.

The effect of the quantity of GII was investigated next. In this case, the $ZnCl_2$ equivalents were kept constant and the amount of GII was changed (Table 4.7). As visible in Figure 4.5**b**, low amounts of GII yielded broad peaks with low M_n. A broad peak corresponding to a M_n of 24 kg/mol was obtained when 0.01 equivalents of GII (with respect to the LGO derivative **5**) were used. Further increasing the amount of GII had no effect on the M_n. These results indicate that both catalysts ($ZnCl_2$ and GII) need to be present in the reaction to obtain a polymer.

Table 4.7.: M_n of p(**5**) obtained using different quantities of GII at 25 °C, with reaction time of 24 hours, concentration of the monomer of 5 mg/mL, 1.0 eq of $ZnCl_2$ and DCM as reaction solvent.

Name	**Equivalent of GII**	**M_n (kg/mol)**	**$Đ$**
p(**5**)_50	0.02	26	1.65
p(**5**)_100	0.01	24	1.62
p(**5**)_500	0.002	1.1	2.48
p(**5**)_1000	0.001	1.3	3.39

Having developed a basic understanding of the catalyst requirements to obtain a polymer, the polymerisation of LGO derivatives **6** and **7** using this co-catalysed process was carried out. As visible in Table 4.8, all three derivatives synthesised in this study yielded a polymeric material using the combination of GII and $ZnCl_2$.

Table 4.8.: Molecular weights of p(**5**), p(**6**) and p(**7**) obtained at 25 °C, with reaction time of 24 hours, DCM as reaction solvent, concentration of the monomer of 5 mg/mL, 1.0 eq of $ZnCl_2$ and 0.01 eq of GII as catalysts .

Product	M_n **(kg/mol)**	**Đ**
p(**5**)	24	1.62
p(**6**)	23	1.60
p(**7**)	28	1.66

The SEC traces of the resulting materials are depicted in Figure 4.6. As noticeable in Figure 4.6, the ethyl-derivative material (p(**7**)) shows a distribution with a shoulder in the low-molecular weight region. In contrast, in the SEC traces of p(**6**) and p(**5**), this low molecular weight shoulder is more accentuated.

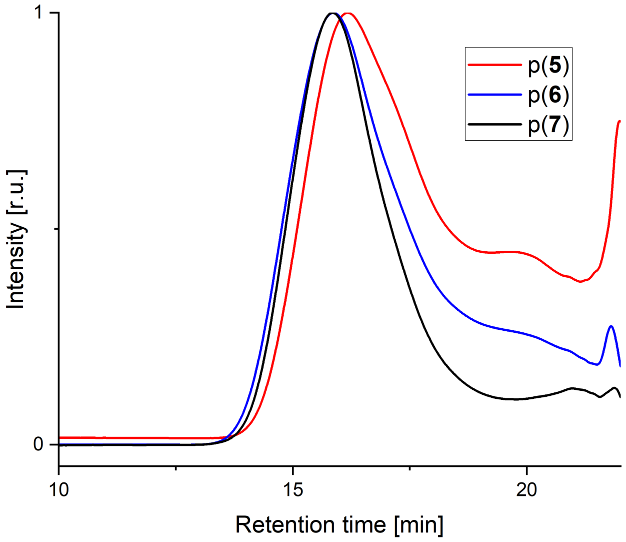

Figure 4.6.: SEC traces of polymeric materials p(**5**); p(**6**); p(**7**) obtained using the conditions reported in Table 4.8.

4.5. Thermal properties of polymeric materials p(5), p(6) and p(7)

The thermal properties of the prepared polymeric materials were tested using thermal gravimetric analysis (TGA, Table 4.9).

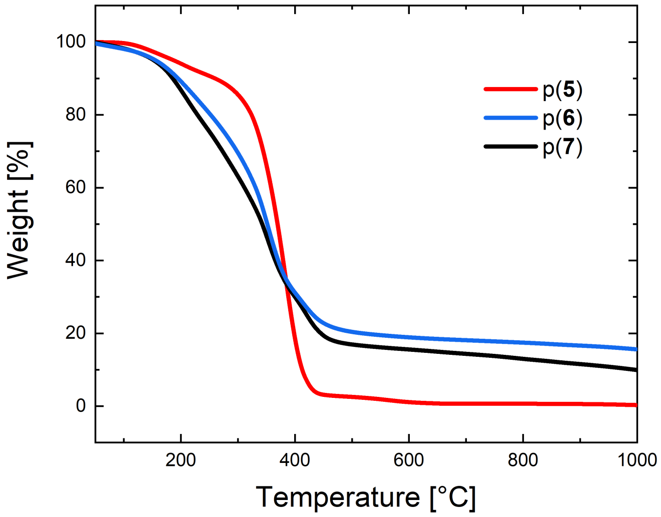

Figure 4.7.: TGA traces of polymeric materials p(**5**), p(**6**) and p(**7**) under N_2 with a heating rate of 10 K/min up to 1000 °C

Table 4.9.: Decomposition and glass transitions temperatures of p(**5**), p(**6**) and p(**7**).

Homopolymer	T_d (°C)	T_g (°C)
p(**5**)	187	-33
p(**6**)	155	-20
p(**7**)	152	-17

The decomposition temperatures are in line with other polymeric materials. For p(**5**), no residue is left after 600 °C (Figure 4.7). However, for p(**6**) and p(**7**), a 20%

residual weight is still present. This difference was surprising given the structural similarity of the three polymers based on NMR and IR spectroscopy data. Furthermore, the decomposition temperature T_d of p(**5**) was significantly higher than that of p(**6**), and p(**7**) (Table 4.9).

Next, differential scanning calorimetry (DSC) was performed. Glass transition temperatures (T_g) were observed and are reported in Table 4.9.

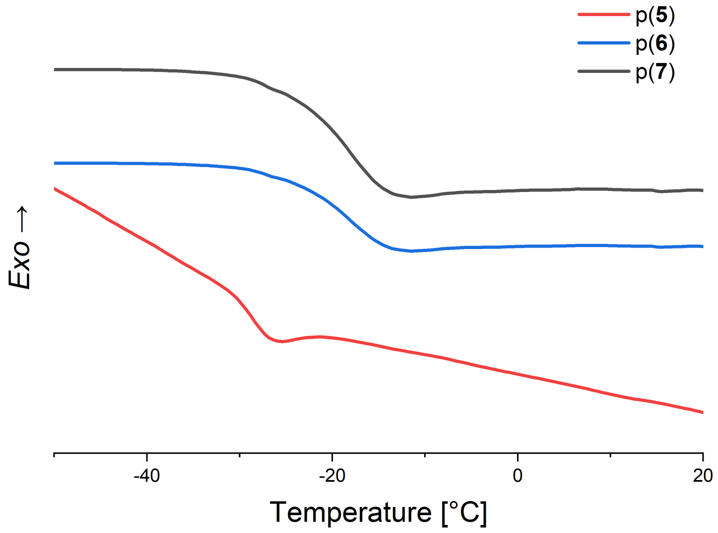

Figure 4.8.: DSC traces of homopolymers p(**5**), p(**6**) and p(**7**)

As visible in Figure 4.8, all glass transition temperatures are below 0 °C, in line with the nature of the products as viscous liquids at room temperature. No melting points were observed in the measured temperature range, indicating the absence of crystallisation. Furthermore, a trend in the T_g of the polymeric materials was observed: p(**7**) exhibited the highest T_g while p(**5**) the lowest. This observation is rather unexpected as the polymers are otherwise similar. Therefore, the lower T_g is ascribed to the presence of low molecular weight chains in p(**5**) and p(**6**). The differences can also be ascribed to the different LGO derivatives employed in the polymerisations. However, since the presence of LGO derivatives cannot be quantified, there is no certainty whether the structural differences themselves play a role in the analysed properties of the obtained polymeric materials.

4.6. Conclusions

In this work, three renewable resourced LGO derivatives (**5**, **6**, and **7**) were synthesised through an electrophilic substitution reaction between furan derivatives and LGO. The conditions for the reaction were optimised and levoglucosenone-derived substituted furans were obtained. The copolymerisation of the LGO derivatives with ethyl vinyl ether was only possible when using a combination of a typical ROMP catalyst, namely GII, and $ZnCl_2$. Interestingly, despite the structural differences between the derivatives, the resulting polymers appeared structurally very similar. Furthermore, their thermal properties varied. This was ascribed to low molecular weight chains in the polymer while the low quantity of levoglucosenone embedded in the final material is likely to also constribute to the differences observed. All synthesised polymers exhibited low T_gs, making them well-suited for further processing, e.g. *via* injection moulding. Further investigations into the polymerisation mechanism and exploiting it for other furan-based monomers are underway. A low molecular weight polymer, obtained by adding a lower quantity of EVE in controlled amounts, should be synthesised. In order to explore the structural characteristics and clarify the mechanism.

5. Materials, methods, calculations and supporting images

5.1. Materials

Furan (Sigma-Aldrich, ≥99%), levoglucosenone (Circa Group, ≥95%), dichloromethane (Sigma-Aldrich, anhydrous, ≥99.8%, contains 40-150 ppm amylene as stabiliser), deuterated dichloromethane (Sigma-Aldrich, ≥99.8% D), 2-methyl-tetrahydrofuran (Honeywell Reagent Grade, contains 150-400 ppm BHT as stabiliser, ≥99.5%), dimethyl carbonate (DMC) (Sigma-Aldrich, ReagentPlus®, 99%), 2-methylfuran (Sigma-Aldrich, stabilised for synthesis), 2-ethylfuran (Sigma-Aldrich ≥99%), 2,3-Dihydrofuran (Sigma-Aldrich ≥99%), allyl ether (Sigma-Aldrich ≥99%), diallyl amine (Sigma-Aldrich ≥99%), N-Methyl diallyl amine (Sigma-Aldrich ≥97%), Allyl sulfide (Sigma-Aldrich ≥97%), Sodium methoxyde (Sigma-Aldrich, reagent grade, ≥95%), 2,5-dimethylfuran (Sigma-Aldrich, 99%), zinc chloride (Alfa Aesar, anhydrous, 98+%), zinc iodide (Thermo Fisher scientific, 98%), hafnium chloride (Alfa Aesar, 98+%, metals basis, Zr<0.5%), aluminium chloride (Alfa Aesar, anhydrous >95%), tris-(6,6,7,7,8,8,8-heptafluor-2,2-dimethyl-3,5-octandionato)-ytterbium (Sigma-Aldrich), zinc triflate (Sigma-Aldrich, 98+%), titanium (IV) chloride (Thermo Fisher scientific, 99+%), Grubbs first generation catalyst (M102, Sigma-Aldrich), Grubbs second generation catalyst (M204, Sigma-Aldrich), Grubbs third generation catalyst (M300, Sigma-Aldrich), DMT-functionalised silica (Sigma-Aldrich, 99+%, molecular loading ≥0.50 mmol/g), chloroform-d (99.8%, Sigma-Aldrich), dimethyl sulfoxide-d6 (99.8% Eurisotop Chemicals), benzophenone (99% Sigma-Aldrich), 2-adamantanone (98%, Fisher scientific), benzaldehyde (99%, Sigma-Aldrich), Xanthone (97% Sigma-Aldrich), Grubbs 3rd generation (Umicore M300, 99% Merck), Grubbs 2nd generation (Umicore M204, 99% Merck), Grubbs first generation (Umicore M102, 97% Merck) Lawessons reagent (97%, Sigma-Aldrich), Hoveyda-Grubbs 2nd generation (Umicore M720, 97% Merck), were used as received. Cyclopentadiene (97%) was freshly distilled before use. Solvents (HPLC grade) were used with no further purification.

Instrumentation

NMR: ^{1}H and ^{13}C spectra were recorded at the Karlsruhe Institute of Technology (KIT, Germany) on a Bruker Avance 400 NMR instrument at 400 MHz for ^{1}H NMR and 101 MHz for ^{13}C NMR. CD_2Cl_2 was used as solvent. Chemical shifts are presented in parts per million (δ) relative to the resonance signal at 5.32 ppm (^{1}H, CD_2Cl_2) and 54.00 ppm (^{13}C, CD_2Cl_2) or 7.26 ppm (^{1}H, $CDCl_3$) and 77.20 ppm (^{13}C, $CDCl_3$). The spin multiplicity and corresponding signal patterns were abbreviated as follows: s = singlet, d = doublet, t = triplet, q = quartet, quint. = quintet, sext. = sextet, m = multiplet and br = broad signal. Coupling constants (J) are reported in Hertz (Hz). All measurements were recorded in a standard fashion at 25 °C unless otherwise stated. Full assignment of structures was aided by 2D NMR analysis (COSY, HSQC and HMBC).

Orbitrap Electrospray-Ionisation Mass Spectrometry (ESI-MS) spectra were recorded on a Q Exactive (Orbitrap) mass spectrometer (Thermo Fisher Scientific, San

Jose, CA, USA) equipped with an atmospheric pressure ionisation source operating in the nebuliser assisted electrospray mode. The instrument was calibrated in the m/z range 150–2,000 using a standard containing caffeine, Met-ArgPhe-Ala acetate (MRFA) and a mixture of fluorinated phosphazenes (Ultramark 1621, all from Sigma-Aldrich). A constant spray voltage of 3.5 kV, a dimensionless sheath gas of 6, and a sweep gas flow rate of 2 were applied. The capillary voltage and the S-lens RF level were set to 68.0 V and 320 °C, respectively. For the interpretation of the spectra, molecular peaks $[M]^+$, peaks of pseudo molecules $[M+H]^+$ and $[M+Na]^+$ characteristic fragment peaks are indicated with their mass to charge ratio (m/z) and their intensity in percent, relative to the most intense peak (100%).

All thin layer chromatography experiments were performed on silica gel coated aluminium foil (silica gel 60 F254, Sigma-Aldrich). Compounds were visualised by staining with Seebach solution (mixture of phosphomolybdic acid hydrate, cerium(IV)-sulfate, sulfuric acid and water).

Size Exclusion Chromatography (SEC) measurements were performed on three different systems based on the solubility of the compound or their size:

For polymers soluble in tetrahydrofuran (THF), a Shimadzu LS 20A system equipped with a SIL-20A autosampler and a RID-20A refractive index detector was used with the solvent mixture THF/2vol% TEA (flow rate 1 mL min^{-1} at 30 °C as the mobile phase. The analysis was performed on the following column system: PSS SDV analytical (5 um, 300x8.0 mm^2, 10,000 Å) and a PSS SDV analytical (5 um, 300x8.0 mm^2, 1.000 Å) with a PSS SDV analytical precolumn (5 um, 50x8.0 mm^2). For the calibration, narrow linear poly(methyl methacrylate) standards (Polymer Standards Service, PPS, Germany) ranging from 1,100 to 981,000 g/mol were used.

For measurements performed using DMAc as solvent, a Polymer Laboratories PL-GPC 50 Plus Integrated System with an autosampler was used. The system was equipped with a PLgel 5 mm bead size guard column 50x7.5 mm, which was followed by three PLgel 5 µm Mixed-C columns and one PLgel 3 µm Mixed-E column 300x7.5 mm. A differential refractive index detector (Agilent Infinity II) was used for detection. The solvent, DMAc, contained 0.3 w% LiBr and a pressure of 1 mL/min at 50 °C was applied. Linear poly(methyl methacrylate) standards ranging from 476 to 2.5×10^6 g mol^{-1}. The polymer samples were dissolved at a concentration of 2 mg mL^{-1} in the eluent and filtered over a 0.2 µL filter prior to the measurement. Signals lower than 1,000 g mol^{-1} correspond to solvent signal.

For p(**3b**) the measurment was performed on Shimadzu LS 20A system equipped with a SIL-20A autosampler, a Varian column oven and a RID-20A refractive index detector was used with THF as solvent (flow rate 1 mL min^{-1} at 30 °C as the mobile phase. The analysis was performed on the following column system: PSS SDV analytical (5 um,300x8.0 mm^2, 10.000 Å) and a PSS SDV analytical (3 um, 300x8.0 mm^2, 1.000 Å) with a PSS SDV analytical precolumn (3 um, 50x8.0 mm^2). For the calibration, narrow linear poly(methyl methacrylate) standards (Polymer Standards Service, PPS, Germany) ranging from 102 to 583,000 g/mol were used.

Differential scanning calorimetry (DSC) experiments were performed on a Mettler Toledo DSC 3 using a Huber Intracooler TC100 and aluminum crucibles (40 and 100 µL). Measurements were performed under nitrogen flow (50 mL min^{-1}) in three consecutive heating-cooling cycles from −80 °C up to 200 °C with a heating rate of 30 K min^{-1} and a cooling rate of 10 K min^{-1}. The maximum temperature for the heating cycle was determinated based on the decomposition temperature of the compound. Each measurement was performed using 3–7 mg of substance for sample preparation. T_g

values were determined as the onset of the transition in the second heating cycle.

Thermogravimetric analysis (TGA) analysis was performed on a TGA5500 from TA instruments. 5–15 mg of a sample was placed in a platinum pan and heated at a rate of $10\,\mathrm{K\,min^{-1}}$ from ambient temperature to 1000 °C under nitrogen flow and then kept at 1000 °C for 5 minutes under air flow. The weight loss was evaluated using the Trios v5.0.044608 software. The T_d was determined by the temperature at which 5% weight loss was observed.

5.2. Calculations

5.2.1. Computational calculations

All DFT calculations were performed according to the method reported by Bazzi *et al.*.[206]

5.2.2. E-factors calculations

For synthesis of 2,5-dihydrofuran from cis-2-buten-1,4-diol

Waste:

Diol = 1.00 g; Sodium metoxide= 1.2 g; Dimethyl carbonate = 4.1 g

Total waste = 6.3 g

Product= 0.78 g

$$\text{E-factor} = \frac{6.3}{0.78} = 8.08 \qquad \text{(Eq. 5.2.1)}$$

For synthesis of 2,5-dihydrofuran from allyl ether

Waste:

Allyl ether = 1.00 g; Catalyst= 0.064 g; Dimethyl carbonate used for the DMT filtration= 5 g; DMT silica used= 0.2 g

Total waste = 6.3 g

Product= 0.64 g

$$\text{E-factor} = \frac{6.3}{0.64} = 9.84 \qquad \text{(Eq. 5.2.2)}$$

From meso-erythtritol to 2,5-DHF (literature reported).[188]

Waste:

meso-erythritol= 1.00 g; 3-octanol= 6.71 g; catalyst= 0.067 g; *para*-toluenesulfonic acid monohydrate = 0.026 g.

Total waste= 7.803 g

Product = 0.316 g

$$\text{E-factor} = \frac{7.803}{0.32} = 24.4 \qquad \text{(Eq. 5.2.3)}$$

From alkyne to 2,3-DHF (literature reported method).[2]

Cyclisation of alkyne (literature reported):[2]

Synthesis of 2,3-DHF

Waste:

reactant = 1.00 g; Catalyst =0.654 g; THF=12.32 g; Silica =40 g; Solvent used in the purification =195 g

Total waste=248.97 g

Product =0.78 g

$$\text{E-factor} = \frac{248.97}{0.78} = 319.20 \qquad \text{(Eq. 5.2.4)}$$

Proposed syntethic pathway from cis-2-buten-1,4-diol to 2,3-DHF

Formation of 2,5-DHF

Waste: Reactant =1.0 g; NaOME=1.2 g; DMC=4.1 g

Isomerisation

Catalyst = 0.094 g; Dimethyl carbonate used for the DMT filtration= 5 g; DMT silica used= 0.2 g

Total waste process=11.59 g

Product=0.56 g

$$\text{E-factor} = \frac{11.59}{0.56} = 20.70 \qquad \text{(Eq. 5.2.5)}$$

Proposed syntethic pathway from allyl ether to 2,3-DHF

RCM of allyl ether and subsequently isomerisation to 2,3-DHF

Waste:

Reactant=1.00 g; Catalyst=0.086 g; DMC used for the DMT filtration=5 g; DMT silica for filtration=0.2 g

Product:0.45 g

Total waste process=6.29 g

$$\text{E-factor} = \frac{6.29}{0.45} = 13.98 \qquad \text{(Eq. 5.2.6)}$$

From alkyne to poly(DHF) Cyclisation of alkyne (literature reported):[2]

Synthesis of 2,3-DHF

Waste:

reactant = 1.00 g; Catalyst =0.654 g; THF=12.32 g; silica =40 g; Solvent used in the purification =195 g

Product =0.78 g

Isomerisation and Polymerisation in one pot:

Waste:

Catalyst= 0.094 g; THF=8.8 g; H_2O_2= 11.25 g; NaOH=3.75 g

Total waste process = 272.86 g

product poly(DHF) obtained =0.523 g

$$\text{E-factor} = \frac{272.86}{0.523} = 521.72 \qquad \text{(Eq. 5.2.7)}$$

Proposed syntethic pathway from cis-2-buten-1,4-diol to poly(DHF)

Formation of 2,5-DHF

Waste: Reactant =1.0 g; NaOME=1.2 g; DMC=4.1 g

Isomerisation and ROMP in one-pot

Catalyst = 0.094 g; THF=8.8 g, H_2O_2=11.25 g; NaOH=3.75 g

Total waste process=30.19 g

Product=0.355 g

$$\text{E-factor} = \frac{30.19}{0.36} = 85.01 \qquad \text{(Eq. 5.2.8)}$$

Proposed syntethic pathway from allyl ether to poly(DHF)

RCM of allyl ether and subsequently isomerisation to 2,3-DHF

Waste:

Reactant=1.00 g; Catalyst=0.086 g; DMC used for the DMT filtration=5 g; DMT silica for filtration=0.2 g

Product:0.45 g

ROMP of 2,3-DHF

Waste:

Catalyst=0.054 g; THF=8.8 g; H_2O_2=11.25 g; NaOH=3.75 g

Total waste process=30.14 g

Product ROMP =0.302 g

$$\text{E-factor} = \frac{30.14}{0.30} = 99.80 \qquad \text{(Eq. 5.2.9)}$$

5.3. Methods and supporting figures

5.4. Pathways to poly(dihydrofuran)

5.4.1. Ring-Closing metathesis of diallyl ether

A solution of Grubbs second-generation catalyst (2.78 mg, 0.0033 mmol, 0.02 eq) in dimethylcarbonate (DMC) (0.7 mL) is added to a crimp-top vial. The solution is bubbled with argon for one minute. After degassing diallyl ether (16 mg, 0.16 mmol, 1.00 eq) is added and the mixture is then argon is bubbled a second time for another minute. The reaction solution is heated up to 40 °C. After 12 hours of stirring the residue is dissolved in DMC (5 mL) and filtered over DMT-functionalised silica, yielding the product as a colourless liquid.

2,5-Dihydrofuran ^{1}H NMR (400 MHZ, DMSO-D$_6$): δ(ppm) = 5.97 (s, 2H,=C**H**-CH2-), 4.51 (s, 2H,=CH-C**H**$_2$-).

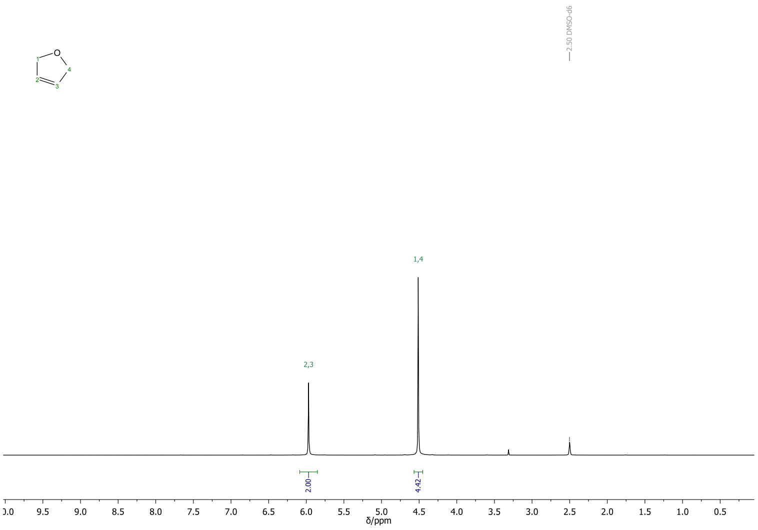

Figure 5.1.: ^{1}H NMR spectrum of 2,5-Dihydrofuran.

5.4.2. One pot isomerisation and ROMP of 2,5-DHF

In a crimp-top vial, 2,5-dihydrofuran (463.5 mg, 1.0 eq , 6.61 mmol, 0.5 mL), previously degassed *via* argon bubbling, and Grubbs catalyst second generation (1.37 mg, 0.1 eq , 0.002 mmol) are added, the solution is agitated at 65 °C for 48 hours. The mixture is then let cool down to room temperature. An aliquot is taken and SEC chromatogram recorded. The residue was subsequently dissolved in a previously-prepared stock solution of 40 mM PCy_3 in THF. A solution of alkaline H_2O_2 was freshly prepared by combining 3 parts aqueous 30% H_2O_2 with one part aqueous 1 M NaOH. The alkaline solution is added drop-wise to the THF solution, until no more precipitation is observed. The residue is filtrated and dried yielding a white solid with yield= 45.5%.

5.4.3. Homopolymerisation test of 2,5-DHF

This method was adapted from the literature method for the synthesis of poly(DHF).[11]

In a crimp-top vial, 2,5-dihydrofuran (463.5 mg,1.0 eq , 6.61 mmol, 0.5 mL), previously degassed *via* argon bubbling, and Grubbs catalyst second generation (1.37 mg, 0.1 eq , 0.002 mmol) are mixed together. After 24 hours, an aliquot is taken and SEC chromatogram and ^{1}H NMR spectrum recorded.

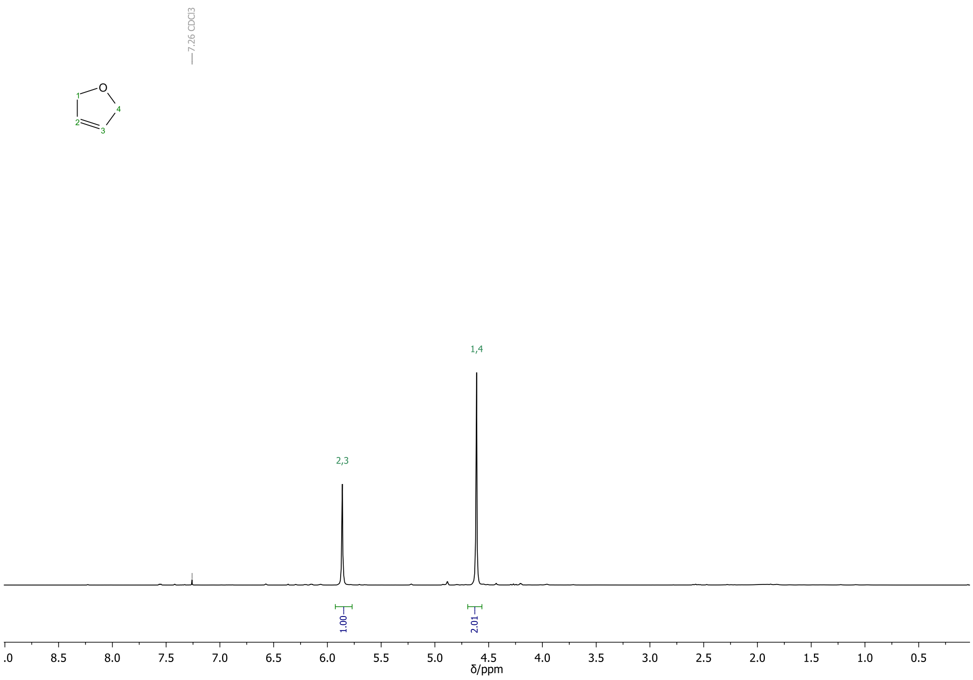

Figure 5.2.: ^{1}H NMR spectrum of unsuccessful polymerisation test of 2,5-Dihydrofuran. Obtained following literature reported method for ROMP of 2,3-DHF.[11]

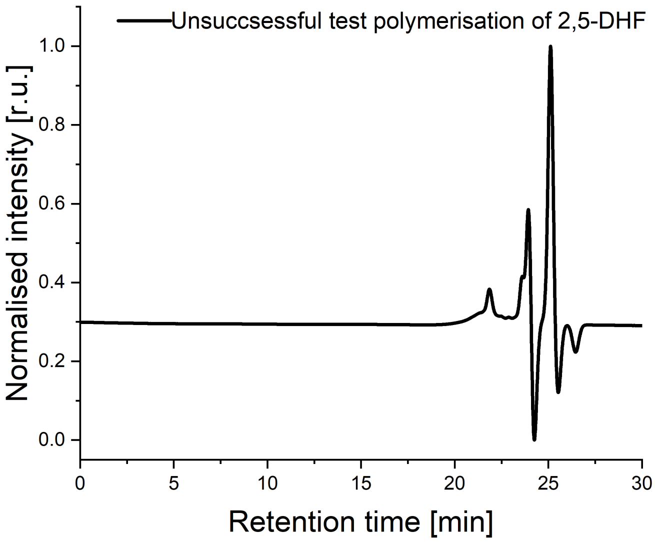

Figure 5.3.: SEC chromatogram of unsuccessful polymerisation test of 2,5-Dihydrofuran. Obtained following literature reported method for ROMP of 2,3-DHF.[11]

5.4.4. Dilution test

In a crimp-top vial, 2,3-Dihydrofuran (463 mg, 1.0 eq , 6.61 mmol, 0.5 mL) and dichloromethane (Table 5.1) are added. The solution is stirred for five minutes. Grubbs catalyst second generation (56 mg,0.01 eq , 0.066 mmol) is then added. After 24 hours, an aliquot is taken and a SEC chromatogram recorded.

Table 5.1.: Dilution rate of 2,3-DHF in DCM.

Product	**Dilution rate monomer:solvent** (v/v)	**Concentration** (M)	**Volume DCM** (mL)
PDHF0	-	-	0
PDHF14	1:1	14	0.5
PDHF7	1:2	7	1.0
PDHF3	1:5	3	2.5

5.4.5. Synthesis of statistical copolymer poly(**N-HexNb**-*co*-**DHF**)

In a crimp-top vial, 2,3-Dihydrofuran (463.5 mg, 1.0 eq , 6.61 mmol, 0.5 mL) and *[N]*-hexyl-*exo*-norbornene-5,6-dicarboximide (200.0 mg, 0.80 mmol, 1.0 eq) is added and the reaction mixture let stirring for five minutes. Grubbs catalyst second generation (1.37 mg, 0.1 eq , 0.002 mmol) is then added. After 24 hours, an aliquot is taken and SEC chromatogram recorded. The residue was subsequently dissolved in a previously-prepared stock solution of 40 mM PCy_3 in THF. A solution of alkaline H_2O_2 was freshly prepared by combining 3 parts aqueous 30% H_2O_2 with one part aqueous 1 M NaOH. The alkaline solution is added drop-wise to the THF solution, until no more precipitation is observed. The residue is filtrated and dried yielding a white solid with yield of 91.7%.

5.4.6. Ring closing metathesis of dienes

The corresponding diene (1.00 eq , 5.10 mmol, Table 5.2) is added to a head space vial and degassed. After degassing Grubbs-Hoveyda second generation catalyst is added to the reaction medium (31.9 mg,0.01 eq , 0.051 mmol). After 2 hours DMC (5 mL) is added to the reaction mixture, the obtained solution is filtered over DMT-functionalised silica to remove the catalyst. The solvent was removed under reduced pressure yielding the product.

Table 5.2.: Dienes quantity employed in the ring-closing metathesis

Diene	**Mass** (mg)	**Volume** (mL)
Allyl sulfide	581.6	0.65
Allyl ether	500.0	0.62
Diallylamine	494.3	0.63
Diallylmethylamine	566	0.72

2,5-dihydrothiophene Colourless oil with yield of 89% ^{1}H NMR (400 MHZ, CDCl3): δ(ppm) = 5.84 (s, 2H,=C**H**-CH2-), 3.74 (s, 2H,=CH-C$\mathbf{H}_2$-).

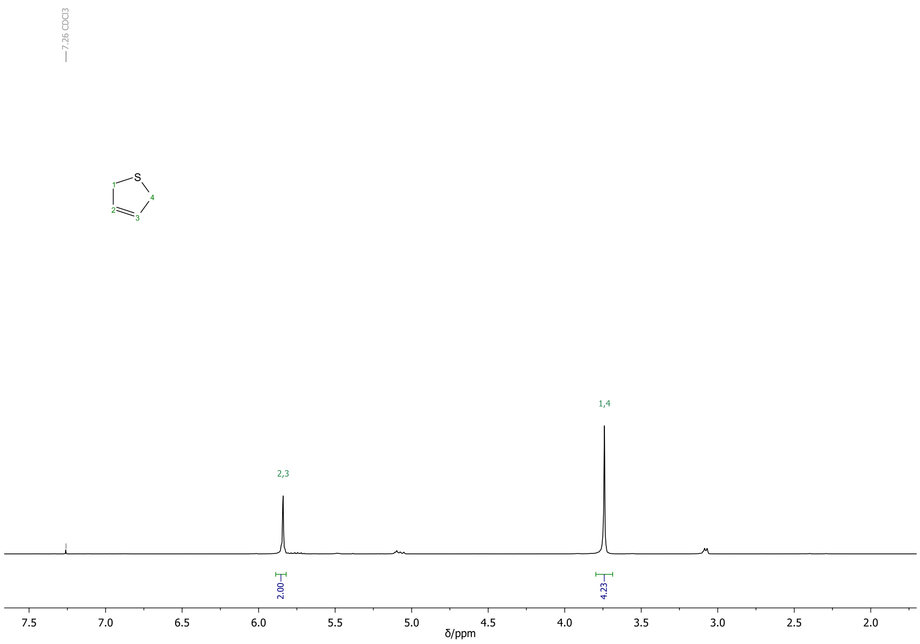

Figure 5.4.: ^{1}H NMR spectrum of 2,5-Dihydrothiophene.

5.5. Ring-Opening Metathesis Polymerisation of Thio-Norbornenes and their Sulfone-Derivatives

5.5.1. Synthesis of thioketones

In a flame-dried round bottom flask, the corresponding ketone or aldehyde (1.00 eq , **Table 5.3**), Lawesson's reagent (0.6 eq) and dry toluene (100 mL) were added under argon. The reaction mixture was heated to 120 °C for 4 hours. It was subsequently cooled down, the solvent was removed under reduced pressure and the mixture was purified *via* column chromatography using a mixture of petroleum ether and triethylamine (3 vol%).

Table 5.3.: Reaction conditions for the synthesis of thiokethones and the thioaldehyde.

Target compound	**Starting compound**	**Mass** (g)	**Moles** (mmol)	**Solvent** (mL)
2a	**1a**	1.00	5.49	100
2b	**1b**	1.00	5.10	100
2c	**1c**	1.00	8.06	100
2d	**1d**	1.00	9.43	100

2a: R_f = 0.26 (cyclohexane 3 vol%Et_3N), ^1H NMR (500 MHz, $CDCl_3$): δ = 7.73 (dd, ^3J = 8.4 Hz, 1.4 Hz, 4 H; *o*-Ar), 7.56 (m, 2 H; *p*-Ar), 7.39 (m, 4 H; *m*-Ar). HRMS (ESI) *m*/*z*: $[M+H]^+$ calc. for $C_{13}H_{10}S$: 199.05760, found: 199.05741.

Thiokethone **2a** synthesised by Kieron Laqua, a bachelor student under the co-supervision of Federico Ferrari and Dr. Roman Nickisch. The author conducted the planning of the synthetic pathway, the final evaluation of the results and the purification of the molecule.

2b: R_f = 0.62 (cyclohexane:EtOAc 40:1), , ^1H NMR (500 MHz, $CDCl_3$): δ = 8.75 (dd, ^3J = 8.2 Hz, 1.7 Hz, 2 H; S=C-C-C**H**=), 7.76 (ddd, ^3J = 8.4 Hz, 7.1 Hz, 1.7 Hz, 2H; -O-C-CH=C**H**-), 7.50 (dd, ^3J = 8.4 Hz, 1.1 Hz, 2H; -O-C-C**H**=), 7.38 (ddd, ^3J = 8.2 Hz, 7.1 Hz, 1.1 Hz, 2H; -O-C-CH=CH-C**H**=). HRMS (ESI) *m*/*z*: $[M+H]^+$ calc. for $C_{13}H_8OS$: 213.03656, found: 213.03686.

2c: R_f = 0.53 (cyclohexanethe 3%Et_3N), , ^1H NMR (500 MHz, $CDCl_3$): δ = 3.45 (app s, 2 H; S=C-C**H**-), 2.07 (m, 12 H). HRMS (ESI) *m*/*z*: $[M+H]^+$ calc. for $C_{10}H_{14}S$: 167.08890, found: 167.08878.

2d was synthesised according to the literature.[238] R_f=0.41, HRMS (ESI) *m*/*z*: $[M+H]^+$ calc. for $C_7H_{10}S$: 123.02648, found: 167.02630.

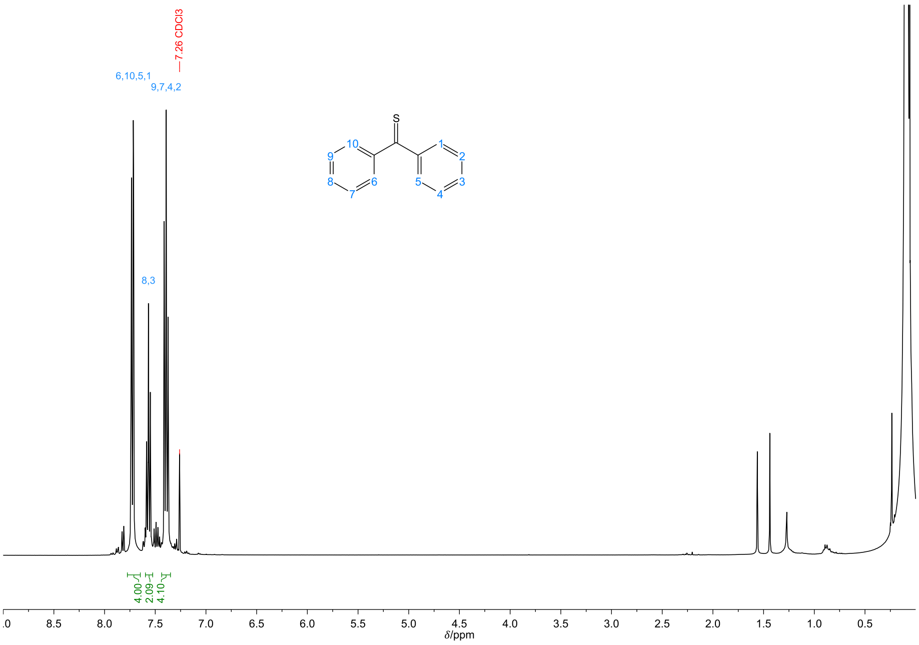

Figure 5.5.: ^{1}H NMR spectrum of **2a**.

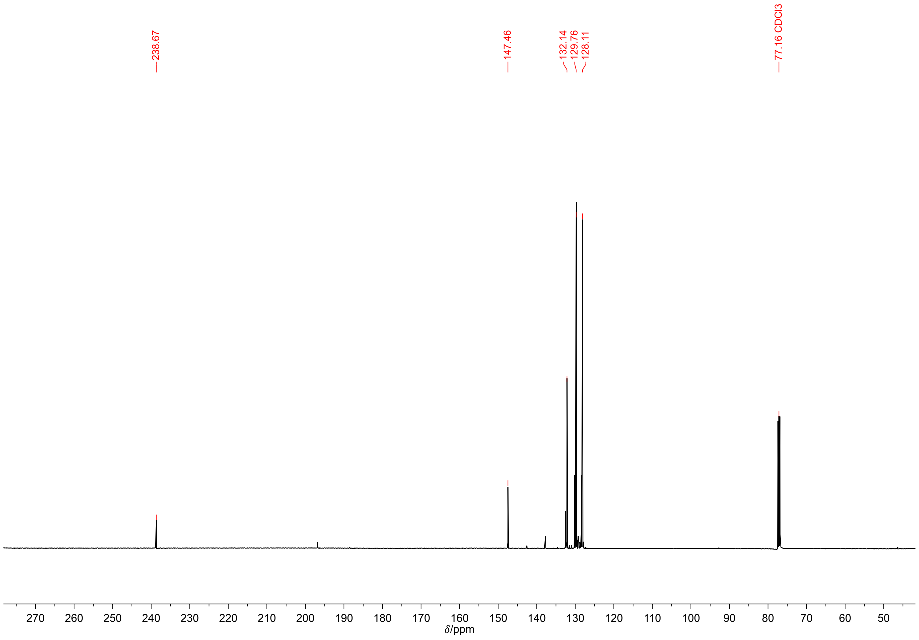

Figure 5.6.: ^{13}C NMR spectrum of **2a**.

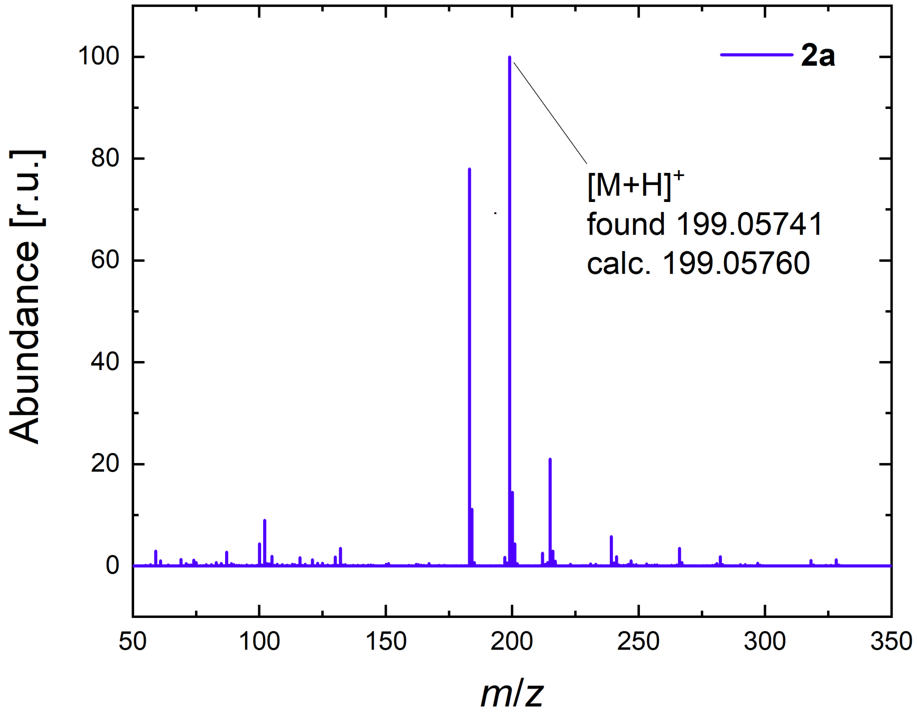

Figure 5.7.: ESI-MS of **2a**.

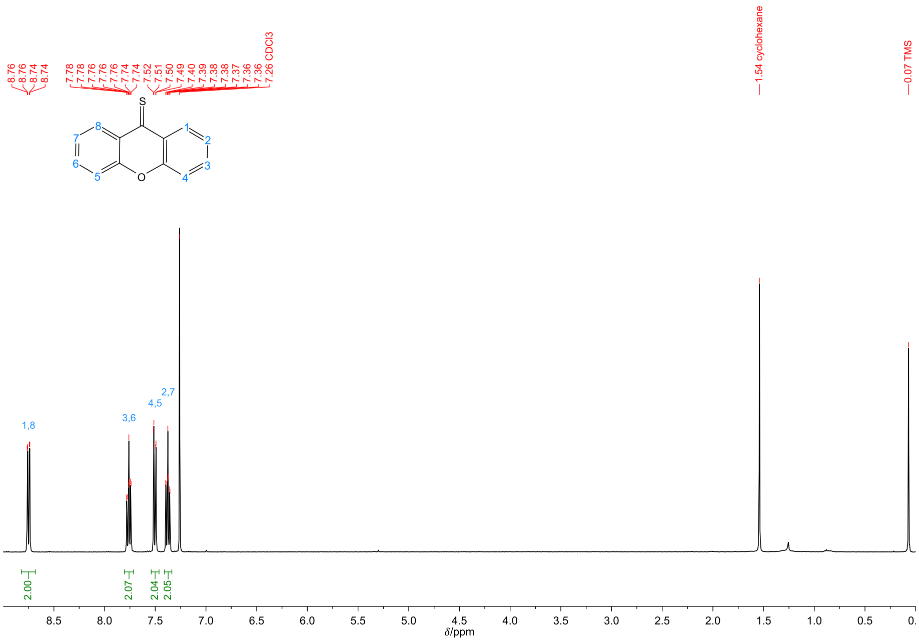

Figure 5.8.: ^{1}H NMR spectrum of **2b**.

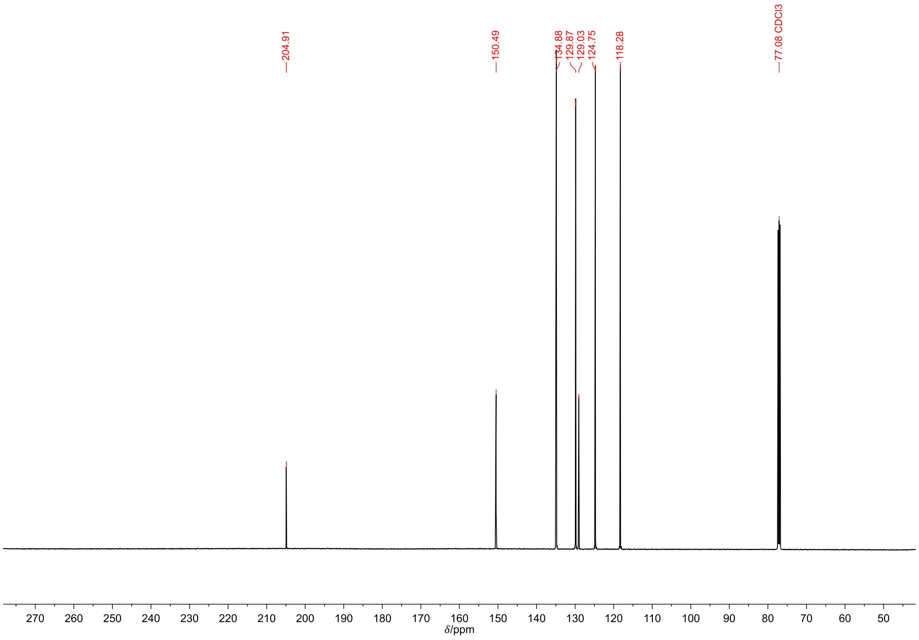

Figure 5.9.: ^{13}C NMR spectrum of **2b**.

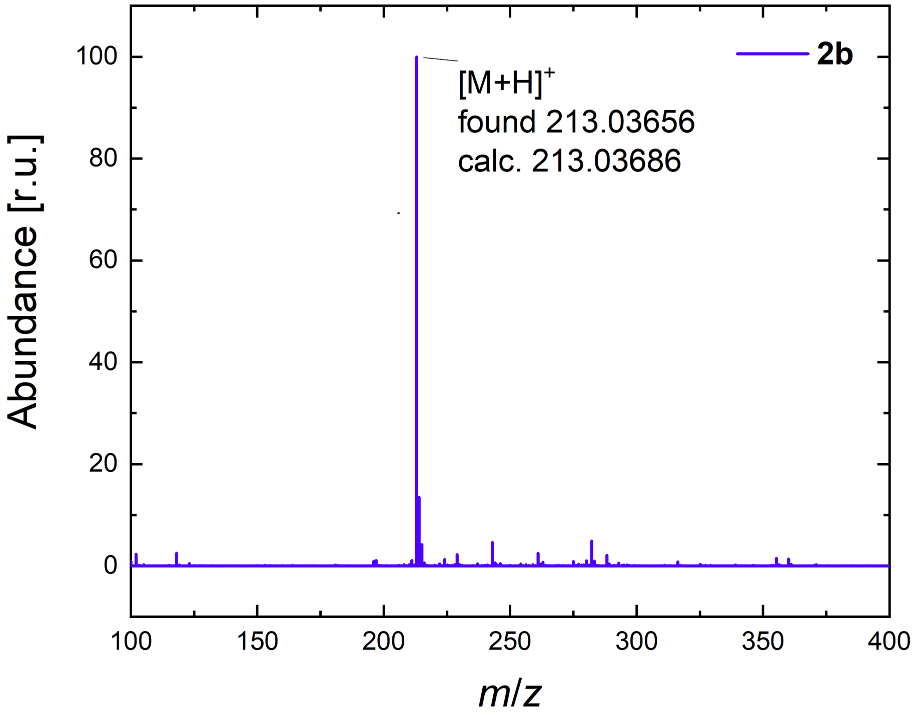

Figure 5.10.: ESI-MS of **2b**.

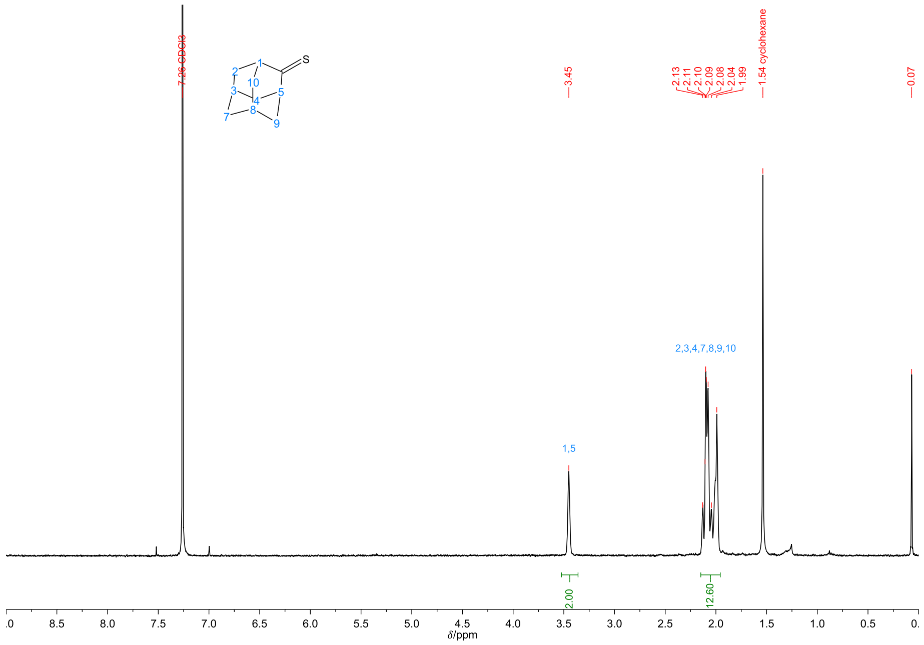

Figure 5.11.: ^{1}H NMR spectrum of **2c**.

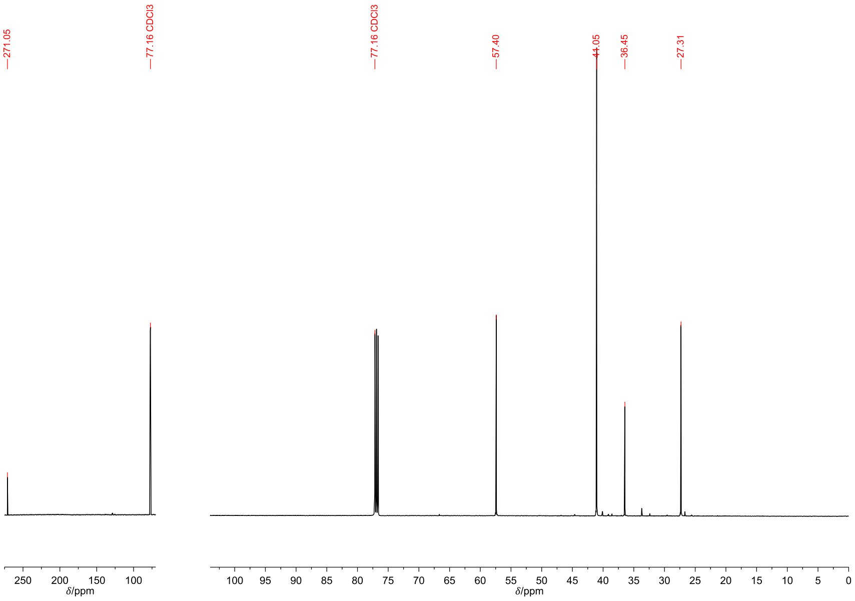

Figure 5.12.: ^{13}C NMR spectrum of **2c**. It is noted that the axis break indicates that the two spectral regions were collected from different measurements to improve the intensity of the C=S peak at 271 ppm.

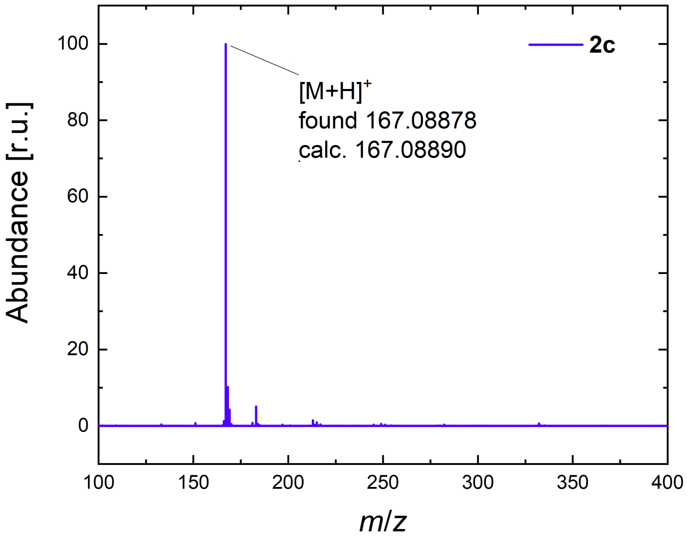

Figure 5.13.: ESI-MS of **2c**.

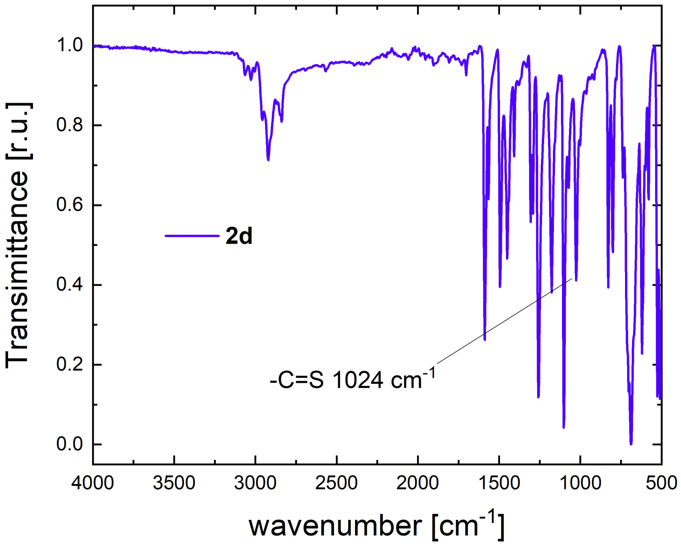

Figure 5.14.: IR spectrum of **2d**.

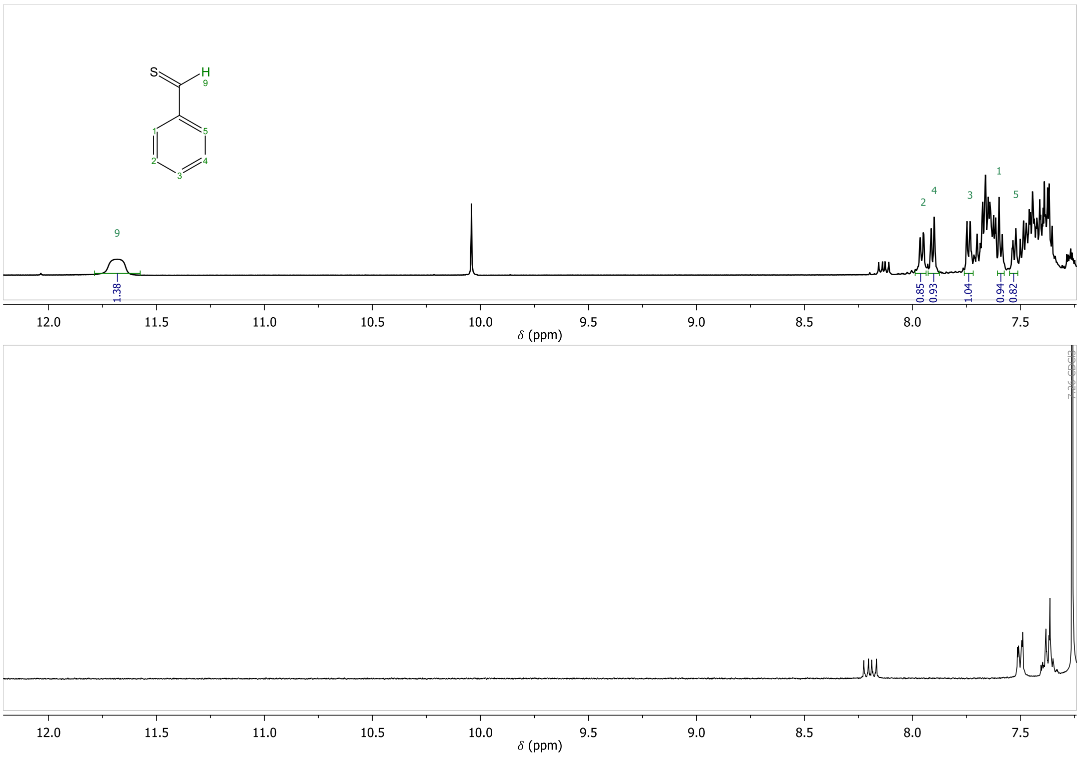

Figure 5.15.: ^{1}H NMR spectra of **2d** compared at room temperature (bottom spectra) and 100 °C (upper spectra).

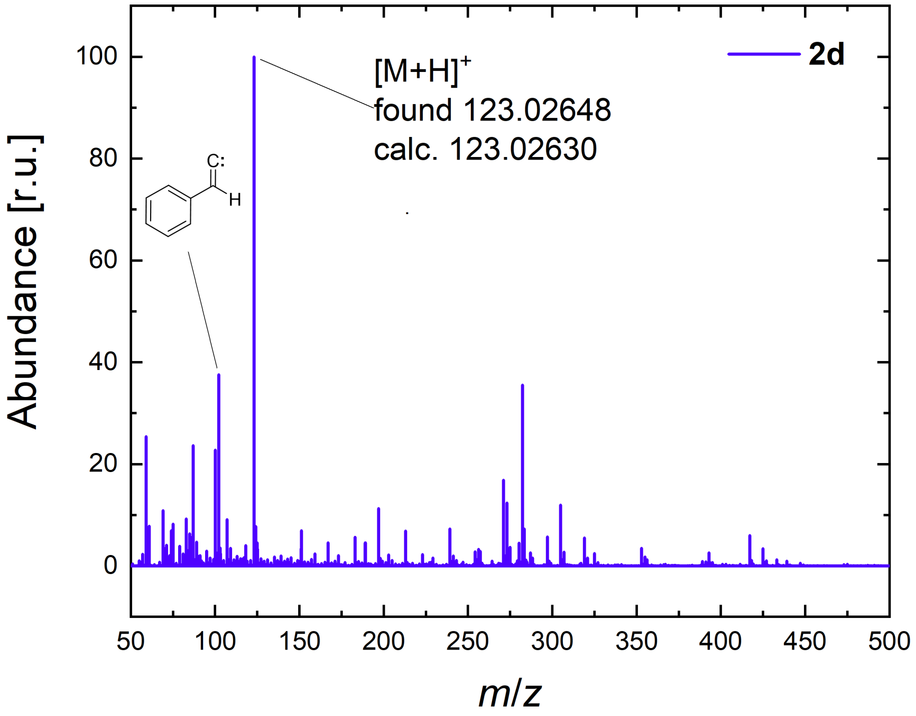

Figure 5.16.: ESI-MS of **2d**.

5.5.2. Synthesis of thionorbornenes

In a pressure tube, the corresponding thioketone (1.0 eq , Table 5.4) was dissolved in dichloromethane (0.7 M). Freshly distilled cyclopentadiene (5.0 eq) was added and the mixture was allowed to stir. Subsequently, the solvent was removed under reduced pressure and the residue purified *via* column chromatography using a mixture of cyclohexane and ethyl acetate (70:30) as eluent.

Table 5.4.: Reaction conditions for the synthesis of TNbs.

Target compound	**Mass** (g)	**Moles** (mmol)	**Solvent**	**Solvent** (mL)	**Reaction time** (h)	**Temperature** (°C)
3a	1	5.05	DCM	7.0	2	25
3c	1	6.02	DCM	8.9	72	25
3d	1	8.20	Toluene	11.7	2	110

3a: R_f = 0.33 (cyclohexane:EtOAc 40:1), , ^{1}H NMR (500 MHz, CDCl$_3$): δ = 8.00−7.00 (m, 10 H; Ar), 6.39 (dd, ^3J = 5.4 Hz, 2.8 Hz, 1 H; =C**H**-CH-S-), 5.58 (dd, ^3J = 5.4 Hz, 3.2 Hz, 1 H; -C**H**=CH-CH-S-), 4.21 (m, 1 H; -C**H**-S-), 4.12 (m, 1 H; -S-C-C**H**-), 2.13 (app d, ^2J = 9.1 Hz, 1 H; bridge), 1.93 (app dt, ^2J = 9.1 Hz, ^3J = 2.3 Hz, 1 H; bridge). HRMS (ESI) *m*/*z*: [M+H]$^+$ calc. for $C_{18}H_{16}S$: 265.10455, found: 265.10463.

Monomer **3a** was synthesised by Kieron Laqua, a bachelor student under the co-supervision of Federico Ferrari and Dr. Roman Nickisch. The author conducted the planning of the synthetic pathway, the final evaluation of the results and the purification of the molecule.

3c: R_f = 0.62 (cyclohexane:EtOAc 40:1), ^{1}H NMR (500 MHz, CDCl$_3$): δ = 6.33 (dd, ^3J = 5.5 Hz, 2.8 Hz, 1 H; =C**H**-CH-S-), 5.96 (dd, ^3J = 5.5 Hz, 3.2 Hz, 1 H; -C**H**=CH-CH-S-), 3.91 (app s, 1 H; -C**H**-S-), 3.52 (app s, 1 H; -S-C-C**H**-), 2.21 (m, 1 H; bridge), 2.04 (app dt, ${}^{2}J$ = 12.6 Hz, ${}^{3}J$ = 2.5 Hz, 1 H; bridge), 1.85 (m, 14 H; adamantyl). HRMS (ESI) *m*/*z*: $[M+H]^+$ calc. for $C_{15}H_{20}S$: 233.13585, found: 233.13589.

3d: R_f = 0.60 (cyclohexane:EtOAc 40:1), ^{1}H NMR (500 MHz, $CDCl_3$): δ = 7.56–7.1 (m, 5H; Ar), 6.52 (dd, ${}^{3}J$ = 5.5 Hz, 2.9 Hz, 1 H; =C**H**-CH-S- *exo*), 6.41 (dd, ${}^{3}J$ = 5.5 Hz, 2.8 Hz, 1 H; =C**H**-CH-S- *endo*), 6.14 (dd, ${}^{3}J$ = 5.5 Hz, 3.2 Hz, 1 H; -S-C**H**-CH- *endo*), 5.53 (dd, ${}^{3}J$ = 5.5 Hz, 3.1 Hz, 1 H; -C**H**=CH-CH-S- *exo*), 4.93 (d, ${}^{3}J$ = 3.8 Hz, 1 H; -S-C**H**-CH- *exo*), 4.22 (app s, 1 H; -C**H**-S- *endo*), 4.15 (app s, 1 H; -C**H**-S- *exo*), 4.03 (app s, 1 H; -S-CH-C**H**-CH= *endo*), 3.57 (app dd, ${}^{3}J$ = 3.3 Hz, 1.7 Hz, 1 H; -S-CH-C**H**-CH= *exo*), 3.26 (app d, ${}^{3}J$ = 1.6 Hz, 1 H; -S-CH-C**H**-CH= *endo*), 1.89 (app d, ${}^{2}J$ = 9.4 Hz, 1 H; bridge *endo*), 1.82 (app d, ${}^{2}J$ = 9.0 Hz, 1 H; bridge *exo*), 1.77 (app dt, ${}^{2}J$ = 9.0 Hz, ${}^{3}J$ = 2.3 Hz, 1 H; bridge *exo*), 1.62 (m, 1 H; bridge *endo*). HRMS (ESI) *m*/*z*: $[M+H]^+$ calc. for $C_{15}H_{20}S$: 233.13585, found: 233.13589.

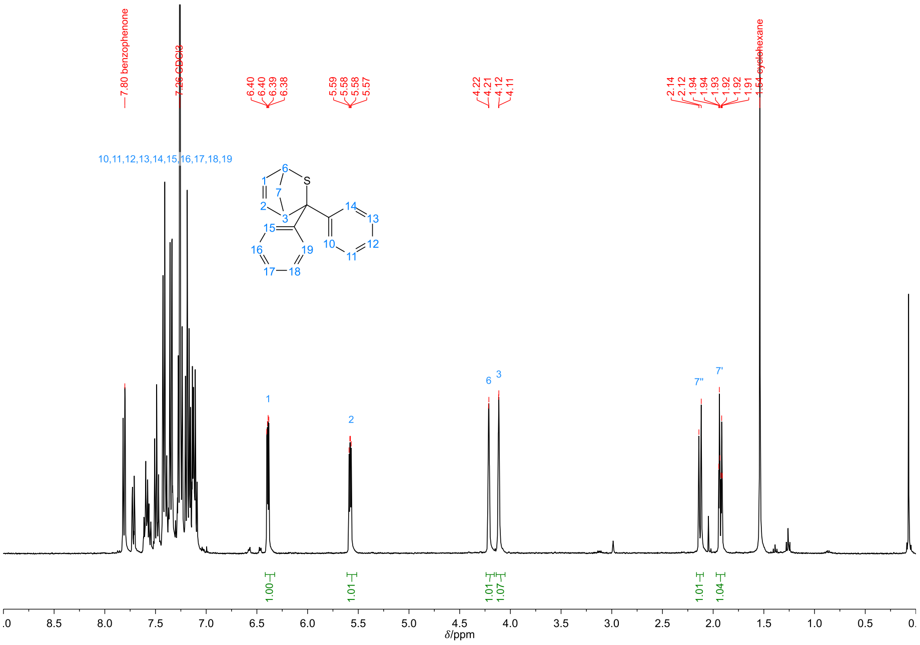

Figure 5.17.: ^{1}H NMR spectrum of **3a**.

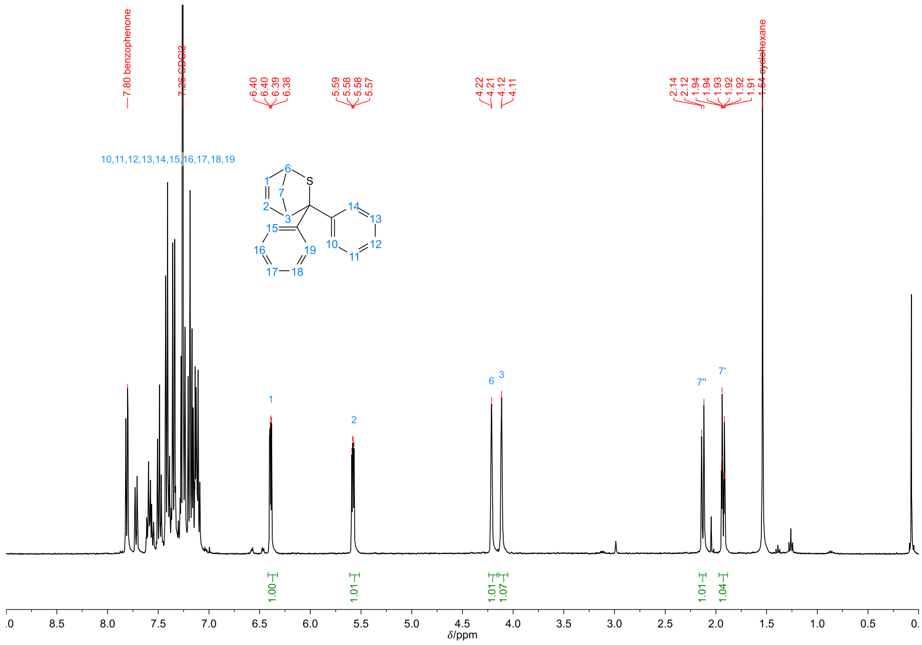

Figure 5.18.: ^{13}C NMR spectrum of **3a**.

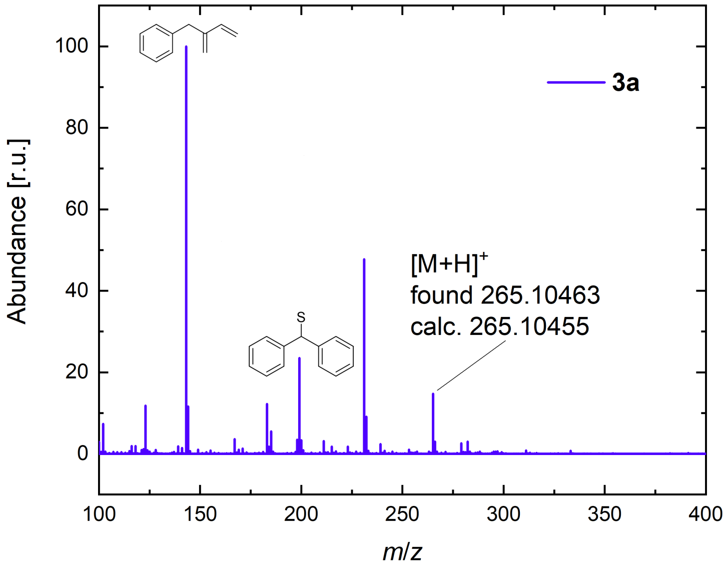

Figure 5.19.: ESI-MS of **3a**.

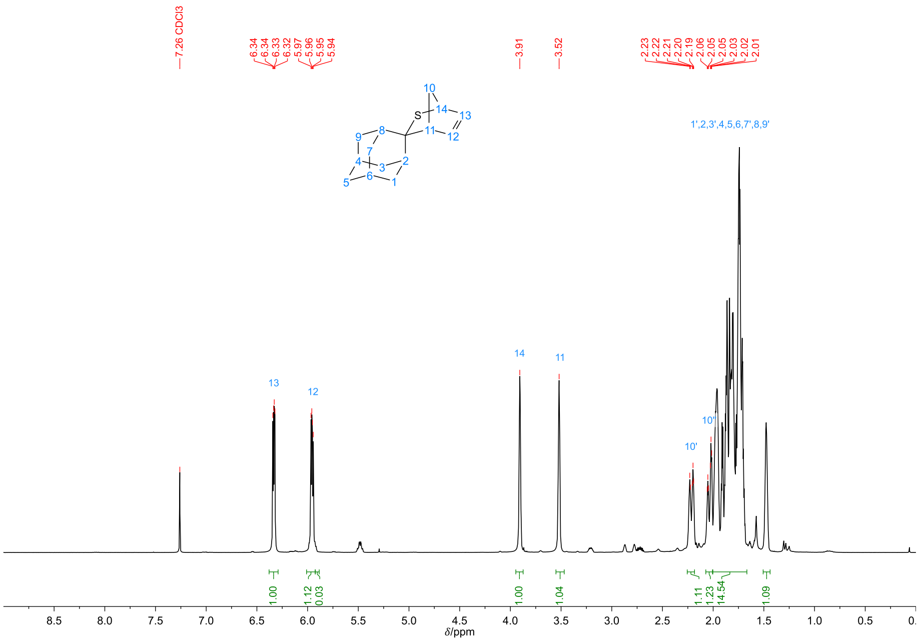

Figure 5.20.: ^{1}H NMR spectrum of **3c**.

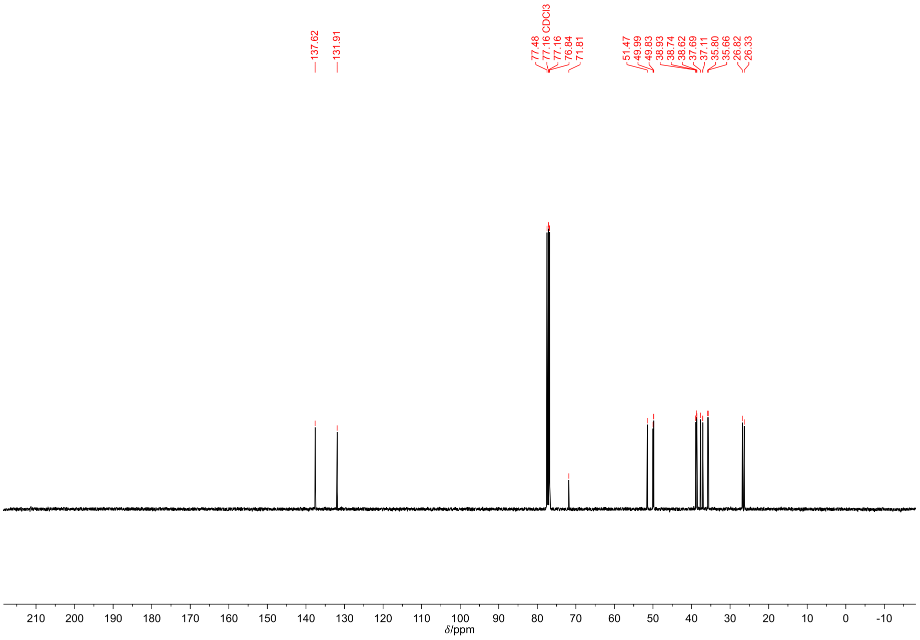

Figure 5.21.: ^{13}C NMR spectrum of **3c**.

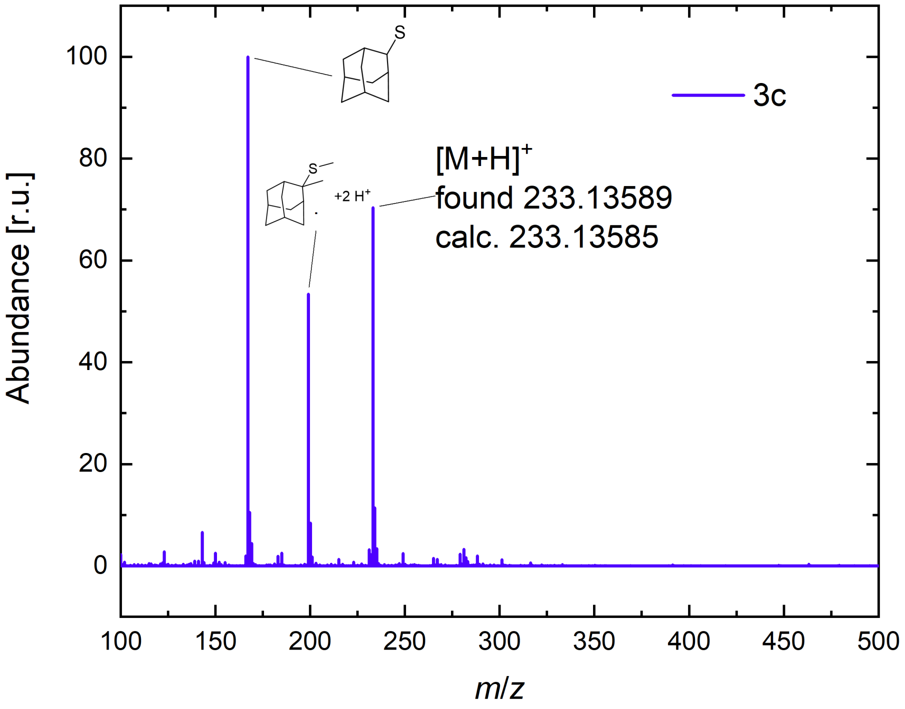

Figure 5.22.: ESI-MS of **3c**.

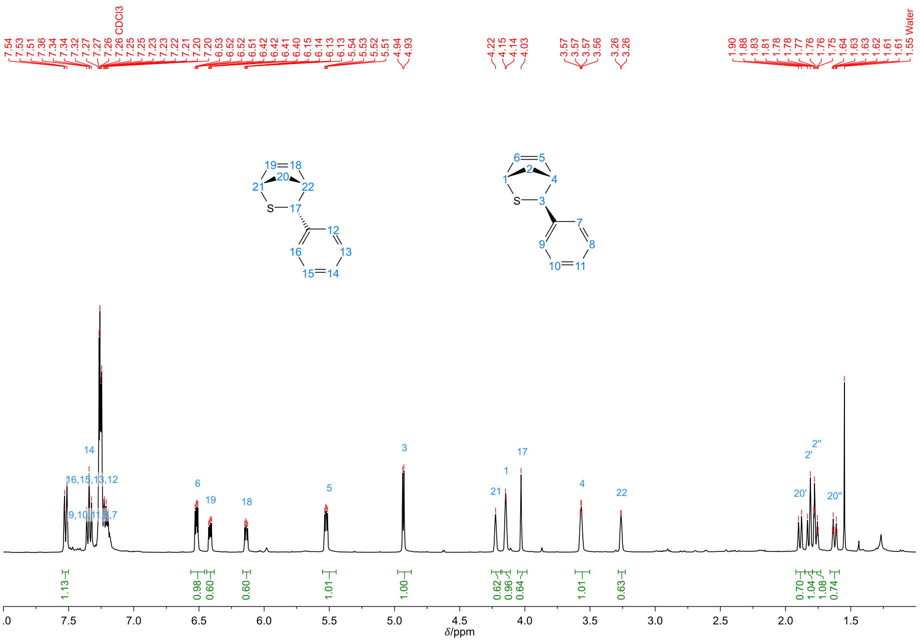

Figure 5.23.: ^{1}H NMR spectrum of **3d** as a mixture of *endo* and *exo* isomers.

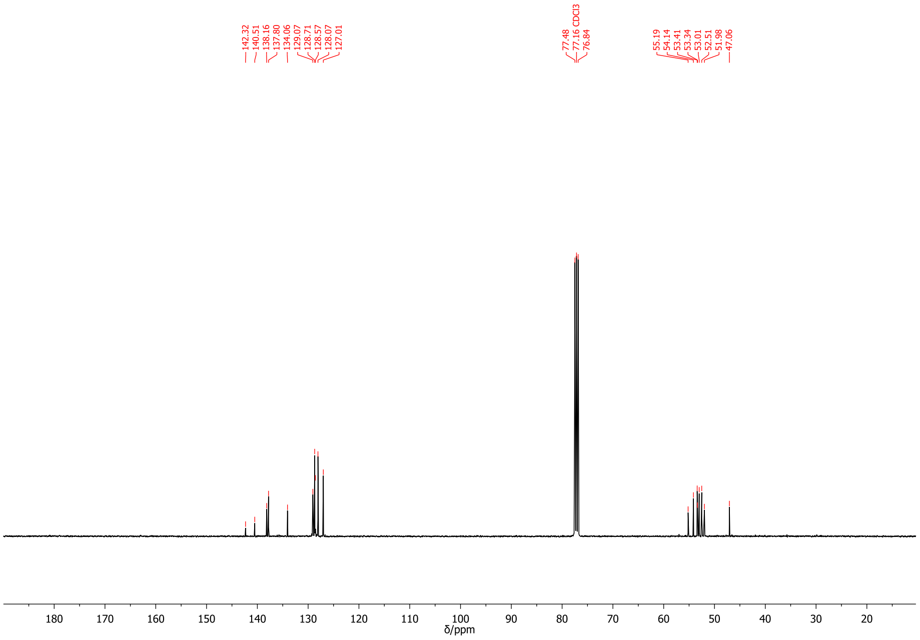

Figure 5.24.: ^{13}C NMR spectrum of **3d**.

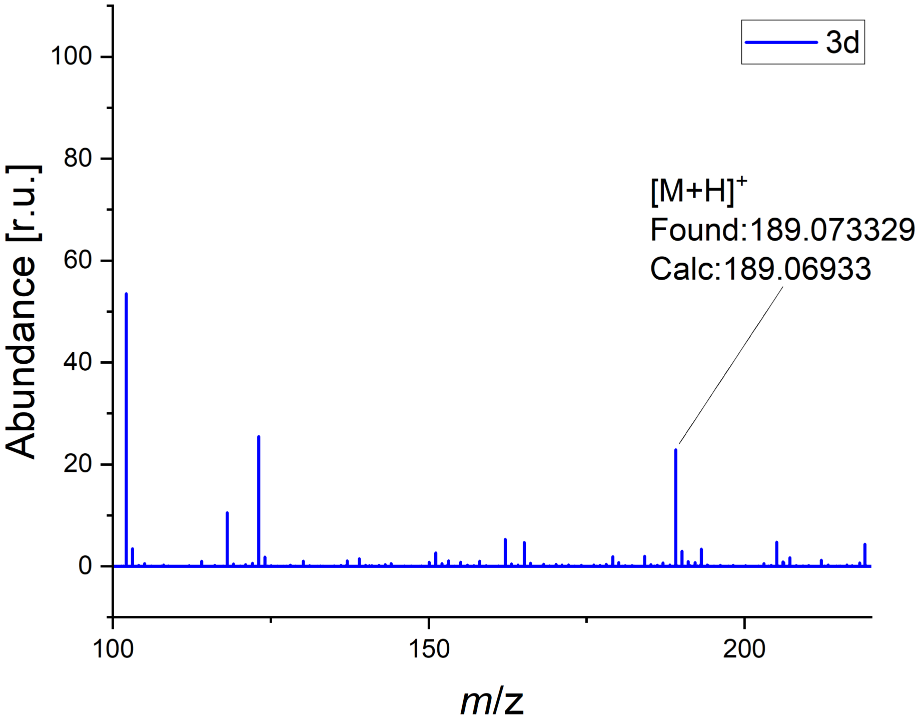

Figure 5.25.: ESI-MS of **3d**.

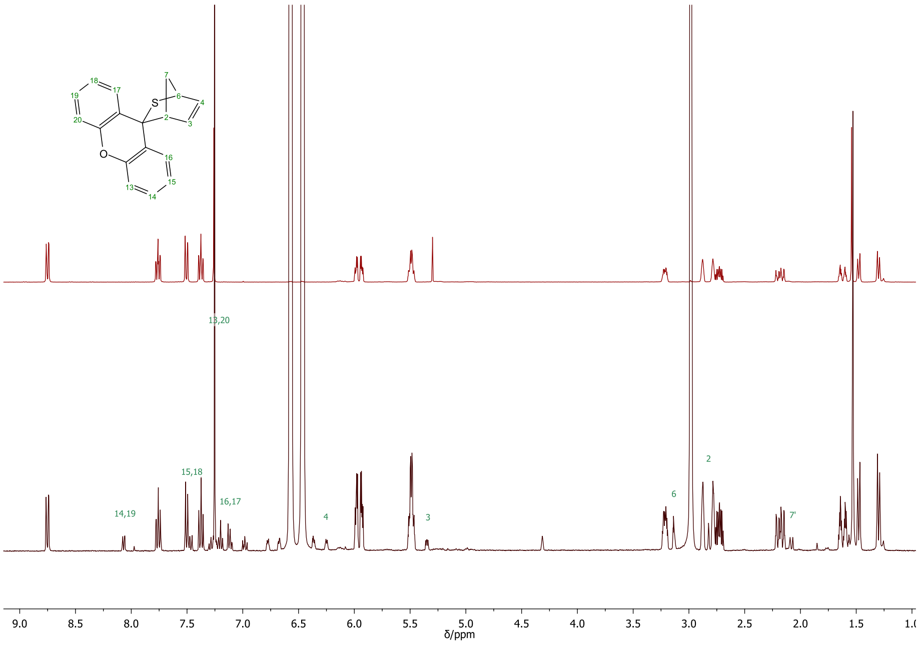

Figure 5.26.: ^{1}H NMR spectra of **3b** before and after removal of the solvent under reduced pressure.

5.5.3. Synthesis of 4a

In a round bottom flask **3a** (1 g, 3.78 mmol, 1.00 eq) and dry DCM (200 mL, 5 mg/mL) were added. The flask was then placed in a cold bath (ca. −78 °C, formed with dry ice and acetone). After bubbling argon through the reaction mixture, mCPBA (1.63 g, 9.45 mmol, 2.50 eq) was added. The reaction was allowed to warm up to room temperature under constant stirring. Subsequently, the reaction mixture was concentrated under reduced pressure and purified *via* column chromatography using a mixture of petroleum ether and triethylamine (3 vol%).

R_f = 0.30 (petroleum ether and triethylamine (3 vol%)

^{1}H NMR (400 MHz, CDCl$_3$): δ = 8.00–7.00 (m, 10 H; Ar), 6.20 (dd, ^3J = 5.7 Hz, 3.1 Hz, 1 H; =C**H**-CH-S-), 6.11 (dd, ^3J = 5.7 Hz, 3.1 Hz, 1 H; -C**H**=CH-CH-S-), 4.14 (m, 1 H; -C**H**-S-), 3.98 (m, 1 H; -S-C-C**H**-), 2.56 (app d, ^2J = 11.3 Hz, 1 H; bridge), 2.31 (app dt, ^2J = 11.3 Hz, ^3J = 3.8 Hz, 1 H; bridge).

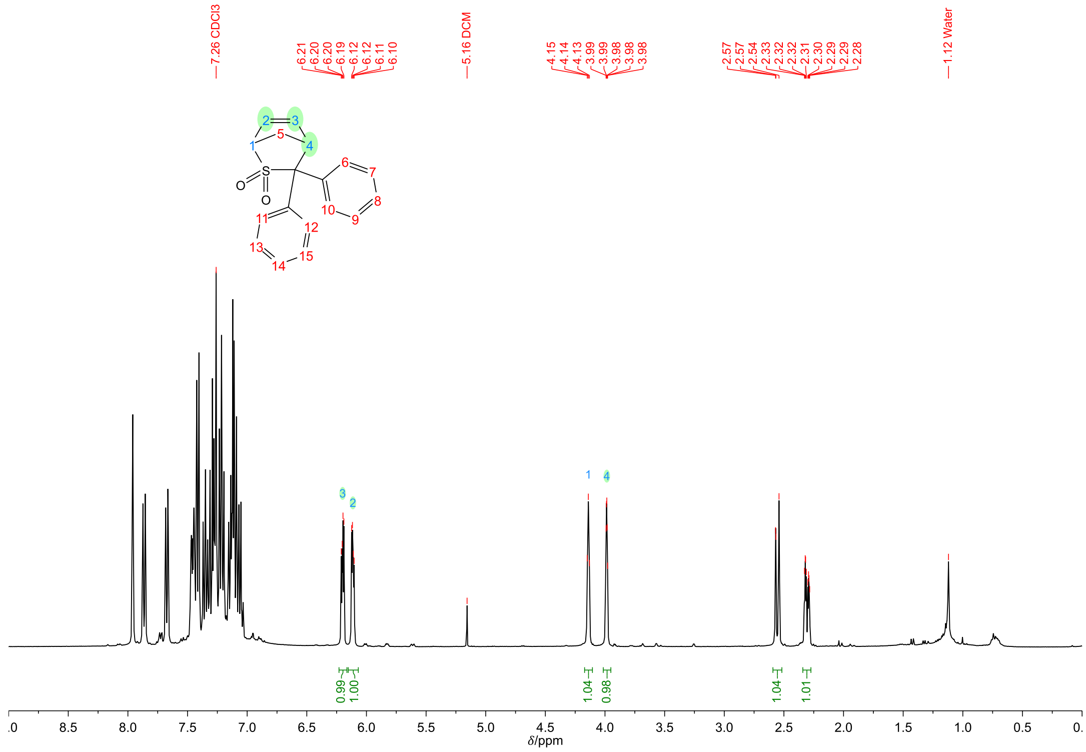

Figure 5.27.: ^{1}H NMR spectrum of **4a**.

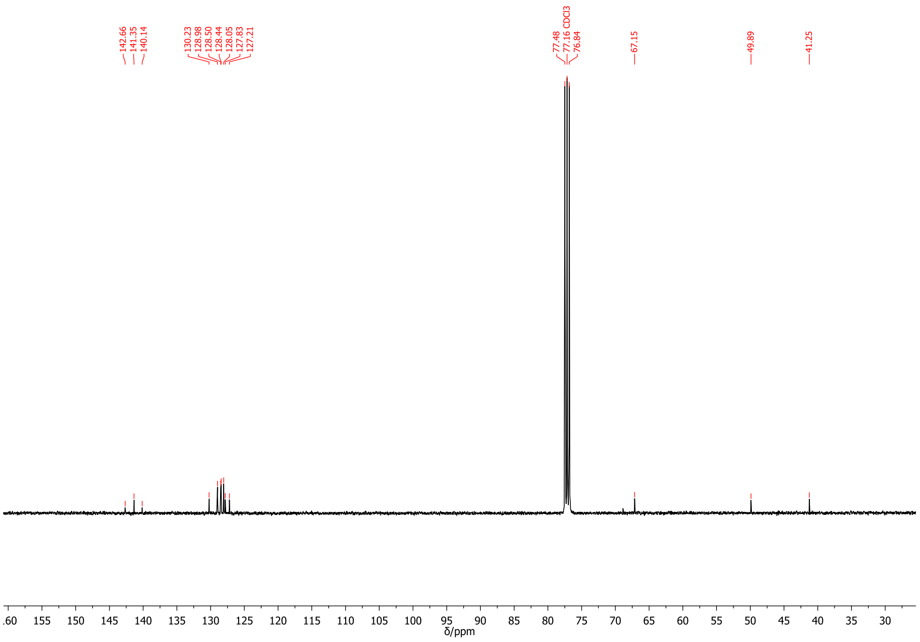

Figure 5.28.: ^{13}C NMR spectrum of **4a**.

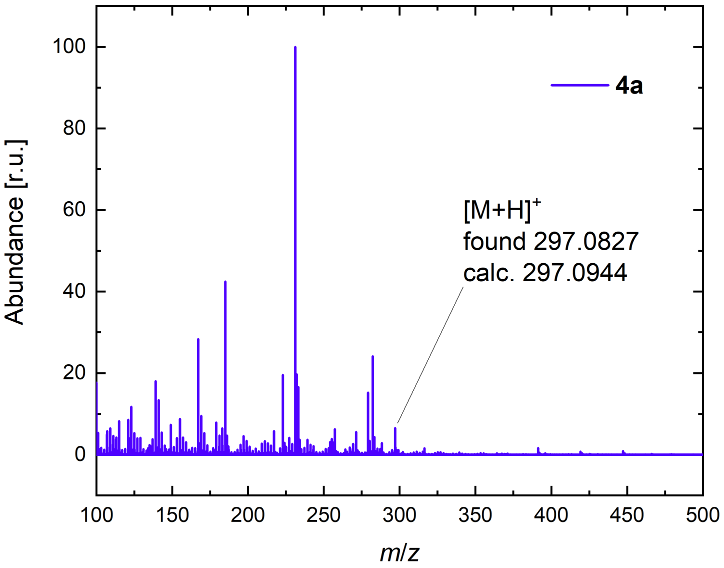

Figure 5.29.: ESI-MS of **4a**.

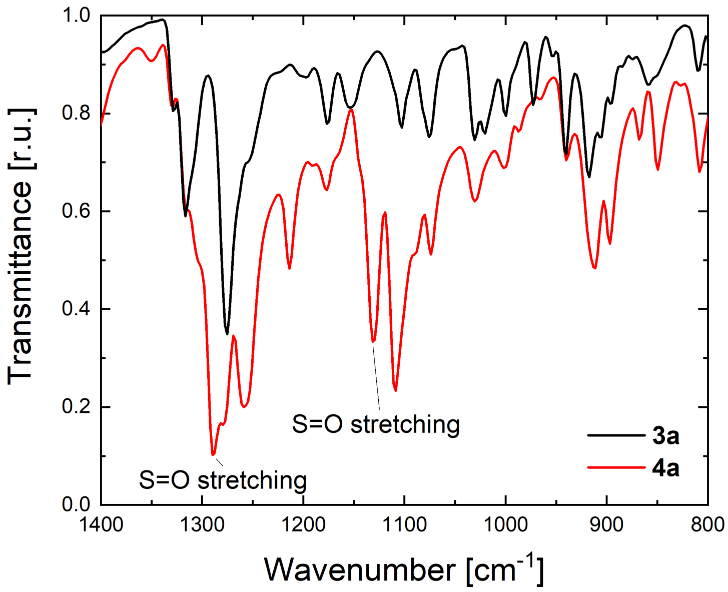

Figure 5.30.: IR spectra of **4a** and **3a**.

5.5.4. Polymerisations of thionorbornenes

For a typical ROMP, the monomer (20 mg, 1.0 eq , **Table 5.5**) was dissolved in dry DCM (4 mL) inside a flame-dried round bottom flask. The solution was then bubbled with argon and the catalyst (0.1 eq) was added *via* a stock solution prepared with 5 mg of catalyst in 2 mL of degassed DCM. The reaction was allowed to stir at 25 °C for one hour. Then, an excess of ethyl vinyl ether was added to quench the polymerisation. The mixture was then concentrated under reduced pressure. Removal of residual monomer was achieved by column chromatography using a mixture of cyclohexane:ethyl acetate 40:1 while metal residues were removed by filtering through a DMT-functionalised silica column.[286]

Table 5.5.: Reaction conditions for the synthesis of homopolymers.

Monomer	**Moles** (mmol)	**Stock solution** (mL)	**Catalyst** (mg)
3a	0.075	0.27	0.63
3c	0.086	0.30	0.76
3d	0.11	0.37	0.94
4a	0.067	0.24	0.59

Polymer p(**3a**) was synthesised by Kieron Laqua, a bachelor student under the co-supervision of Federico Ferrari and Dr. Roman Nickisch. The author conducted the planning of the synthetic pathway, the final evaluation of the results and the purification of the molecule.

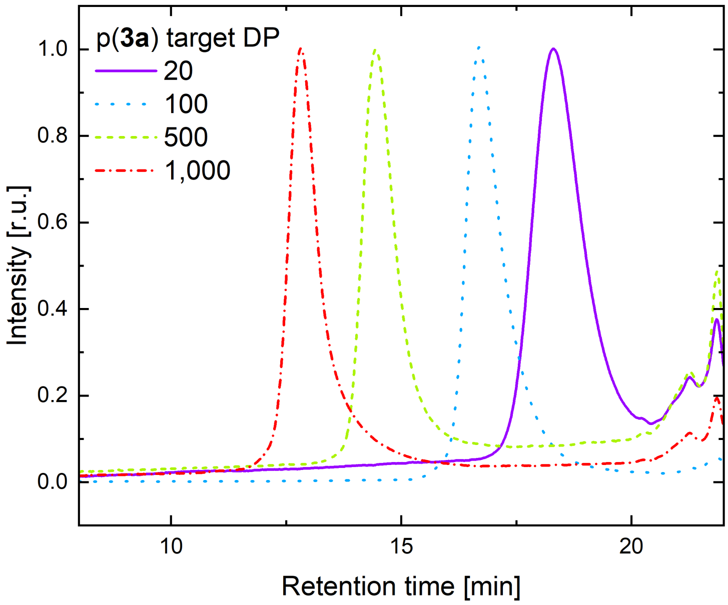

Target DP	**Conversion** (%)	**M_n** (kg mol^{-1})	**Đ**
20	97	6	1.16
100	99	16	1.21
500	99	100	1.21
1000	99	350	1.26

Figure 5.31.: SEC curves and results from the polymerisation of **3a** catalysed by G3, targeting different DPs by variation of the catalyst concentration.

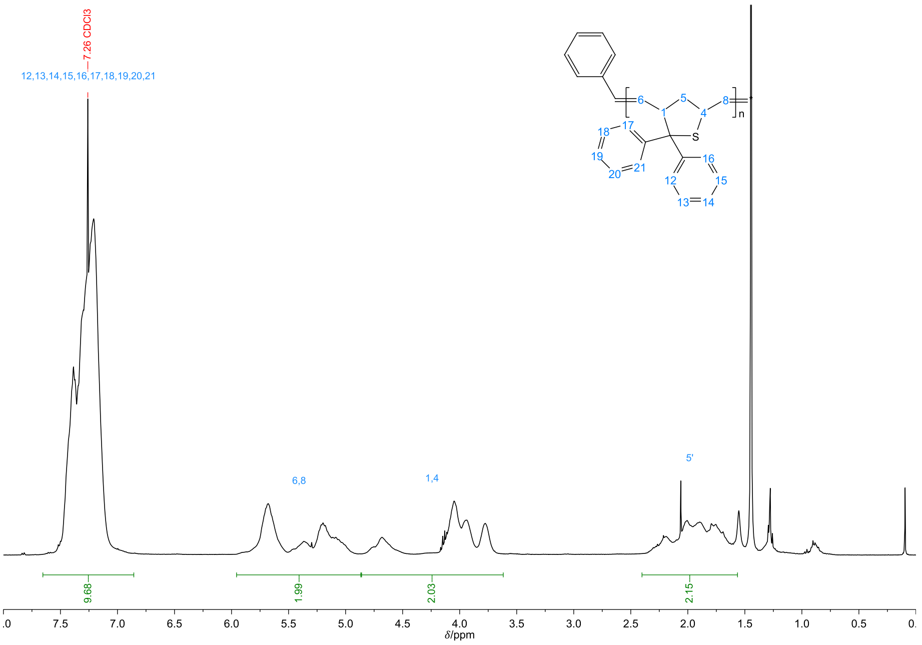

Figure 5.32.: ^{1}H NMR spectrum of p(**3a**).

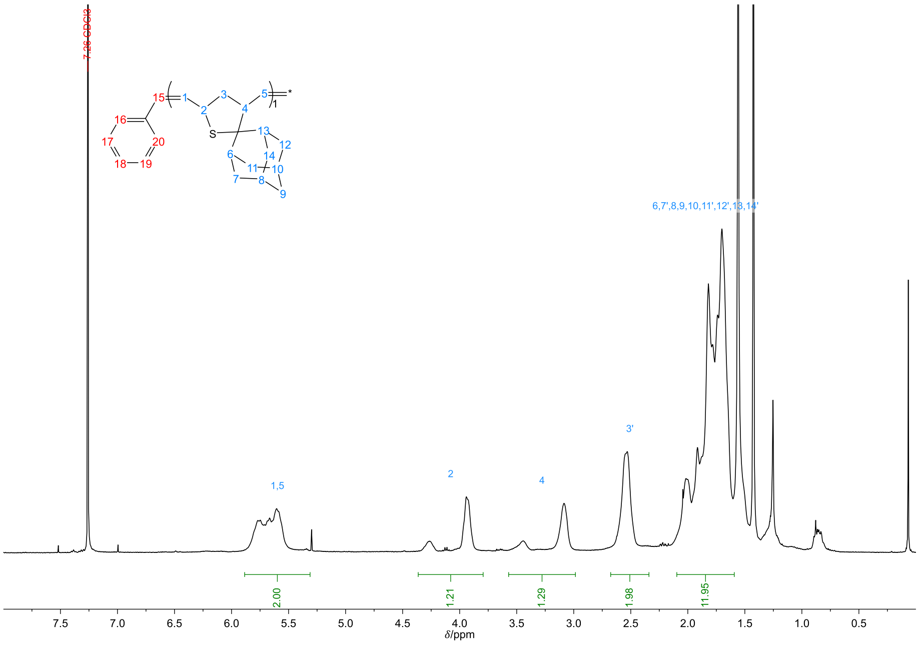

Figure 5.33.: ^{1}H NMR spectrum of p(**3c**).

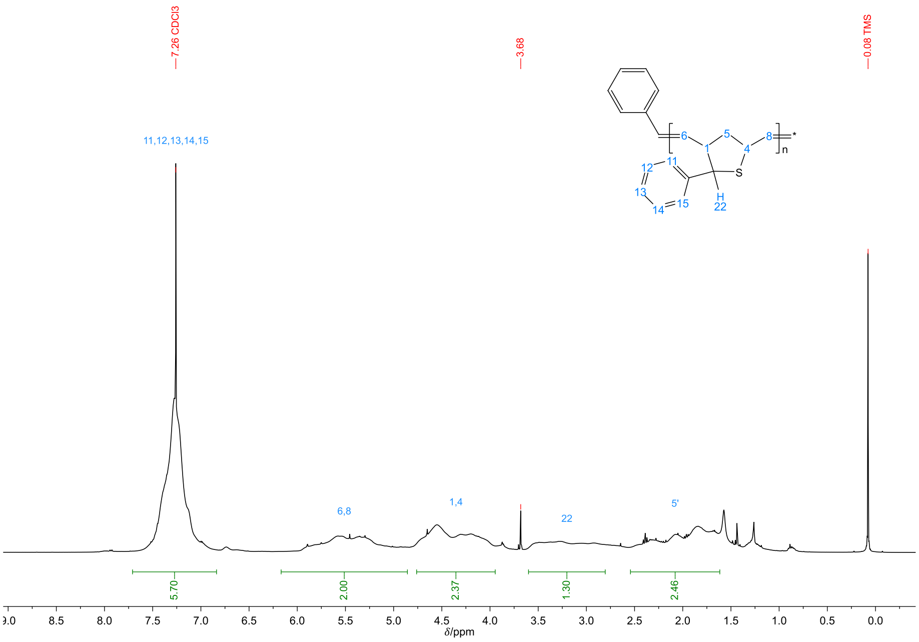

Figure 5.34.: ^{1}H NMR spectrum of p(**3d**).

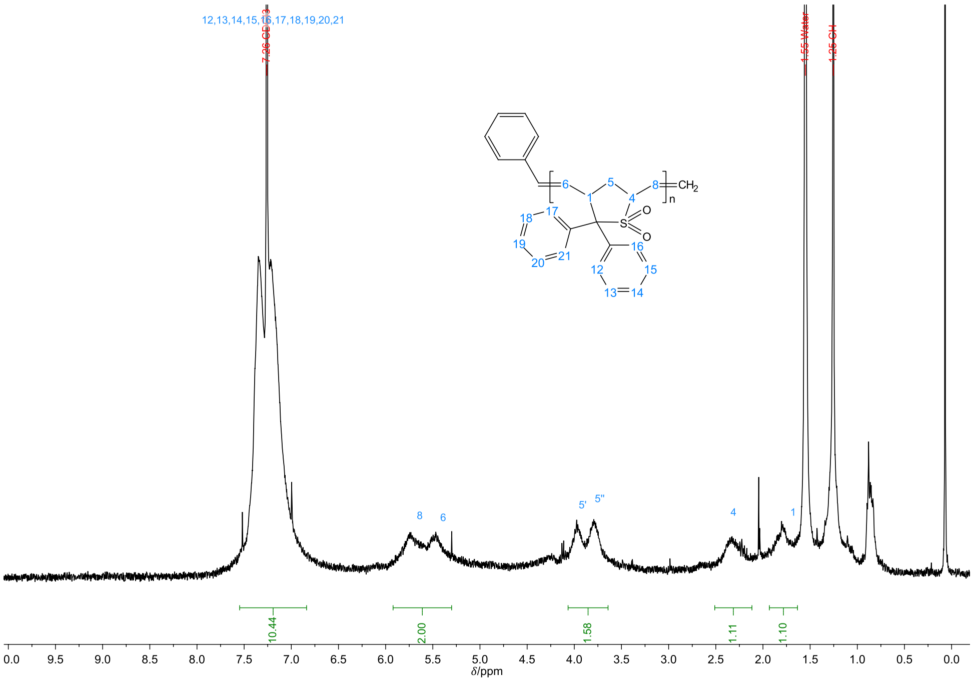

Figure 5.35.: ^{1}H NMR spectrum of p(**4a**)i.

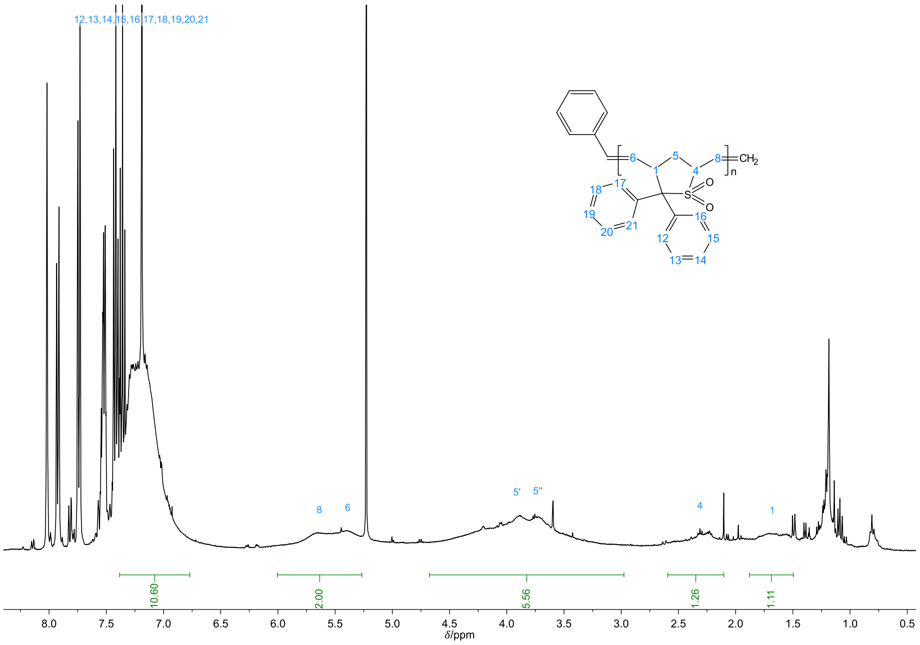

Figure 5.36.: ^{1}H NMR spectrum of p(**4a**)ii (prior to purification).

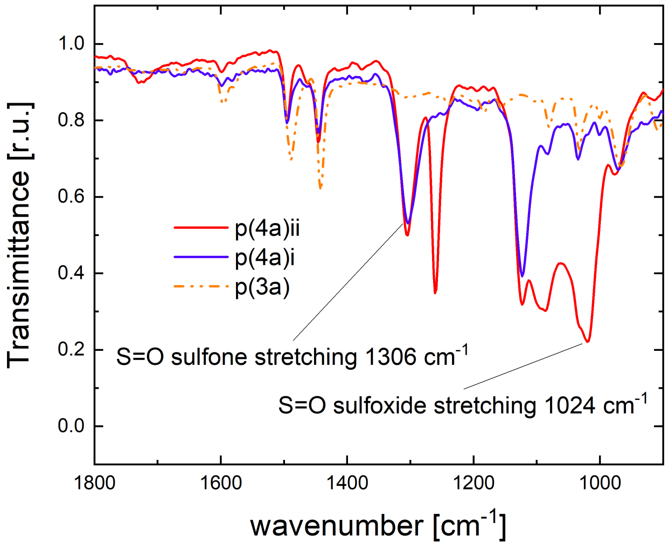

Figure 5.37.: IR spectra of p(**3a**), p(**4ai**) and p(**4aii**).

For the synthesis of p(**3b**), in a round bottom flask, thioketone **3b** (500 mg, 1.0 eq , 2.36 mmol) and freshly distilled cyclopentadiene (7.78 g,50 eq , 118 mmol, 9.72 mL) were allowed to stir for 30 minutes. Then, the catalyst (20 mg, 0.1 eq , 0.024 mmol) was added as a stock solution prepared with 40 mg of G3 in 2 mL of degassed DCM. The reaction was allowed to stir at 25 °C for one hour. Then, an excess of ethyl vinyl ether was added to quench the polymerisation. The mixture was then concentrated under reduced pressure. Removal of residual monomer was achieved by column chromatography using a mixture of cyclohexane:ethyl acetate 40:1 while metal residues were removed by filtering through a DMT-functionalised silica column.[286]

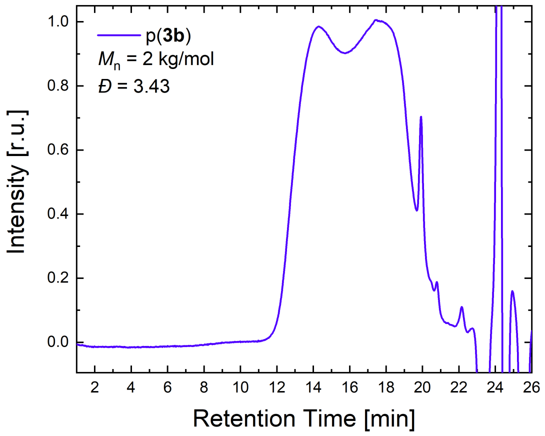

Figure 5.38.: SEC of p(**3b**) on a system equipped with columns for low molecular weight polymers.

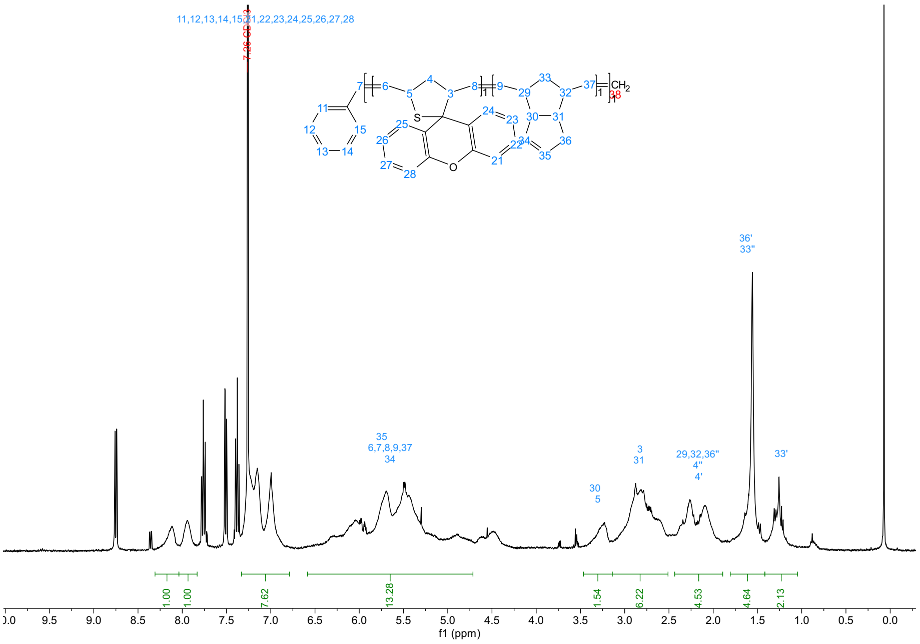

Figure 5.39.: ^{1}H NMR spectrum of p(**3b**).

The synthesis of the block copolymer p(**3a**-*b*-**4a**) was as follows. Monomer **3a** (20 mg, 1.0 eq , 0.075 mmol) was dissolved in dry DCM (4 mL) in a flame-dried round bottom flask. The solution was then bubbled with argon and placed in an acetone/dry ice bath at −15 °C. The catalyst (1.25 mg, 0.1 eq) was then added from a stock solution prepared with 2.5 mg of G3 in 2 mL of degassed DCM. The reaction was allowed to stir at −15 °C for six hours. A small aliquot (0.1 mL) was removed from the reaction for SEC analyses before a solution of **4a** (20 mg, 1.0 eq , 0.067 mmol) in dry DCM (4 mL) was cooled to −15 °C and added to the reaction vessel. The reaction mixture was then allowed to stir for 24 additional hours. Then, an excess of ethyl vinyl ether was added to quench the polymerisation. The mixture was then concentrated under reduced pressure. Removal of residual monomer was achieved by column chromatography using a mixture of cyclohexane:ethyl acetate 40:1 while metal residues were removed by filtering through a DMT-functionalised silica column.[286]

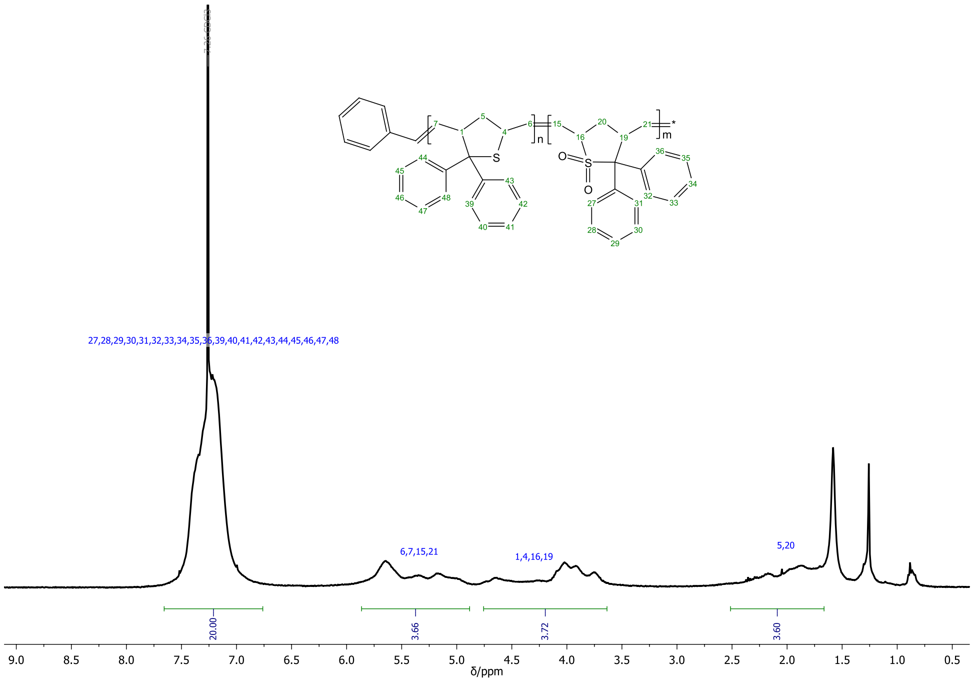

Figure 5.40.: ^{1}H NMR spectrum of copolymer p(**3a**-*b*-**4a**).

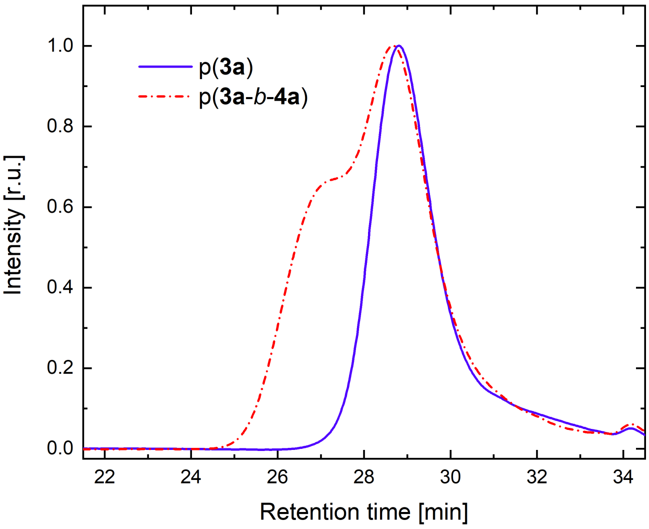

Figure 5.41.: SEC traces of the p(**3a**) homopolymer and the incomplete chain extension with **4a** to obtain p(**3a**-*b*-**4a**) at room temperature.

The synthesis of the statistical copolymer p(**3a**-*co*-**4a**) was as follows. Monomer **3a** (20 mg, 1.0 eq , 0.075 mmol) and monomer **4a** (20 mg, 1.0 eq , 0.067 mmol) were dissolved in dry DCM (8 mL) in a flame-dried round bottom flask. The solution was then bubbled with argon and the catalyst (1.25 mg, 0.1 eq) was added from a stock solution prepared with 2.5 mg of G3 in 2 mL of degassed DCM. The reaction was allowed to stir at 25 °C for one hour. Then, an excess of ethyl vinyl ether was added to quench the polymerisation. The mixture was then concentrated under reduced pressure. Removal of residual monomer was achieved by column chromatography using a mixture of cyclohexane:ethyl acetate 40:1 while metal residues were removed by filtering through a DMT-functionalised silica column.[286]

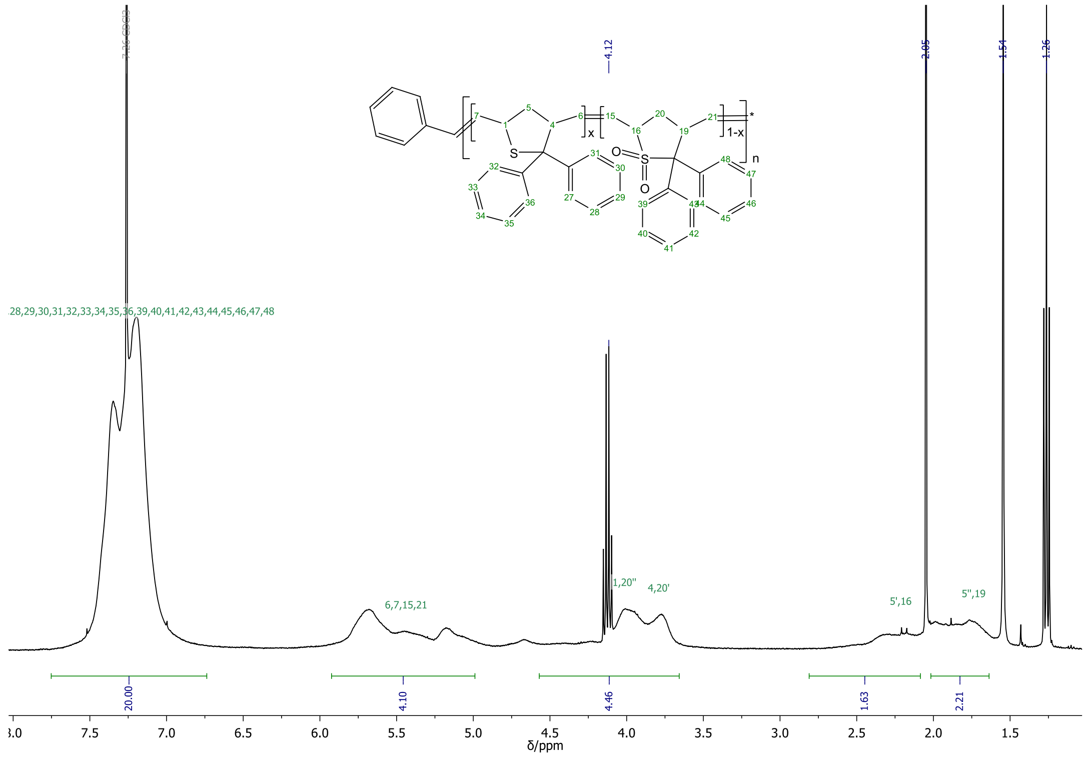

Figure 5.42.: ^{1}H NMR spectrum of copolymer p(**3a**-*co*-**4a)**

5.5.5. Thermal properties of Thionorbornenes derivated polymers.

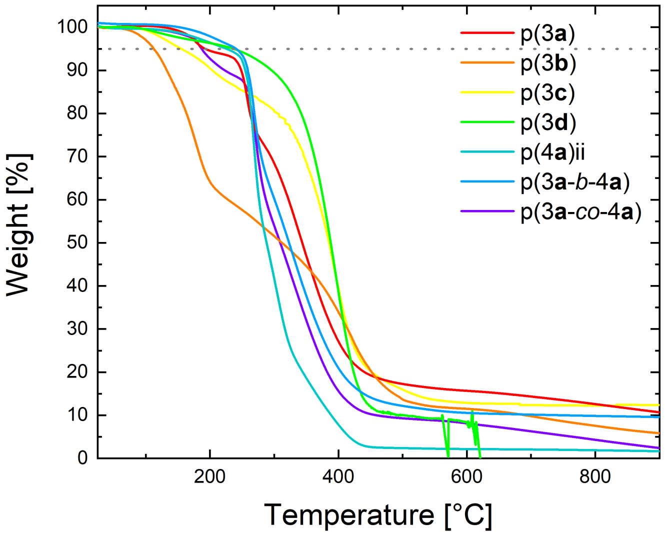

Figure 5.43.: TGA of polymers synthesised in this study. The 5% weight loss line is shown for clarity.

5.5.6. Solubility of Thionorbornenes derivated polymers

Table 5.6.: Solubility of homopolymers and copolymers in common solvents.

Polymers	**DCM**	**Acetone**	**HFIP**	**DMAc**	**THF**	**Hexane**	**Water**
p(**3a**)	✓	✗	✗	✓	✓	✗	✗
p(**3b**)	✓	✗	✗	✓	✓	✗	✗
p(**3c**)	✓	✗	✗	✓	✓	✗	✗
p(**3d**)	✓	✗	✗	✓	✓	✗	✗
p(**3a**-*b*-**4a**)	✓	✗	✓	✓	✓	✗	✗
p(**3a**-*co*-**4a**)	✓	✗	✓	✓	✓	✗	✗
p(**4a**)i	✓	✗	✓	✓	✗	✗	✗

5.5.7. Spectra of Poly(Norbornene) synthesised

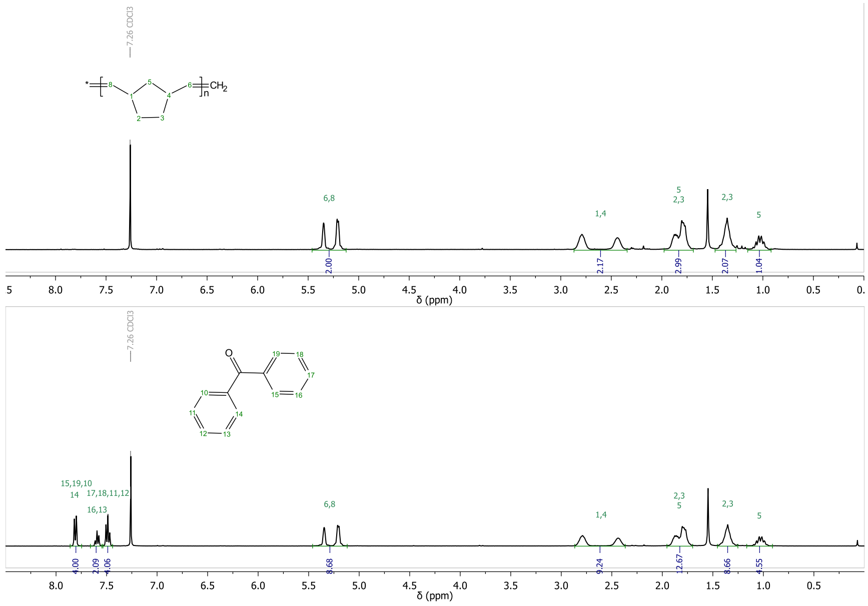

Figure 5.44.: ^{1}H NMR spectra of poly(norbornene) obtained *via* ROMP in the absence (upper spectrum) and the presence (lower spectrum) of 10% mol benzophenone as additive.

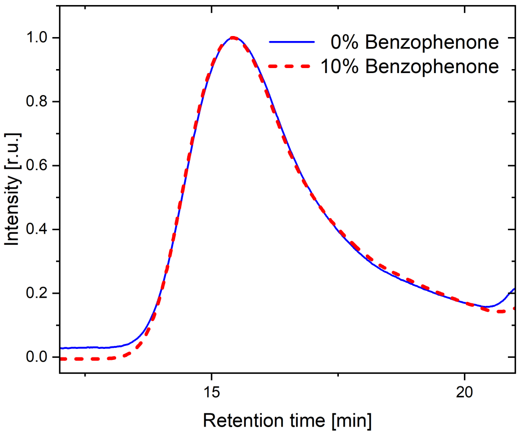

Figure 5.45.: SEC traces of the polymers obtained from the ROMP of norbornene in the absence (blue curve) and the presence (red curve) of 10 mol% of benzophenone.

5.6. Synthesis of Levoglucosenone derivatives

5.6.1. Synthesis of 2-(2-Furyl)-6,8-dioxabicyclo[3.2.1]octan-4-one (**5**)

Dimethyl carbonate (0.2 mL) was added to a crimp-top vial. After degassing *via* argon bubbling, levoglucosenone (65 mg, 0.515 mmol, 1.00 eq), furan (52.5 mg, 0.773 mmol, 1.50 eq) and zinc chloride (3.52 mg, 25.8 µmol, 0.05 eq) were added to the solvent and stirred for 5 days at 55 °C. Subsequently, the solvent was removed under reduced pressure and the mixture was purified *via* column chromatography (3:2 cyclohexane:ethyl acetate). The product was obtained as a colourless liquid with a yield of 72.3%.

^{1}H NMR (400 MHz, CD_2Cl_2): δ (ppm) = 7.39 (1H, d, J = 1.9 Hz, -O-CH=), 1H, dd, J = 3.3, 1.9 Hz, -O-CH=CH-), 6.21 (1H, dt, J = 3.3, 1.1 Hz, -O-C-CH-), 5.09 (1H, s, O=C-CH-), 4.90 (1H, m, -O-CH-CH_2-), 4.16 (1H, dd, J = 7.8, 1.0 Hz, -O-CH_2-CH), 4.04 (1H, dd, J = 7.8, 5.5 Hz, -O-CH_2-CH), 3.53 (1H, app d, J = 8.3 Hz, -O-C-CH-), 3.01 (1H, dd, J = 16.6, 8.4 Hz, O=C-CH_2-), 2.60 (1H, m, O=C-CH_2-).

^{13}C NMR (101 MHz, CD_2Cl_2): δ(ppm) = 199.01, 154.27, 141.90, 110.37, 106.60, 101.70, 75.47, 67.46, 40.55, 34.99.

HRMS (ESI): m/z for $C_{10}H_{10}O_4$ $[M+H]^+$ calculated: 195.06519 found: 195.06513, Δ=0.06 mmu

R_f= 0.55 (3:2 cyclohexane:ethyl acetate) This molecule was synthesised by Luca Heusser, a bachelor student under the co-supervision of Federico Ferrari. The author performed the evaluation on the obtained results and ideated the synthetic pathway.

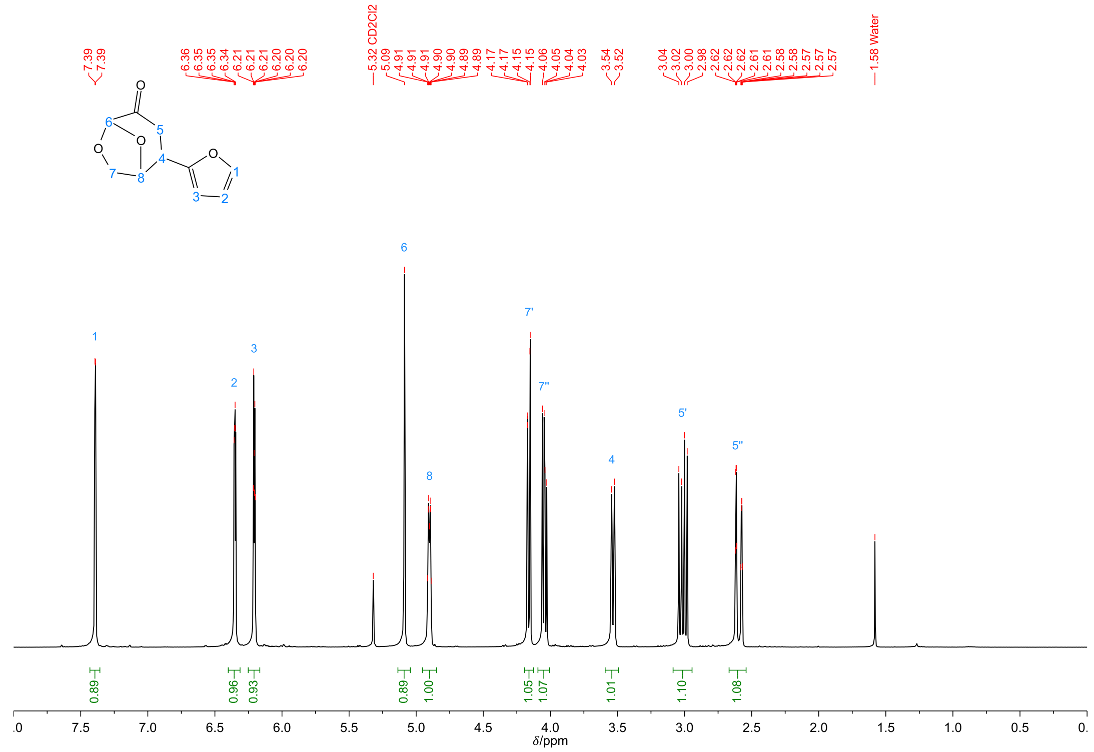

Figure 5.46.: ^{1}H NMR spectrum of **5**.

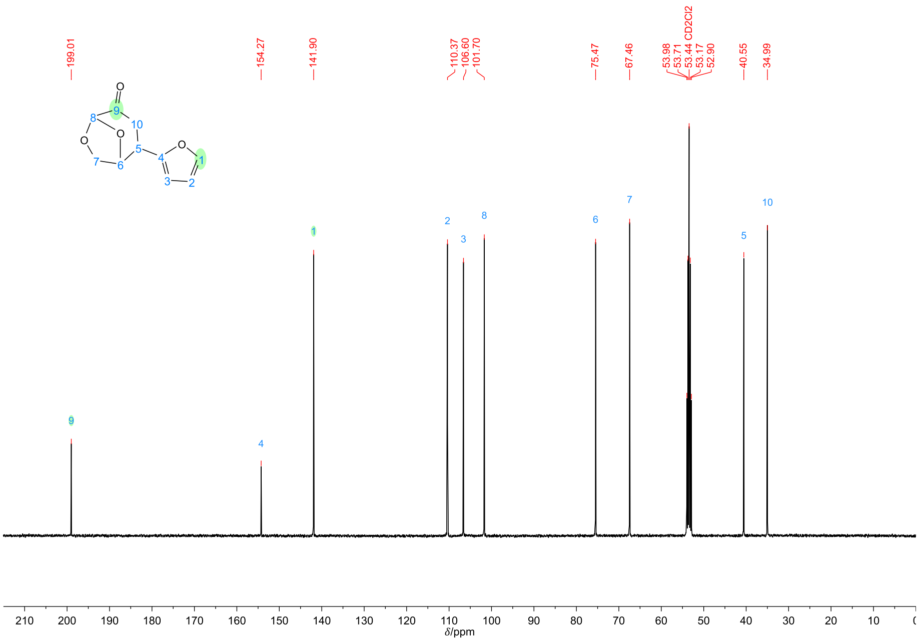

Figure 5.47.: ^{13}C-NMR spectrum of **5**.

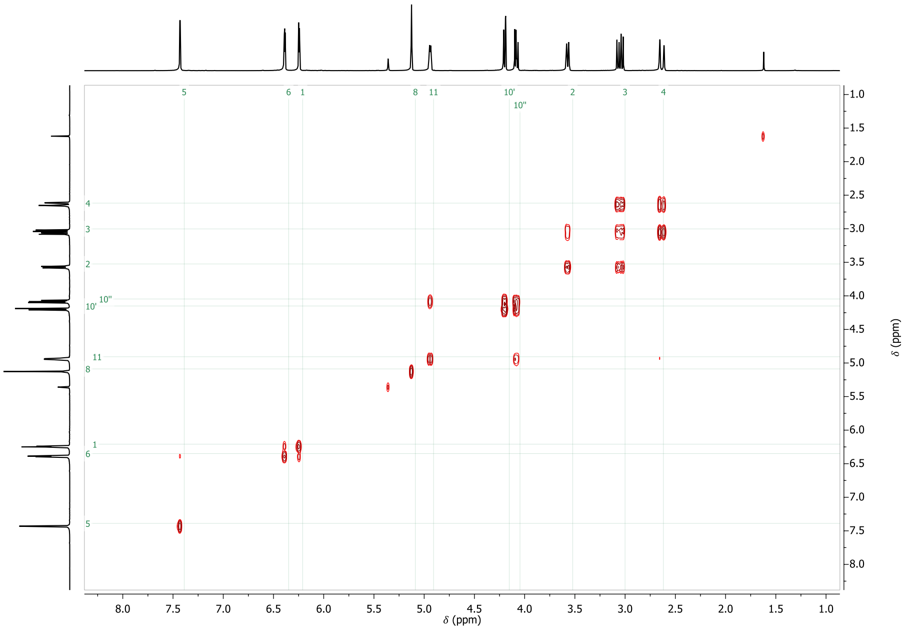

Figure 5.48.: COSY spectrum of **5**.

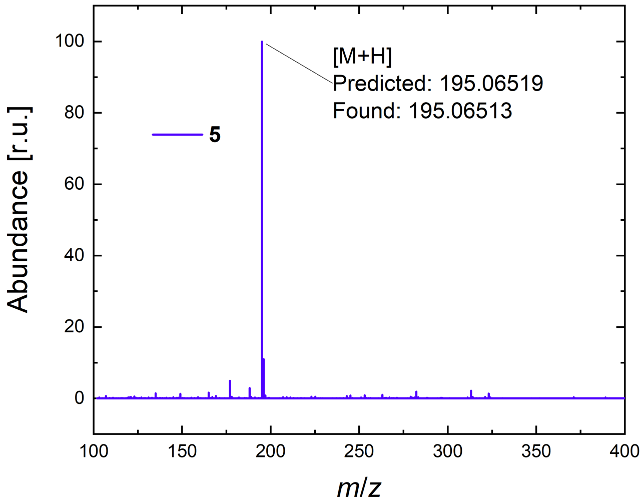

Figure 5.49.: ESI mass spectrum of **5**.

5.6.2. Synthesis of 2-(5-Methyl-2-furyl)-6,8-dioxabicyclo[3.2.1]octan-4-one (6)

In a crimp-top vial, dimethyl carbonate (0.1 mL) was bubbled with argon for 3 minutes. Levoglucosenone (32.5 mg, 0.0258 mmol, 1.00 eq), 2-methylfuran (109 mg, 1.29 mmol, 5.00 eq) and zinc chloride (1.76 mg, 0.0129 mmol, 0.05 eq) were added to the solvent and stirred for 5 days at 55 °C. The solvent was removed under reduced pressure and the mixture purified *via* column chromatography (3:2 cyclohexane:ethyl acetate to 4:1 cyclohexane:ethyl acetate). The product was obtained as a colourless liquid with a yield of 58.2%.

^{1}H NMR (400 MHz, CD_2Cl_2): δ (ppm) = 6.05 (1H, d, J = 3.1 Hz, $CH_3-C=CH$), 5.91 (1H, d, J = 3.1 Hz, $-O-C=CH$), 5.07 (1H, s, $-O-CH-O-$), 4.90 (1H, app d, J = 5.3 Hz, $-O-CH-$), 4.14 (1H, app d, J = 7.7 Hz, $-O-CH_2-$), 4.03 (1H, dd, J = 7.7, 5.2 Hz,

$-O-CH_2-$), 3.47 (1H, app d, J = 8.3 Hz, $-CH=C-CH-$), 2.98 (1H, dd, J = 16.6, 8.3 Hz, $O=C-CH_2$-), 2.57 (1H, dd, J = 16.6, 1.9 Hz, $O=C-CH_2$-), 2.26 (3H, s, $-CH_3$).

^{13}C NMR (101 MHz, CD_2Cl_2): δ (ppm) = 199.21, 152.26, 151.62, 107.32, 106.09, 101.68, 75.45, 67.43, 40.54, 34.95, 13.19.

HRMS (ESI): m/z for $C_{11}H_{12}O_4[M+H]^+$ calculated: 209.08084 found: 209.08064, Δ=0.20 mmu

R_f: 0.67 (3:2 cyclohexane : ethyl acetate)

This molecule was synthesised by Luca Heusser, a bachelor student under the co-supervision of Federico Ferrari. The author performed the evaluation on the obtained results and ideated the synthetic pathway.

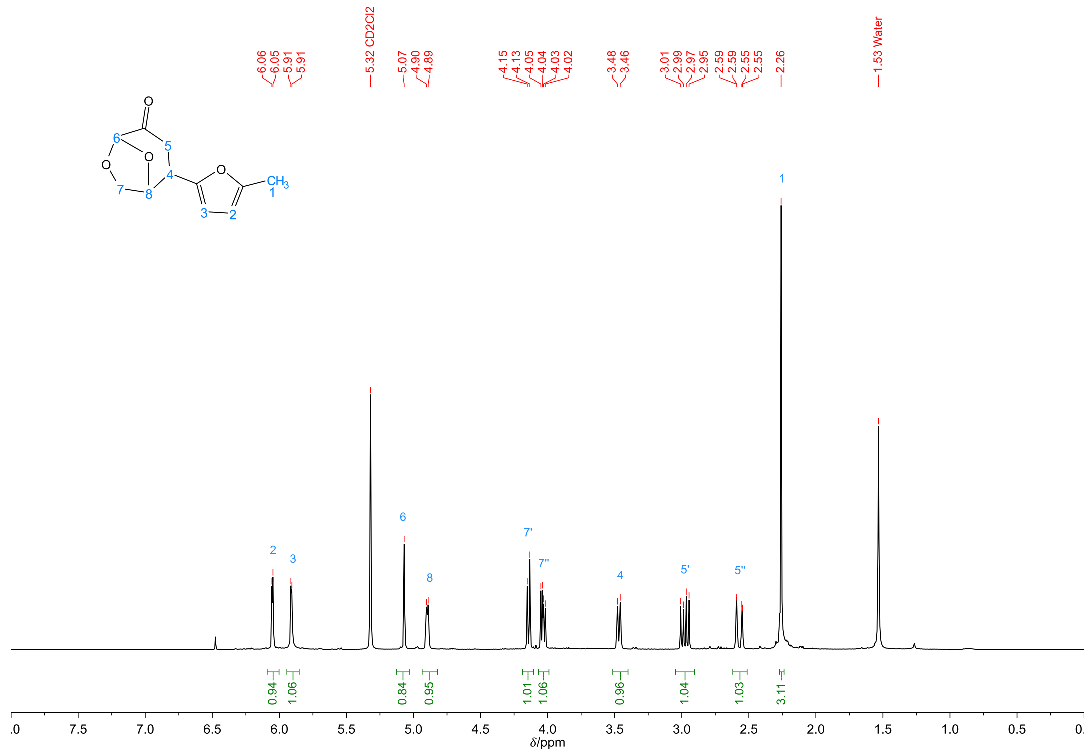

Figure 5.50.: ^{1}H NMR spectrum of **6**.

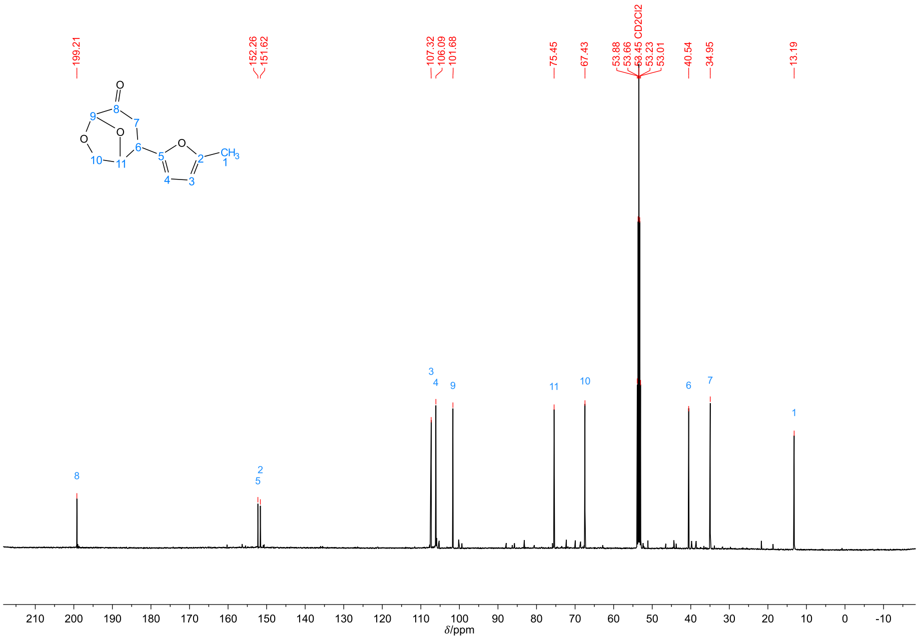

Figure 5.51.: ^{13}C NMR spectrum of **6**.

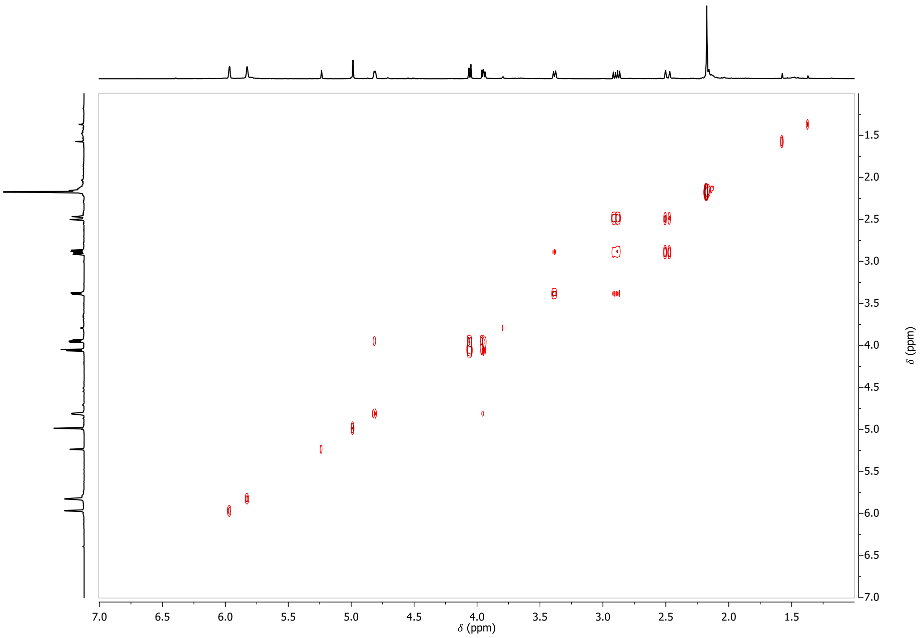

Figure 5.52.: COSY spectrum of **6**.

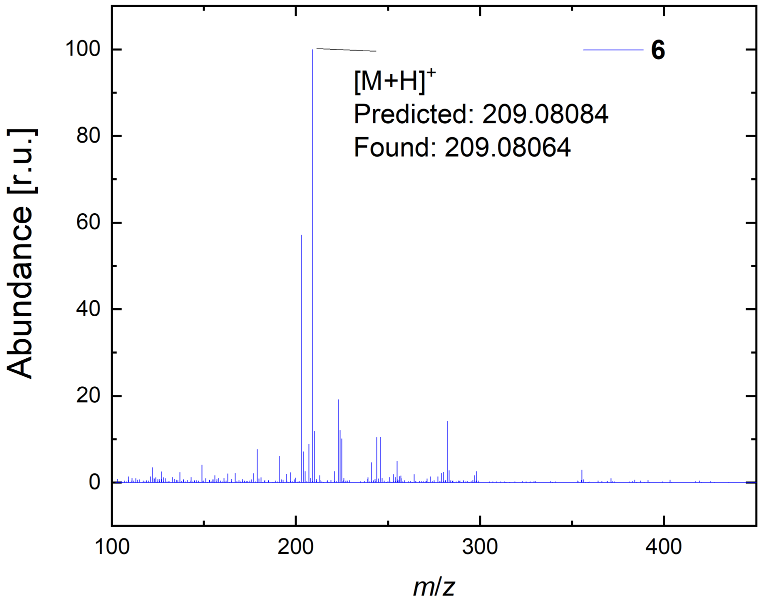

Figure 5.53.: ESI mass spectrum of **6**.

5.6.3. Synthesis of 2-(5-Ethyl-2-furyl)-6,8-dioxabicyclo[3.2.1]octan-4-one (7)

Dimethyl carbonate was added to a crimp-top vial after degassing *via* argon bubbling. Levoglucosenone (32.5 mg, 0.0258 mmol, 1.00 eq), 2-ethylfuran (124 mg, 1.29 mmol, 5.00 eq) and zinc chloride (1.76 mg, 0.0129 mmol, 0.05 eq) were added and stirred for 5 days at 55 °C. The solvent was removed under reduced pressure and the mixture purified *via* column chromatography (3:2 cyclohexane : ethyl acetate; 4:1 cyclohexane : ethyl acetate). The product was obtained as a yellow liquid with a yield of 70.5%.

^{1}H NMR (400 MHz, CD_2Cl_2): δ (ppm) = 6.06 (1H, d, J = 3.1 Hz, $-O-C=CH-$), 5.92 (1H, d, J = 3.1 Hz, $-C=CH-$), 5.07 (1H, s, $-O-CH-O-$), 4.90 (1H, app d, J = 5.5 Hz,

$-O-CH-$), 4.14 (1H, m, $-O-CH_2-$), 4.03 (1H, dd, *J* = 7.7, 5.2 Hz, $-O-CH_2-$), 3.48 (1H, app d, *J* = 8.3 Hz, $-CH=C-CH-$), 2.98 (1H, dd, *J* = 16.6, 8.3 Hz, $O=C-CH_2$-), 2.60 (3H, m, $O=C-CH_2$- and CH_3-CH_2-), 1.21 (3H, t, *J* = 7.6 Hz, $-CH_3$).

^{13}C NMR (101 MHz, CD_2Cl_2): δ (ppm) = 199.22, 157.32, 152.11, 107.09, 104.49, 101.68, 75.44, 67.43, 40.57, 31.95, 21.25, 11.85.

HRMS (ESI): m/z for $C_{12}H_{14}O_4[M+H]^+$ calculated: 223.09649 found: 223.09627, Δ=0.22 mmu

R_f= 0.69 (3:2 cyclohexane : ethyl acetate)

This molecule was synthesised by Luca Heusser, a bachelor student under the co-supervision of Federico Ferrari. The author performed the evaluation on the obtained results and ideated the synthetic pathway.

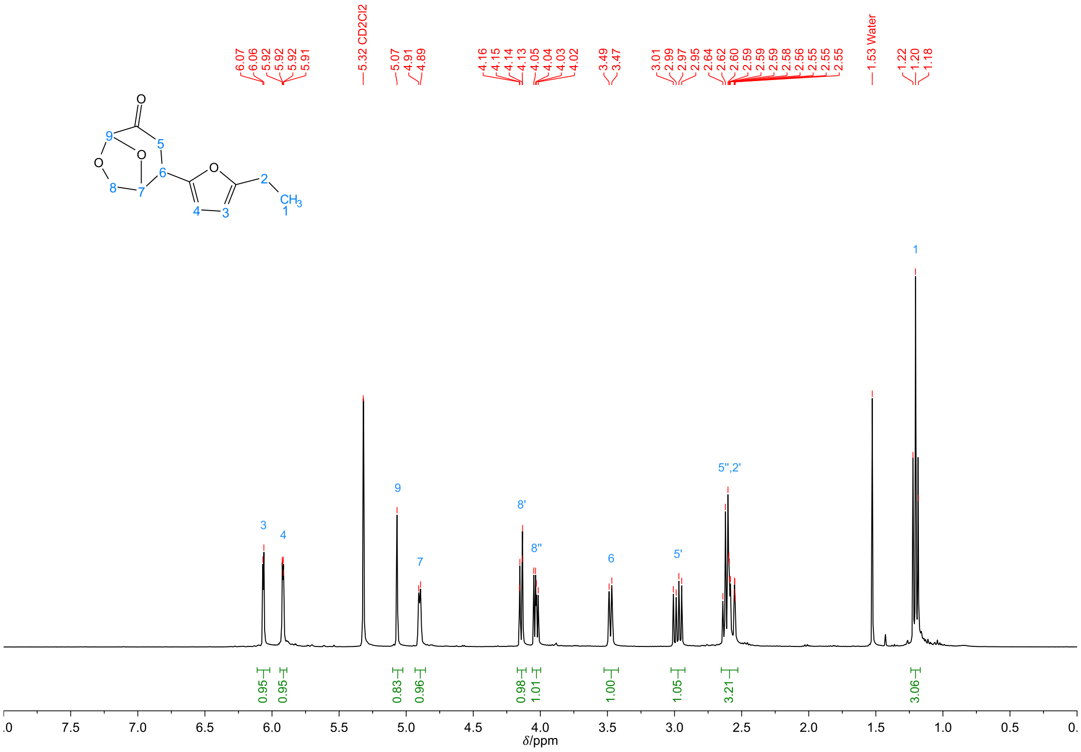

Figure 5.54.: ^{1}H NMR spectrum of **7**.

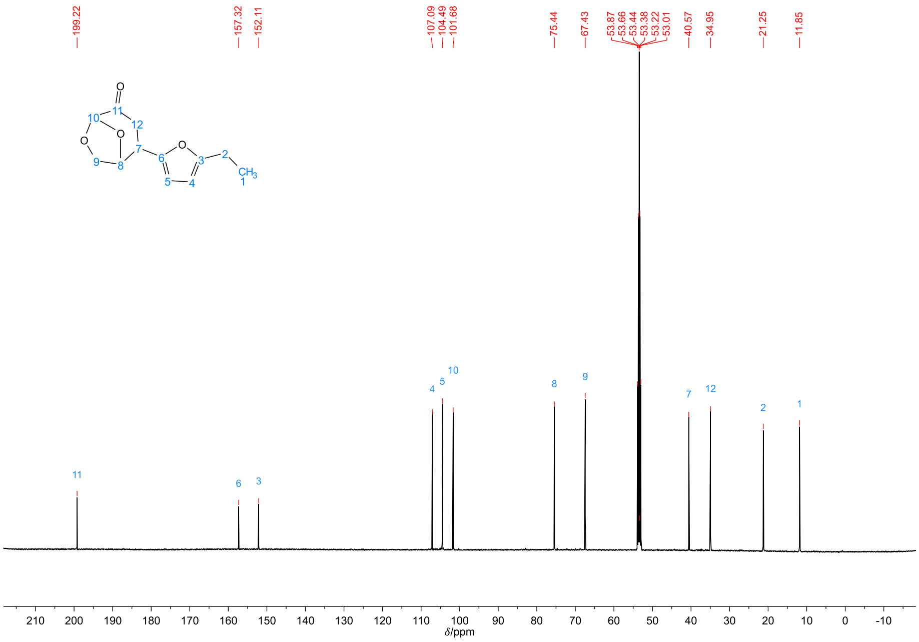

Figure 5.55.: ^{13}C NMR spectrum of **7**.

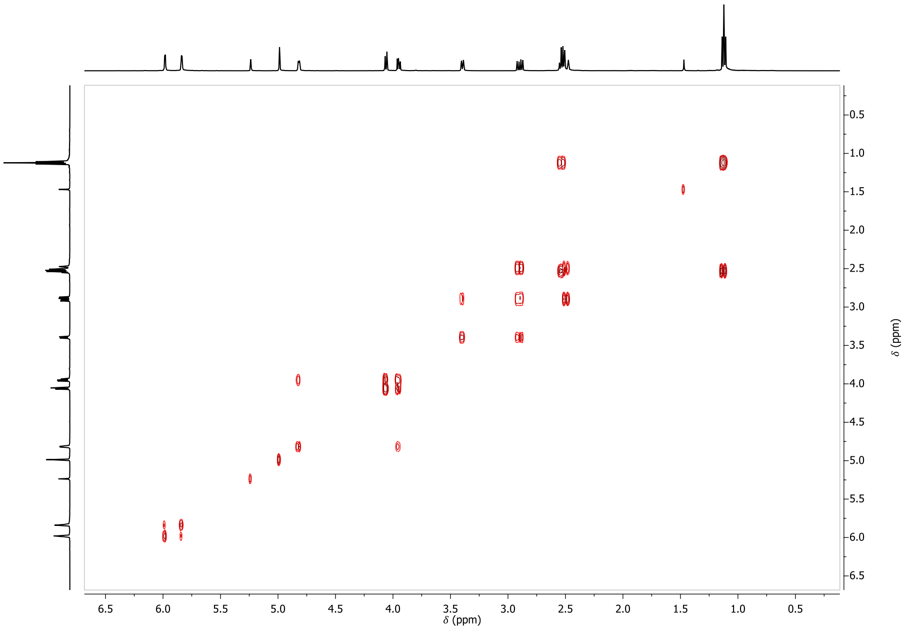

Figure 5.56.: COSY spectrum of **7**.

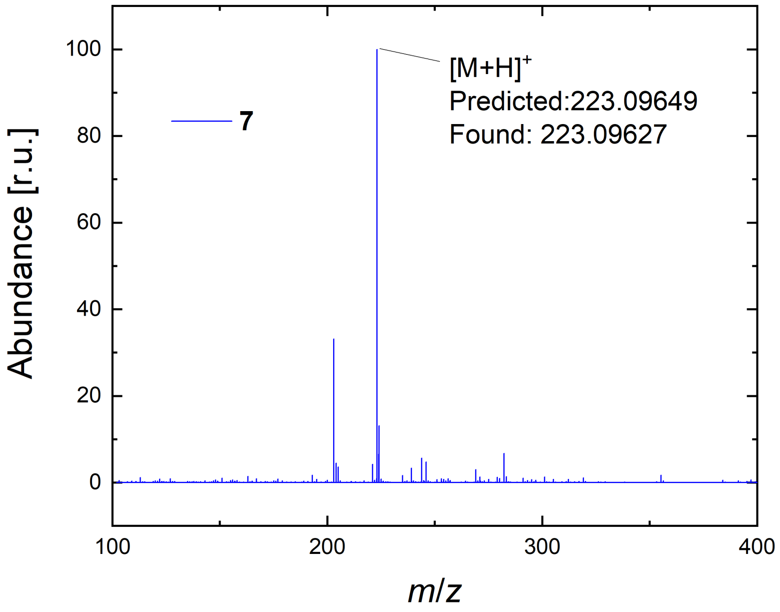

Figure 5.57.: ESI mass spectrum of **7**.

5.6.4. Synthesis of p(**5**), p(**6**) and p(**7**)

In a typical procedure (table 5.7), the monomer (1.00 eq) was added to a crimp-top vial. Dichloromethane (5 mL) (DCM) was added to the reaction vial together with $ZnCl_2$ (1.00 eq) and the mixture was stirred for 20 minutes. After that, Grubbs second generation catalyst M204 (GII, 0.01 eq) from a freshly prepared stock solution (4 mg/mL) was added and the reaction mixture was stirred for 24 hours at 25 °C. Subsequently, an excess of ethyl vinyl ether (1.0 mL) was added to quench the reaction. Then, after one hour, the solvent was removed under reduced pressure. The obtained residue was then dissolved in dichloromethane (5.00 mL) and filtered through DMT-functionalised silica. After filtration, the solvent was removed under reduced pressure and a ^1H NMR spectrum and SEC chromatogram as well as an IR spectrum were recorded.

Table 5.7.: Quantities of reagents used for the polymerisation reactions.

	Monomer		**GII**		**$ZnCl_2$**	
	(mg)	(mmol)	(mg)	(mmol)	(mg)	(mmol)
5	25	128.86	1.09	1.28	17.5	128.86
6	25	120.2	1.02	1.20	16.3	120.2
7	25	112.6	0.95	1.13	15.2	112.6

Polymeric material (p(**5**)) was synthesised by Luca Heusser, a bachelor student under the co-supervision of Federico Ferrari. The author performed the evaluation on the obtained results and ideated the synthetic pathway.

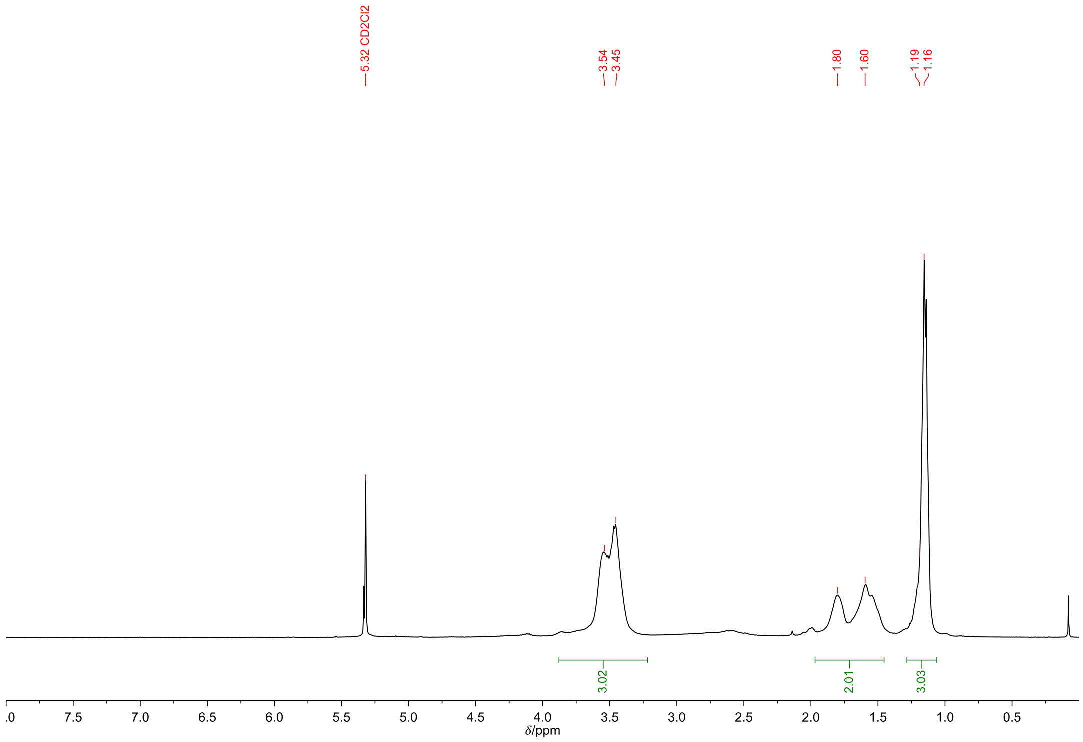

Figure 5.58.: ^{1}H NMR spectrum of p(**5**).

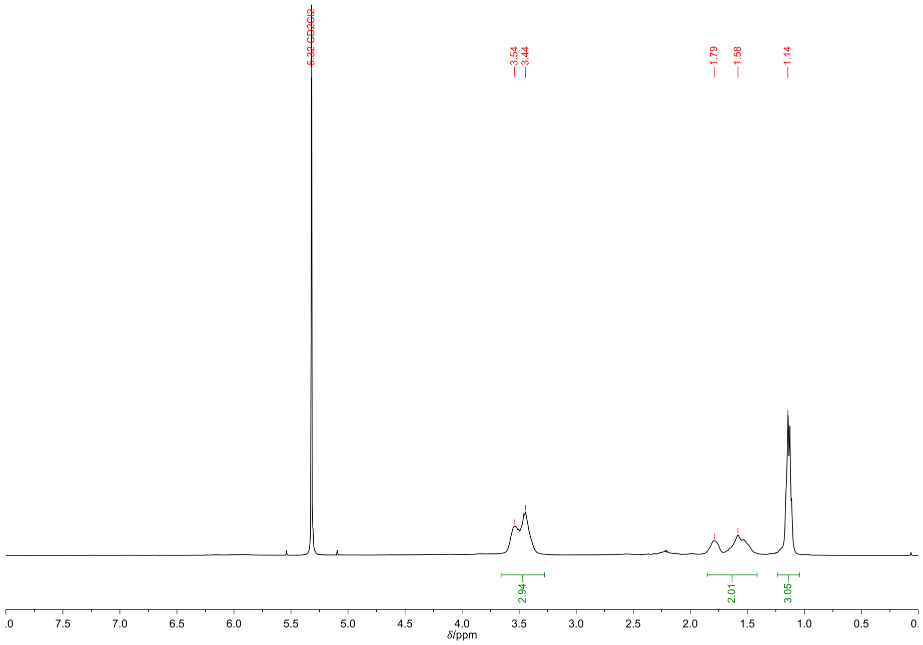

Figure 5.59.: ^{1}H NMR spectrum of p(**6**).

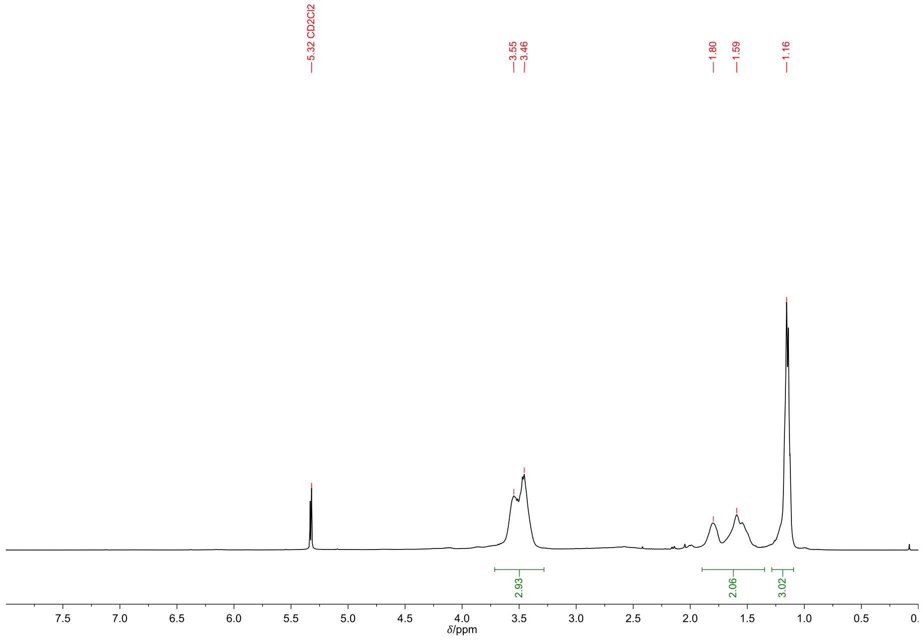

Figure 5.60.: ^{1}H NMR spectrum of p(**7**).

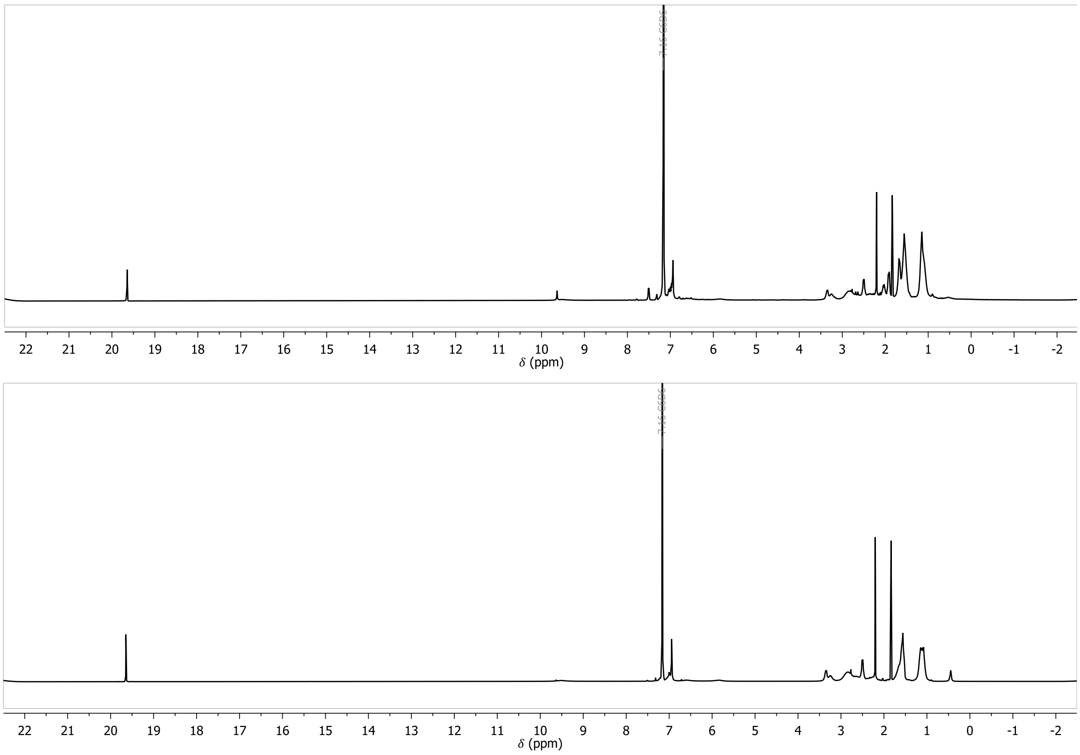

Figure 5.61.: ^{1}H NMR spectrum of GII and $ZnCl_2$ in C_6D_6 (top) and GII in C_6D_6 (bottom).

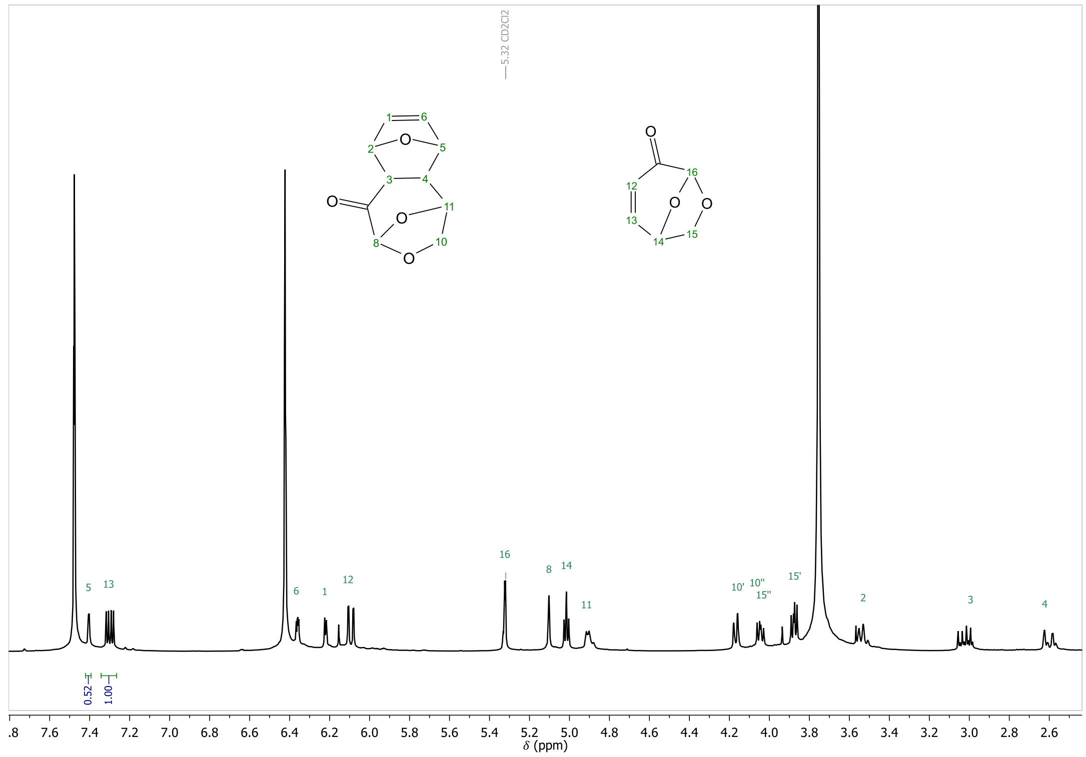

Figure 5.62.: ^{1}H NMR spectrum of crude reaction mixture of **5** after 24 hours at 55 °C with $ZnCl_2$ as catalyst.

5.6.5. IR spectroscopy investigation of poly(EVE)

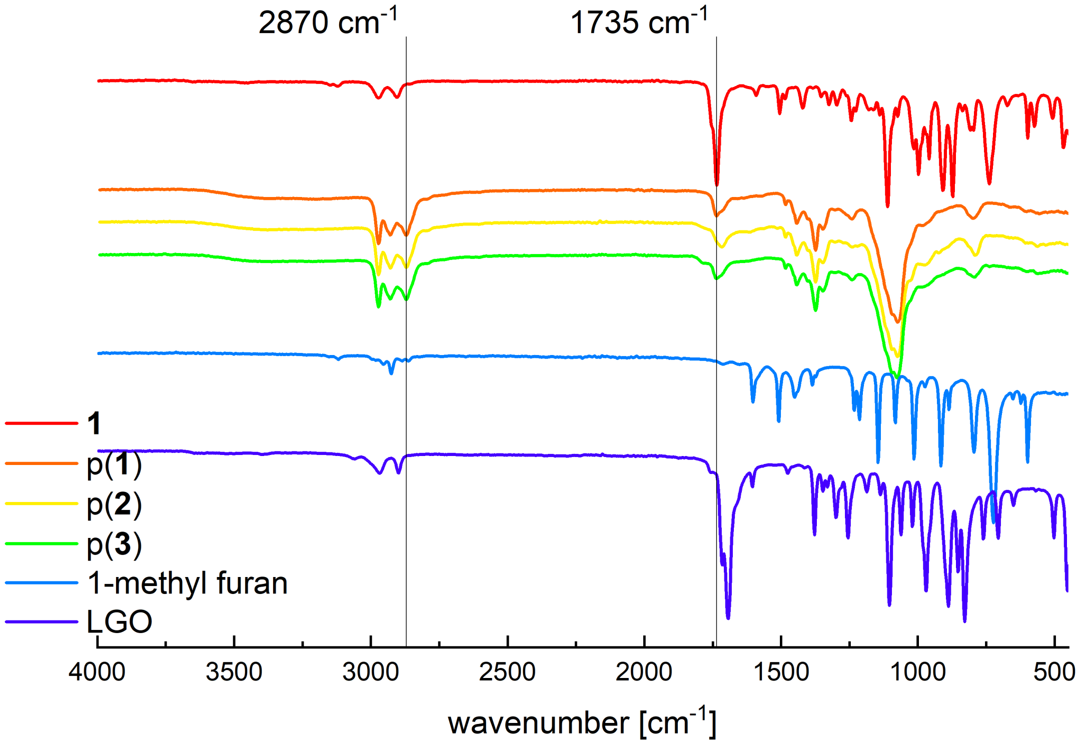

Figure 5.63.: IR spectra of **5**, p(**5**), p(**6**), and p(**7**), as well as 1-methyl furan and LGO, for comparison. The bands at 1735 cm^{-1} and 2870 cm^{-1} are indicated.

5.6.6. Test homopolymerisation of 5 without quenching

Monomer **5** (25 mg, 1.00 eq , 128.86 mmol) was added to a crimp-top vial. Dichloromethane (5 mL) (DCM) was added to the reaction vial together with $ZnCl_2$ (17.5 mg, 1.00 eq , 128.86 mmol) and the mixture was stirred for 20 minutes. After that, Grubbs second generation catalyst M204 (GII, 1.09 mg, 0.01 eq , 1.28 mmol) from a freshly prepared stock solution (4 mg/mL) was added and the reaction mixture was stirred for 24 hours at 25 °C. After 24 hours the solvent was removed under reduced pressure. The obtained residue was then dissolved in dichloromethane (5.00 mL) and filtered through DMT-functionalised silica. After filtration, the solvent was removed under reduced pressure and a ^{1}H NMR spectrum and SEC chromatogram were recorded.

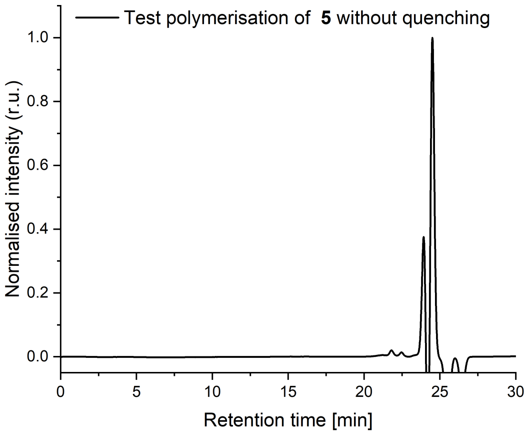

Figure 5.64.: SEC chromatogram of test homopolymerisation of **5** without quenching

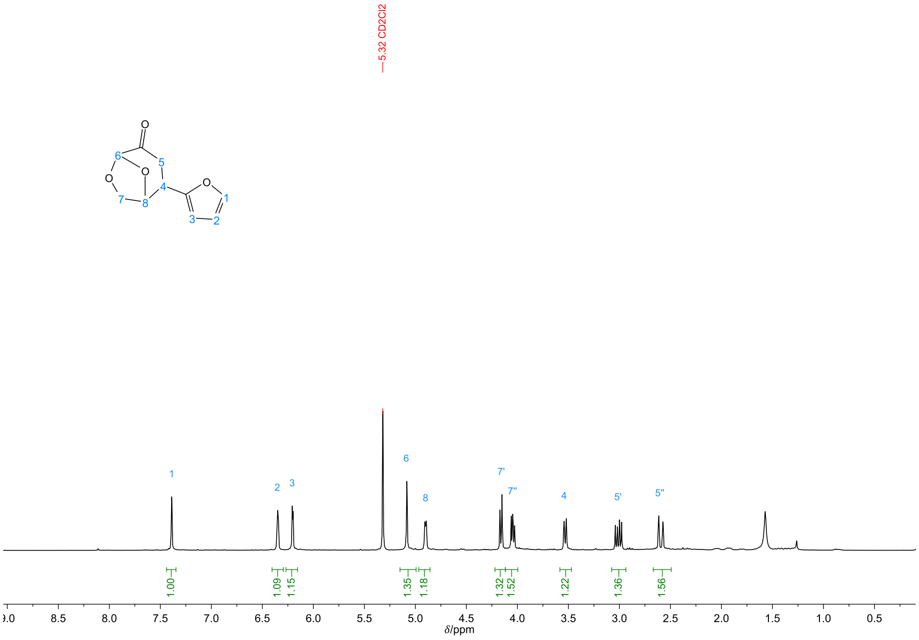

Figure 5.65.: ^{1}H NMR spectrum of test homopolymerisation of **5** without quenching

5.6.7. Test homopolymerisation of EVE

Ethyl vinyl ether (EVE) (753 mg, 1.00 eq , 10.76 mmol, 1.00 mL) was added to a crimp-top vial. Dichloromethane (5 mL) (DCM) was added to the reaction vial together with $ZnCl_2$ (17.5 mg, 11.90 eq , 128.86 mmol) and the mixture was stirred for 20 minutes. After that, Grubbs second generation catalyst M204 (GII, 1.09 mg, 0.12 eq , 1.28 mmol) from a freshly prepared stock solution (4 mg/mL) was added and the reaction mixture was stirred for 24 hours at 25 °C. After 24 hours the solvent was removed under reduced pressure. The obtained residue was then dissolved in dichloromethane (5.00 mL) and filtered through DMT-functionalised silica. After filtration, the solvent was removed under reduced pressure and a ^{1}H NMR spectrum and SEC chromatogram were recorded.

6. Conclusion and outlook

In this thesis, two novel pathways for poly(DHF) production were designed and investigated. Both improved pathways propose 2,5-dihydrofuran(2,5-DHF) as an intermediary and its subsequential isomerisation to 2,3-dihydrofuran (2,3-DHF), the monomer of poly(DHF). One pathway proposed using diallyl ether, its ring-closing metathesis and isomerisation to yield 2,3-DHF. The second one involved the use of *cis*-2-but-1,4-ene and *via* a carbonated mediated etherification, previously reported in the literature,[180], to produce 2,5-DHF that will be then converted into 2,3-DHF. After screening, the best conditions to perform ring-closing metathesis on diallyl ether were established, using Grubbs-Hoveyda II in bulk. Then, the partial kinetic of the isomerisation from 2,3-DHF to 2,5-DHF was recorded, showing that the process is favoured at higher temperatures, the absence of solvent allows also to perform a one-pot procedure combining isomerisation and ring-opening metathesis polymerisation (ROMP). One-pot processes are desirable since they enhance the overall green metrics of a process. The environmental factors for the hypothesised pathways were calculated, overall and for each step, and compared to literature-reported pathways toward poly(DHF) and intermediates. The lowest E-factor for poly(DHF) production, between the one compared, is posses by the pathways that start from *cis*-2-but-1,4-ene. Then, the dilution limit in the homopolymerisation of dihydrofuran was investigated, leading to the discovery that even with a high concentration of monomer (14 M) the polymerisation process shows a reduction of molecular weight compared to the bulk obtained product. This is ascribed to chain-transfer phenomena with the solvent chosen. As outlook, new solvents should be tested to understand how the nature of the solvent influence the polymerisation. However, high concentration of monomer (14 M) still allows obtaining a polymer with a molecular weight comparable to the predicted one, even if somewhat lower. A statistical copolymer of DHF was synthesised, using a norbornene derivative as a test molecule to establish the polymerisation conditions. Its structure was determinate *via* NMR, and the product was thermally characterised using DSC, revealing an increase in the transition glass temperature compared to poly(DHF).It would be interesting to exchange the norbornene derivatives for more sustainable oxanorbornenes in future studies. Five-membered ring heterocycles as an equivalent of DHF in ROMP were studied, and the ring-closing and isomerisation cycle developed for DHF was applied to other heteroatom containing dienes. The poor results obtained showed that diallyl sulfide could be ring-closed, but neither could this molecule be isomerised to the hypothesised monomer. However, ring-strain values for oxygen and sulfur-containing heterocycles were calculated, showing that dihydrothiophenes possess lower ring-strain than their oxygen counterparts, reducing the possibility of this monomers to be effective for ROMP. Even if thiophenes derivatives were not suitable for ROMP, another approach towards sulfur-containing monomers for ROMP was taken. Four thionorbornenes were synthesised, and their polymerisability by ring-opening metathesis polymerisation was investigated. Utilising GIII as catalyst yielded homopolymers with well-defined molecular weights and low dispersities. Furthermore, a sulfone-functional norbornene was prepared by oxidation, and its polymerisation was successfully shown. A sulfone-functional polymer was also obtained by post-polymerisation oxidation of a polythionorbornene, albeit the reaction was incomplete. The high control of the ROMP of the herein prepared monomers was further demonstrated by chain-extension of a polythionorbornene with the sulfone-functional norbornene. The resulting block copolymer exhibited properties similar to the corresponding homopolymers. Finally, the thermal properties of the herein synthesised polymers were investigated, finding a correlation between the structure of the repeat units. Lastly, three renewable Levoglucosenone (LGO) derivatives (**5**, **6**, and **7**) were synthesised through an electrophilic substitution reaction between furan derivatives and LGO. The conditions for the reaction were optimised, and levoglucosenone-derived molecules were obtained. The polymerisation of the monomers was only possible when using a combination of a typical ROMP catalyst, namely GII and $ZnCl_2$. The quenching agent used for the polymerisation, ethyl vinyl ether, was shown to be taking place in the polymerisation processes. The IR investigation of the obtained materials revealed peaks attributed to both ethyl vinyl ether and the levoglucosenone derivatives synthesised. Thermal investigations on the obtained materials revealed that all synthesised polymers exhibited low T_gs, making them well-suited for further processing. Further investigations into the polymerisation mechanism and exploiting it for other furan-based monomers are underway. These monomers (**5**, **6**, **7**) could also be tested as dienes in Diels-Alder reactions since the reactivity of furan derivatives in this type of pericyclic reaction is well known.[262] The bicyclic structures possibly obtained from the DA reaction should be then tested out as monomers in a ring-opening metathesis polymerisation (ROMP).

Bibliography

[1] Y. Zhong, P. Godwin, Y. Jin, H. Xiao, *Advanced Industrial and Engineering Polymer Research* **2020**, *3*, 27–35.

[2] P. N. Liu, F. H. Su, T. B. Wen, H. H. Y. Sung, I. D. Williams, G. Jia, *Chemistry – A European Journal* **2010**, *16*, 7889–7897.

[3] S. Son, G. C. Fu, *Journal of the American Chemical Society* **2007**, *129*, 1046–1047.

[4] C. Jehanno, J. W. Alty, M. Roosen, S. De Meester, A. P. Dove, E. Y.-X. Chen, F. A. Leibfarth, H. Sardon, *Nature* **2022**, *603*, 803–814.

[5] D. Kawecki, P. R. Scheeder, B. Nowack, *Environmental science & technology* **2018**, *52*, 9874–9888.

[6] T. Charoonsuk, R. Muanghlua, S. Sriphan, S. Pongampai, N. Vittayakorn, *Sustainable Materials and Technologies* **2021**, *27*, e00239.

[7] H. A. Maddah, *Am. J. Polym. Sci* **2016**, *6*, 1–11.

[8] J. M. Millican, S. Agarwal, *Macromolecules* **2021**, *54*, 4455–4469.

[9] G. W. Coates, Y. D. Getzler, *Nature Reviews Materials* **2020**, *5*, 501–516.

[10] G. Li, M. Zhao, F. Xu, B. Yang, X. Li, X. Meng, L. Teng, F. Sun, Y. Li, *Molecules* **2020**, *25*, 5023.

[11] J. D. Feist, Y. Xia, *Journal of the American Chemical Society* **2020**, *142*, 1186–1189.

[12] K. J. Jem, B. Tan, *Advanced Industrial and Engineering Polymer Research* **2020**, *3*, 60–70.

[13] A. Amobonye, P. Bhagwat, S. Singh, S. Pillai, *Science of The Total Environment* **2021**, *759*, 143536.

[14] T. Thiounn, R. C. Smith, *Journal of Polymer Science* **2020**, *58*, 1347–1364.

[15] T. P. Haider, C. Völker, J. Kramm, K. Landfester, F. R. Wurm, *Angewandte Chemie International Edition* **2019**, *58*, 50–62.

[16] P. G. Jessop, S. Trakhtenberg, J. Warner in ACS Publications, **2009**.

[17] I. T. Horvath, P. T. Anastas, *Chemical reviews* **2007**, *107*, 2169–2173.

[18] P. C. Sabapathy, S. Devaraj, K. Meixner, P. Anburajan, P. Kathirvel, Y. Ravikumar, H. M. Zabed, X. Qi, *Bioresource technology* **2020**, *306*, 123132.

[19] T. Debsharma, F. N. Behrendt, A. Laschewsky, H. Schlaad, *Angewandte Chemie International Edition* **2019**, *58*, 6718–6721.

[20] R. J. Hickey, A. E. Pelling, *Front Bioeng Biotechnol* **2019**, *7*, 45.

[21] D. Lu, C. Xiao, S. Xu, *Express polymer letters* **2009**, *3*, 366–375.

[22] K. Matyjaszewski, T. E. Patten, J. Xia, *Journal of the American Chemical Society* **1997**, *119*, 674–680.

[23] H. Wang, Z. Jin, X. Hu, Q. Jin, S. Tan, A. Reza Mahdavian, N. Zhu, K. Guo, *Chemical Engineering Journal* **2022**, *430*, 132791.

[24] A. Forens, K. Roos, C. Dire, B. Gadenne, S. Carlotti, *Polymer* **2018**, *153*, 103–122.

[25] O. Nuyken, S. D. Pask, *Polymers* **2013**, *5*, 361–403.

[26] I. Mandal, A. Mandal, M. A. Rahman, A. F. Kilbinger, *Chemical science* **2022**, *13*, 12469–12478.

[27] S. Varlas, S. B. Lawrenson, L. A. Arkinstall, R. K. O'Reilly, J. C. Foster, *Progress in Polymer Science* **2020**, *107*, 101278.

[28] Y. Yamauchi, N. N. Horimoto, K. Yamada, Y. Matsushita, M. Takeuchi, Y. Ishida, *Angewandte Chemie* **2021**, *133*, 1552–1558.

[29] J. Chen, X. Chen, C. Zhu, J. Zhu, *Journal of Molecular Catalysis A: Chemical* **2014**, *394*, 198–204.

[30] M. Shetty, V. A. Kothapalli, C. E. Hobbs, *Polymer* **2015**, *80*, 64–66.

[31] H. G. Shin, H. S. Lee, E. J. Hong, J. G. Kim, *Bulletin of the Korean Chemical Society* **2021**, *42*, 502–505.

[32] L. C. So, S. Faucher, S. Zhu, *Macromolecular Reaction Engineering* **2013**, *7*, 684–698.

[33] J. McQuade, M. I. Serrano, F. Jäkle, *Polymer* **2022**, *246*, 124739.

[34] K. O. Kim, T.-L. Choi, *ACS Macro Letters* **2012**, *1*, 445–448.

[35] H. Jeong, V. W. Ng, J. Börner, R. R. Schrock, *Macromolecules* **2015**, *48*, 2006–2012.

[36] S. Song, Z. Zhang, X. Liu, Z. Fu, J. Xu, Z. Fan, *Journal of Polymer Science Part A: Polymer Chemistry* **2017**, *55*, 4027–4036.

[37] M. H. Kim, S. H. Kim, B. S. Kim, J.-W. Wee, B.-H. Choi, *Composites Science and Technology* **2018**, *168*, 272–278.

[38] K. Liu, H. Zhao, D. Ye, J. Zhang, *Chemical Engineering Journal* **2021**, *417*, 129309.

[39] F. Ferrari, MA thesis, Alma Mater Studiorum (University of Bologna), **2019**.

[40] A. Caraculacu, S. Coseri, *Progress in Polymer Science* **2001**, *26*, 799–851.

[41] T. Yokozawa, A. Yokoyama, *The Chemical Record* **2005**, *5*, 47–57.

[42] J. Bicerano, **1998**.

[43] D. Colombani, *Progress in polymer science* **1997**, *22*, 1649–1720.

[44] M. Adam, V. Arrighi, R. Ocone, *Chemical Engineering Research and Design* **2012**, *90*, 2287–2292.

[45] H. Uegaki, Y. Kotani, M. Kamigaito, M. Sawamoto, *Macromolecules* **1997**, *30*, 2249–2253.

[46] P. Miao, S. Lin, G. L. Rempel, Q. Pan, *Journal of Applied Polymer Science* **2018**, *135*, 46622.

[47] M. Abdollahi, M. Akbari Hajiataloo, *Journal of Polymer Research* **2021**, *28*, 1–16.

[48] C. M. Abreu, A. C. Fonseca, N. M. Rocha, J. T. Guthrie, A. C. Serra, J. F. Coelho, *Progress in Polymer Science* **2018**, *87*, 34–69.

[49] C. Lu, Y. Liu, X. Liu, C. Wang, J. Wang, F. Chu, *ACS Sustainable Chemistry & Engineering* **2018**, *6*, 6527–6535.

[50] T. Bahry, Z. Cui, A. Dazzi, M. Gervais, C. Sollogoub, F. Goubard, T.-T. Bui, S. Remita, *Radiation Physics and Chemistry* **2021**, *180*, 109291.

[51] Y. Wang, L. Fu, K. Matyjaszewski, *ACS macro letters* **2018**, *7*, 1317–1321.

[52] S. Molina-Gutiérrez, V. Ladmiral, R. Bongiovanni, S. Caillol, P. Lacroix-Desmazes, *Green Chemistry* **2019**, *21*, 36–53.

[53] R. Whitfield, N. P. Truong, D. Messmer, K. Parkatzidis, M. Rolland, A. Anastasaki, *Chemical Science* **2019**, *10*, 8724–8734.

[54] M. Rogošić, H. J. Mencer, Z. Gomzi, *European Polymer Journal* **1996**, *32*, 1337–1344.

[55] M. Kruk, B. Dufour, E. B. Celer, T. Kowalewski, M. Jaroniec, K. Matyjaszewski, *Macromolecules* **2008**, *41*, 8584–8591.

[56] J. Yeow, R. Chapman, A. J. Gormley, C. Boyer, *Chemical Society Reviews* **2018**, *47*, 4357–4387.

[57] J. Phommalysack-Lovan, Y. Chu, C. Boyer, J. Xu, *Chemical communications* **2018**, *54*, 6591–6606.

[58] X. Guo, B. Choi, A. Feng, S. H. Thang, *Macromolecular Rapid Communications* **2018**, *39*, 1800479.

[59] N. Corrigan, K. Jung, G. Moad, C. J. Hawker, K. Matyjaszewski, C. Boyer, *Progress in Polymer Science* **2020**, *111*, 101311.

[60] M. Edeleva, P. H. Van Steenberge, D. R. D'hooge, *Industrial & Engineering Chemistry Research* **2021**, *60*, 16981–16992.

[61] R. Cuatepotzo-Díaz, B. L. López-Méndez, P. López-Domínguez, M. E. Albores-Velasco, A. Penlidis, E. Vivaldo-Lima, *Industrial & Engineering Chemistry Research* **2020**, *59*, 17786–17795.

[62] J. Nicolas, Y. Guillaneuf, C. Lefay, D. Bertin, D. Gigmes, B. Charleux, *Progress in Polymer Science* **2013**, *38*, 63–235.

[63] M. D. Nothling, Q. Fu, A. Reyhani, S. Allison-Logan, K. Jung, J. Zhu, M. Kamigaito, C. Boyer, G. G. Qiao, *Advanced Science* **2020**, *7*, 2001656.

[64] C. Barner-Kowollik, M. Buback, B. Charleux, M. L. Coote, M. Drache, T. Fukuda, A. Goto, B. Klumperman, A. B. Lowe, J. B. Mcleary, G. Moad, M. J. Monteiro, R. D. Sanderson, M. P. Tonge, P. Vana, *Journal of Polymer Science Part A: Polymer Chemistry* **2006**, *44*, 5809–5831.

[65] G. Moad, E. Rizzardo, S. H. Thang, *Chemistry – An Asian Journal* **2013**, *8*, 1634–1644.

[66] M. Kato, M. Kamigaito, M. Sawamoto, T. Higashimura, *Macromolecules* **1995**, *28*, 1721–1723.

[67] J.-S. Wang, K. Matyjaszewski, *Journal of the American Chemical Society* **1995**, *117*, 5614–5615.

[68] K. Matyjaszewski, *Macromolecules* **2012**, *45*, 4015–4039.

[69] N. P. Truong, G. R. Jones, K. G. E. Bradford, D. Konkolewicz, A. Anastasaki, *Nature Reviews Chemistry* **2021**, *5*, 859–869.

[70] N. P. Truong, G. R. Jones, K. G. Bradford, D. Konkolewicz, A. Anastasaki, *Nature Reviews Chemistry* **2021**, *5*, 859–869.

[71] J. B. Zimmerman, P. T. Anastas, H. C. Erythropel, W. Leitner, *Science* **2020**, *367*, 397–400.

[72] T.-L. Chen, H. Kim, S.-Y. Pan, P.-C. Tseng, Y.-P. Lin, P.-C. Chiang, *Science of the Total Environment* **2020**, *716*, 136998.

[73] C. Jiménez-González, D. J. Constable, C. S. Ponder, *Chemical Society Reviews* **2012**, *41*, 1485–1498.

[74] A. P. Dicks, A. Hent in Green Chemistry Metrics, Springer, **2015**, pp. 17–44.

[75] D. J. Constable, A. D. Curzons, V. L. Cunningham, *Green Chemistry* **2002**, *4*, 521–527.

[76] V. Nanjappa, S. Vink, J. Dunlop, M. N. Krosch, R. Mann, *Marine and Freshwater Research* **2022**.

[77] R. A. Sheldon, *Green Chemistry* **2007**, *9*, 1273–1283.

[78] E. R. Monteith, P. Mampuys, L. Summerton, J. H. Clark, B. U. Maes, C. R. McElroy, *Green Chemistry* **2020**, *22*, 123–135.

[79] J. Liu, R. Liu, Y. Wei, M. Shi, *Trends in Chemistry* **2019**, *1*, 779–793.

[80] O. Diels, *Ber. Dtsch. Chem. Ges* **1929**, *62*, 554–562.

[81] M.-Y. Chang, M.-H. Wu, *Tetrahedron Letters* **2012**, *53*, 3173–3177.

[82] B. Yang, S. Gao, *Chemical Society Reviews* **2018**, *47*, 7926–7953.

[83] R. C. Cioc, T. J. Smak, M. Crockatt, J. C. Van Der Waal, P. C. Bruijnincx, *Green Chemistry* **2021**, *23*, 5503–5510.

[84] R. Gara, M. O. Zouaghi, L. M. H. ALshandoudi, Y. Arfaoui, *Journal of molecular modeling* **2021**, *27*, 1–12.

[85] K. Nishimoto, S. Kim, Y. Kitano, M. Tada, K. Chiba, *Organic Letters* **2006**, *8*, 5545–5547.

[86] J. Engberts, E. Fernández, L. García-Río, J. Leis, *The Journal of Organic Chemistry* **2006**, *71*, 4111–4117.

[87] D. Huertas, M. Florscher, V. Dragojlovic, *Green Chemistry* **2009**, *11*, 91–95.

[88] R. Woodward, H. Baer, *Journal of the American Chemical Society* **1948**, *70*, 1161–1166.

[89] Y. Lu, M.-M. Xu, Z.-M. Zhang, J. Zhang, Q. Cai, *Angewandte Chemie International Edition* **2021**, *60*, 26610–26615.

[90] B. A. Parsons, V. Dragojlovic, *Journal of Chemical Education* **2011**, *88*, 1553–1557.

[91] B. Oliveira, Z. Guo, G. Bernardes, *Chemical Society Reviews* **2017**, *46*, 4895–4950.

[92] K. Houk, Y. T. Lin, F. K. Brown, *Journal of the American Chemical Society* **1986**, *108*, 554–556.

[93] P. Vermeeren, T. A. Hamlin, F. M. Bickelhaupt, *Physical Chemistry Chemical Physics* **2021**, *23*, 20095–20106.

[94] X. Jiang, R. Wang, *Chemical Reviews* **2013**, *113*, 5515–5546.

[95] J. G. Martin, R. K. Hill, *Chemical Reviews* **1961**, *61*, 537–562.

[96] M. Arca, B. K. Sharma, N. P. Price, J. M. Perez, K. M. Doll, *Journal of the American Oil Chemists' Society* **2012**, *89*, 987–994.

[97] T. S. Powers, W. Jiang, J. Su, W. D. Wulff, B. E. Waltermire, A. L. Rheingold, *Journal of the American Chemical Society* **1997**, *119*, 6438–6439.

[98] T. Dinadayalane, R. Vijaya, A. Smitha, G. N. Sastry, *The Journal of Physical Chemistry A* **2002**, *106*, 1627–1633.

[99] S. M. Park, J. Choi, H. L. Kim, C. H. Kwon, *Physical Chemistry Chemical Physics* **2020**, *22*, 28383–28392.

[100] Y. Chung, B. F. Duerr, T. A. McKelvey, P. Nanjappan, A. W. Czarnik, *The Journal of Organic Chemistry* **1989**, *54*, 1018–1032.

[101] V. D. Kiselev, A. I. Konovalov, *Journal of Physical Organic Chemistry* **2009**, *22*, 466–483.

[102] M. De Rosa, D. Arnold, E. Blythe, M. S. Farrell, T. Seals, K. Wills, M. Medved, *Heterocyclic Communications* **2007**, *13*, 97–100.

[103] P. Vermeeren, M. D. Tiezza, M. van Dongen, I. Fernández, F. M. Bickelhaupt, T. A. Hamlin, *Chemistry–A European Journal* **2021**, *27*, 10610–10620.

[104] P. Vermeeren, T. A. Hamlin, I. Fernández, F. M. Bickelhaupt, *Angewandte Chemie* **2020**, *132*, 6260–6265.

[105] J. J. Vollmer, K. L. Servis, *Journal of Chemical Education* **1970**, *47*, 491.

[106] A. R. Izzotti, J. L. Gleason, *Chemistry–A European Journal* **2022**, *28*, e202201418.

[107] N. D. Epiotis, *Journal of the American Chemical Society* **1973**, *95*, 1191–1200.

[108] B. J. Levandowski, D. Svatunek, B. Sohr, H. Mikula, K. Houk, *Journal of the American Chemical Society* **2019**, *141*, 2224–2227.

[109] W. C. Herndon, L. H. Hall, *Tetrahedron Letters* **1967**, *8*, 3095–3100.

[110] M. Hatano, T. Sakamoto, T. Mizuno, Y. Goto, K. Ishihara, *Journal of the American Chemical Society* **2018**, *140*, 16253–16263.

[111] J. A. Berson, R. D. Reynolds, W. M. Jones, *Journal of the American Chemical Society* **1956**, *78*, 6049–6053.

[112] M. Schuster, S. Blechert, *Angewandte Chemie International Edition in English* **1997**, *36*, 2036–2056.

[113] H. Ehrhorn, M. Tamm, *Chemistry–A European Journal* **2019**, *25*, 3190–3208.

[114] S. Planer, P. Małecki, B. Trzaskowski, A. Kajetanowicz, K. Grela, *ACS catalysis* **2020**, *10*, 11394–11404.

[115] Y.-N. Yin, R.-Q. Ding, D.-C. Ouyang, Q. Zhang, R. Zhu, *Nature communications* **2021**, *12*, 1–10.

[116] A. Abera Tsedalu, *Journal of Chemistry* **2021**, *2021*.

[117] S. J. Connon, S. Blechert, *Angewandte Chemie International Edition* **2003**, *42*, 1900–1923.

[118] M. Yu, S. Lou, F. Gonzalez-Bobes, *Organic Process Research & Development* **2018**, *22*, 918–946.

[119] J. A. Tallarico, P. J. Bonitatebus, M. L. Snapper, *Journal of the American Chemical Society* **1997**, *119*, 7157–7158.

[120] M. Piccini, D. J. Leak, C. J. Chuck, A. Buchard, *Polymer Chemistry* **2020**, *11*, 2681–2691.

[121] S. Monfette, D. E. Fogg, *Chemical Reviews* **2009**, *109*, 3783–3816.

[122] H. Ehrhorn, M. Tamm, *Chemistry–A European Journal* **2019**, *25*, 3190–3208.

[123] T. P. Montgomery, A. M. Johns, R. H. Grubbs, *Catalysts* **2017**, *7*, 87.

[124] J. Louie, R. H. Grubbs, *Angewandte Chemie International Edition* **2001**, *40*, 247–249.

[125] D. S. La, E. S. Sattely, J. G. Ford, R. R. Schrock, A. H. Hoveyda, *Journal of the American Chemical Society* **2001**, *123*, 7767–7778.

[126] F. D. Mango, *Journal of the American Chemical Society* **1977**, *99*, 6117–6119.

[127] R. T. Mathers, *Handbook of Transition Metal Polymerization Catalysts* **2018**, 631–659.

[128] A. K. Chatterjee, T.-L. Choi, D. P. Sanders, R. H. Grubbs, *Journal of the American Chemical Society* **2003**, *125*, 11360–11370.

[129] S. T. Nguyen, L. K. Johnson, R. H. Grubbs, J. W. Ziller, *Journal of the American Chemical Society* **1992**, *114*, 3974–3975.

[130] M. G. Holland, V. E. Griffith, M. B. France, S. G. Desjardins, *Journal of Polymer Science Part A: Polymer Chemistry* **2003**, *41*, 2125–2131.

[131] R. Walker, R. M. Conrad, R. H. Grubbs, *Macromolecules* **2009**, *42*, 599–605.

[132] G. Hondrogiannis, R. M. Pagni, G. W. Kabalka, P. Anosike, R. Kurt, *Tetrahedron letters* **1990**, *31*, 5433–5436.

[133] Y. Chen, M. M. Abdellatif, K. Nomura, *Tetrahedron* **2018**, *74*, 619–643.

[134] W. R. Gutekunst, C. J. Hawker, *Journal of the American Chemical Society* **2015**, *137*, 8038–8041.

[135] C. W. Bielawski, R. H. Grubbs, *Progress in Polymer Science* **2007**, *32*, 1–29.

[136] J. A. Johnson, Y. Y. Lu, A. O. Burts, Y. Xia, A. C. Durrell, D. A. Tirrell, R. H. Grubbs, *Macromolecules* **2010**, *43*, 10326–10335.

[137] W. Crowe, J. Mitchell, V. Gibson, R. Schrock, *Macromolecules* **1990**, *23*, 3534–3536.

[138] A. Mandal, I. Mandal, A. F. M. Kilbinger, *Macromolecules* **2022**, *55*, 7827–7833.

[139] S. Varlas, S. B. Lawrenson, L. A. Arkinstall, R. K. O'Reilly, J. C. Foster, *Progress in Polymer Science* **2020**, *107*, 101278.

[140] B. Kong, J. K. Lee, I. S. Choi, *Langmuir* **2007**, *23*, 6761–6765.

[141] T. Steinbach, E. M. Alexandrino, C. Wahlen, K. Landfester, F. R. Wurm, *Macromolecules* **2014**, *47*, 4884–4893.

[142] R. Li, X. Li, Y. Zhang, A. O. Delawder, N. D. Colley, E. A. Whiting, J. C. Barnes, *Polymer Chemistry* **2020**, *11*, 541–550.

[143] S. A. Isarov, P. W. Lee, J. K. Pokorski, *Biomacromolecules* **2016**, *17*, 641–648.

[144] P. Shieh, H. V.-T. Nguyen, J. A. Johnson, *Nature chemistry* **2019**, *11*, 1124–1132.

[145] H. Li, Z. Wang, B. He, *Journal of Molecular Catalysis A: Chemical* **1999**, *147*, 83–88.

[146] P. Preishuber-Pflügl, P. Buchacher, E. Eder, R. M. Schitter, F. Stelzer, *Journal of Molecular Catalysis A: Chemical* **1998**, *133*, 151–158.

[147] K. G. Moloy, *Journal of molecular catalysis* **1994**, *91*, 291–302.

[148] B. Novak, W. Risse, R. Grubbs, *Polymer Synthesis Oxidation Processes* **1992**, 47–72.

[149] D. H. McConville, J. R. Wolf, R. R. Schrock, *Journal of the American Chemical Society* **1993**, *115*, 4413–4414.

[150] S. Wache, *Journal of organometallic chemistry* **1995**, *494*, 235–240.

[151] M. A. Hillmyer, W. R. Laredo, R. H. Grubbs, *Macromolecules* **1995**, *28*, 6311–6316.

[152] B. Novak, W. Risse, R. Grubbs, *Polymer Synthesis Oxidation Processes* **1992**, 47–72.

[153] C. L. Dwyer, M. M. Kirk, W. H. Meyer, W. Janse van Rensburg, G. S. Forman, *Organometallics* **2006**, *25*, 3806–3812.

[154] B. F. Straub, *Angewandte Chemie International Edition* **2005**, *44*, 5974–5978.

[155] S. J. P'Poo, H.-J. Schanz, *Journal of the American Chemical Society* **2007**, *129*, 14200–14212.

[156] D. J. Walsh, S. H. Lau, M. G. Hyatt, D. Guironnet, *Journal of the American Chemical Society* **2017**, *139*, 13644–13647.

[157] L. H. Peeck, S. Leuthäusser, H. Plenio, *Organometallics* **2010**, *29*, 4339–4345.

[158] G. Borja, R. Pleixats, R. Alibés, X. Cattoën, M. W. C. Man, *Molecules* **2010**, *15*, 5756–5767.

[159] M. Bocus, L. Vanduyfhuys, F. De Proft, B. M. Weckhuysen, V. Van Speybroeck, *JACS Au* **2022**, *2*, 502–514.

[160] M. Ohmori, K. Kimura, Y. Yamashita, Y. Sakaguchi, *Sen'i Gakkaishi* **2006**, *62*, 141–149.

[161] Y. Kamitori, M. Hojo, R. Msuda, T. Yoshida, S. Ohara, K. Yamada, N. Yoshikawa, *The Journal of Organic Chemistry* **1988**, *53*, 519–526.

[162] D. Lenoir, *Angewandte Chemie International Edition* **2003**, *42*, 854–857.

[163] P. Mondal, G. Jana, T. S. Pal, P. K. Chattaraj, N. K. Singha, *Polymer Chemistry* **2021**, *12*, 6283–6290.

[164] K. Leja, G. Lewandowicz, *Polish Journal of Environmental Studies* **2010**, *19*.

[165] S. Binauld, M. H. Stenzel, *Chemical communications* **2013**, *49*, 2082–2102.

[166] K. Ogino, J.-S. Chen, C. K. Ober, *Chemistry of materials* **1998**, *10*, 3833–3838.

[167] M. MacLeod, H. P. H. Arp, M. B. Tekman, A. Jahnke, *Science* **2021**, *373*, 61–65.

[168] N. Ibrahim, A. N. Shamsuddin, *Malaysian Journal of Chemical Engineering and Technology (MJCET)* **2021**, *4*, 15–23.

[169] M. Bartnikowski, T. R. Dargaville, S. Ivanovski, D. W. Hutmacher, *Progress in Polymer Science* **2019**, *96*, 1–20.

[170] M. Aslam, M. A. Kalyar, Z. A. Raza, *Polymer Engineering & Science* **2018**, *58*, 2119–2132.

[171] S. Pirsa, K. Aghbolagh Sharifi, *Journal of Chemistry Letters* **2020**, *1*, 47–58.

[172] O. Coulembier, P. Degée, J. L. Hedrick, P. Dubois, *Progress in Polymer Science* **2006**, *31*, 723–747.

[173] H. M. Younes, E. Bravo-Grimaldo, B. G. Amsden, *Biomaterials* **2004**, *25*, 5261–5269.

[174] P. A. Fokou, M. A. Meier, *Journal of the American Chemical Society* **2009**, *131*, 1664–1665.

[175] D. H. Kim, W. Jang, K. Choi, J. S. Choi, J. Pyun, J. Lim, K. Char, S. G. Im, *Science advances* **2020**, *6*, eabb5320.

[176] E. Cruickshank, M. Salamończyk, D. Pociecha, G. J. Strachan, J. M. Storey, C. Wang, J. Feng, C. Zhu, E. Gorecka, C. T. Imrie, *Liquid Crystals* **2019**, *46*, 1595–1609.

[177] J. Caner, Z. Liu, Y. Takada, A. Kudo, H. Naka, S. Saito, *Catalysis Science & Technology* **2014**, *4*, 4093–4098.

[178] Y. Gu, F. Jérôme, *Green Chemistry* **2010**, *12*, 1127–1138.

[179] C. Kim, B. A. Ondrusek, H. Chung, *Organic Letters* **2018**, *20*, 736–739.

[180] F. Aricò, P. Tundo, A. Maranzana, G. Tonachini, *ChemSusChem* **2012**, *5*, 1578–1586.

[181] E. Fuhrmann, J. Talbiersky, *Organic Process Research & Development* **2005**, *9*, 206–211.

[182] J. Li, S. Yang, W. Wu, C. Qi, Z. Deng, H. Jiang, *Tetrahedron* **2014**, *70*, 1516–1523.

[183] M. Y. Al-Enezi, E. John, Y. A. Ibrahim, N. A. Al-Awadi, *RSC advances* **2021**, *11*, 37866–37876.

[184] A. Horváth, D. Depré, W. A. Vermeulen, S. L. Wuyts, S. R. Harutyunyan, G. Binot, J. Cuypers, W. Couck, D. V. Den Heuvel, *The Journal of Organic Chemistry* **2019**, *84*, 4932–4939.

[185] E. S. Greenwood, P. J. Parsons, M. J. Young, *Synthetic Communications* **2003**, *33*, 223–228.

[186] T. Mandal, J. Dash, *Organic & Biomolecular Chemistry* **2021**, *19*, 9797–9808.

[187] D. Seo, *Environ Anal Health Toxicol* **2021**, *36*, e2021012–.

[188] E. Arceo, J. A. Ellman, R. G. Bergman, *Journal of the American Chemical Society* **2010**, *132*, 11408–11409.

[189] A. Sen, T. W. Lai, *Inorganic chemistry* **1984**, *23*, 3257–3258.

[190] P. Formentín, N. Gimeno, J. H. G. Steinke, R. Vilar, *The Journal of Organic Chemistry* **2005**, *70*, 8235–8238.

[191] S. Hanessian, S. Giroux, A. Larsson, *Organic Letters* **2006**, *8*, 5481–5484.

[192] I. W. Ashworth, I. H. Hillier, D. J. Nelson, J. M. Percy, M. A. Vincent, *European Journal of Organic Chemistry* **2012**, *2012*, 5673–5677.

[193] R. Maghrebi, M. Buffi, P. Bondioli, D. Chiaramonti, *Renewable and Sustainable Energy Reviews* **2021**, *149*, 111264.

[194] T. Neveselý, M. Wienhold, J. J. Molloy, R. Gilmour, *Chemical Reviews* **2021**, *122*, 2650–2694.

[195] R. H. Crabtree, *Chemical reviews* **2015**, *115*, 127–150.

[196] Y. Bai, M. De bruyn, J. H. Clark, J. R. Dodson, T. J. Farmer, M. Honoré, I. D. V. Ingram, M. Naguib, A. C. Whitwood, M. North, *Green Chemistry* **2016**, *18*, 3945–3948.

[197] B. Wang, K. Mireles, M. Rock, Y. Li, V. K. Thakur, D. Gao, M. R. Kessler, *Macromolecular Chemistry and Physics* **2016**, *217*, 871–879.

[198] F. Joubert, O. M. Musa, D. R. Hodgson, N. R. Cameron, *Chemical Society Reviews* **2014**, *43*, 7217–7235.

[199] D. Barther, D. Moatsou, *Macromolecular rapid communications* **2021**, *42*, 2100027.

[200] K. Hase, S.-i. Matsuoka, M. Suzuki, *Macromolecules* **2022**, *55*, 6811–6819.

[201] M. Naguib, K. L. Nixon, D. J. Keddie, *Polymer Chemistry* **2022**, *13*, 1401–1410.

[202] G. A. Edwards, P. A. Culp, J. M. Chalker, *Chemical Communications* **2015**, *51*, 515–518.

[203] F. Nuñez-Zarur, X. Solans-Monfort, L. Rodríguez-Santiago, R. Pleixats, M. Sodupe, *Chemistry–A European Journal* **2011**, *17*, 7506–7520.

[204] D. V. Deubel, T. Ziegler, *Organometallics* **2002**, *21*, 1603–1611.

[205] G. Spagnol, M.-P. Heck, S. P. Nolan, C. Mioskowski, *Organic Letters* **2002**, *4*, 1767–1770.

[206] A. R. Hlil, J. Balogh, S. Moncho, H.-L. Su, R. Tuba, E. N. Brothers, M. Al-Hashimi, H. S. Bazzi, *Journal of Polymer Science Part A: Polymer Chemistry* **2017**, *55*, 3137–3145.

[207] W. M. McGregor, D. C. Sherrington, *Chemical Society Reviews* **1993**, *22*, 199–204.

[208] A. U. Augustin, M. Sensse, P. G. Jones, D. B. Werz, *Angewandte Chemie International Edition* **2017**, *56*, 14293–14296.

[209] T. Ozturk, E. Ertas, O. Mert, *Chemical reviews* **2007**, *107*, 5210–5278.

[210] P. Matczak, M. Domagała, *J Mol Model* **2017**, *23*, 268.

[211] E. Vedejs, J. Stults, R. Wilde, *Journal of the American Chemical Society* **1988**, *110*, 5452–5460.

[212] B. Briou, B. Améduri, B. Boutevin, *Chemical Society Reviews* **2021**, *50*, 11055–11097.

[213] G. Duret, V. Le Fouler, P. Bisseret, V. Bizet, N. Blanchard, *European Journal of Organic Chemistry* **2017**, *2017*, 6816–6830.

[214] J. Sauer, *Angewandte Chemie International Edition in English* **1966**, *5*, 211–230.

[215] P. Laszlo, P. v. R. Schleyer, *Journal of the American Chemical Society* **1964**, *86*, 1171–1179.

[216] S. Elyashiv-Barad, N. Greinert, A. Sen, *Macromolecules* **2002**, *35*, 7521–7526.

[217] G. Hu, S. Lin, B. Zhao, F. Ng, Q. Pan, *European Polymer Journal* **2022**, *168*, 111085.

[218] E. Szuromi, H. Shen, B. L. Goodall, R. F. Jordan, *Organometallics* **2008**, *27*, 402–409.

[219] C. Janiak, P. G. Lassahn, *Macromolecular Rapid Communications* **2001**, *22*, 479–493.

[220] A. Leitgeb, J. Wappel, C. Slugovc, *Polymer* **2010**, *51*, 2927–2946.

[221] G. Leone, A. Boglia, A. C. Boccia, S. T. Scafati, F. Bertini, G. Ricci, *Macromolecules* **2009**, *42*, 9231–9237.

[222] G. C. Vougioukalakis, I. Stamatopoulos, N. Petzetakis, C. P. Raptopoulou, V. Psycharis, A. Terzis, P. Kyritsis, M. Pitsikalis, N. Hadjichristidis, *Journal of Polymer Science Part A: Polymer Chemistry* **2009**, *47*, 5241–5250.

[223] I. Choinopoulos, *Polymers* **2019**, *11*, 298.

[224] X. Liu, F. Liu, W. Liu, H. Gu, *Polymer Reviews* **2021**, *61*, 1–53.

[225] D. Smith, E. B. Pentzer, S. T. Nguyen, *Polymer Reviews* **2007**, *47*, 419–459.

[226] I. Dragutan, V. Dragutan, P. Filip, B. C. Simionescu, A. Demonceau, *Molecules* **2016**, *21*, 198.

[227] P. H. Nguyen, S. Spoljaric, J. Seppälä, *Polymer* **2018**, *153*, 183–192.

[228] J. Liao, J. Wang, Z. Liu, Z. Ye, *ACS Applied Energy Materials* **2019**, *2*, 6732–6740.

[229] I. Aranberri, S. Montes, I. Azcune, A. Rekondo, H.-J. Grande, *Polymers* **2018**, *10*, 1056.

[230] F. Chu, S. Qiu, S. Zhang, Z. Xu, Y. Zhou, X. Luo, X. Jiang, L. Song, W. Hu, Y. Hu, *Journal of Colloid and Interface Science* **2022**, *608*, 142–157.

[231] A. Kausar, S. Zulfiqar, M. I. Sarwar, *Polymer Reviews* **2014**, *54*, 185–267.

[232] T.-J. Yue, W.-M. Ren, L. Chen, G.-G. Gu, Y. Liu, X.-B. Lu, *Angewandte Chemie* **2018**, *130*, 12852–12856.

[233] X. Chen, L. Fang, J. Wang, F. He, X. Chen, Y. Wang, J. Zhou, Y. Tao, J. Sun, Q. Fang, *Macromolecules* **2018**, *51*, 7567–7573.

[234] D. Mecerreyes, L. Porcarelli, N. Casado, *Macromolecular Chemistry and Physics* **2020**, *221*, 1900490.

[235] N. Ramnath, V. Ramesh, V. Ramamurthy, *The Journal of Organic Chemistry* **1983**, *48*, 214–222.

[236] R. Mayer, J. Morgenstern, J. Fabian, *Angewandte Chemie International Edition in English* **1964**, *3*, 277–286.

[237] M. M. Cambell, D. Evgenios, *Journal of the Chemical Society Perkin Transactions 1* **1973**, 2862–2866.

[238] D. Bansal, S. Pandey, G. Hundal, R. Gupta, *New Journal of Chemistry* **2015**, *39*, 9772–9781.

[239] T. Clark, J. S. Murray, P. Lane, P. Politzer, *Journal of Molecular Modeling* **2008**, *14*, 689–697.

[240] J. A. Smulik, A. J. Giessert, S. T. Diver, *Tetrahedron Letters* **2002**, *43*, 209–211.

[241] Z. Cheng, P. Sun, A. Tang, W. Jin, C. Liu, *Organic Letters* **2019**, *21*, 8925–8929.

[242] S. Watanabe, T. Takayama, H. Nishio, K. Matsushima, Y. Tanaka, S. Saito, Y. Sun, K. Oyaizu, *Polymer Chemistry* **2022**, *13*, 1705–1711.

[243] M. A. Guerrero-Robles, M. A. Vilchis-Reyes, E. M. Ramos-Rivera, C. Alvarado, *ChemistrySelect* **2019**, *4*, 13698–13708.

[244] R. P. Babu, K. O'Connor, R. Seeram, *Progress in Biomaterials* **2013**, *2*, 8.

[245] M. N. Siddiqui, H. H. Redhwi, A. A. Al-Arfaj, D. S. Achilias, *Sustainability* **2021**, *13*, 10528.

[246] S. A. Rafiqah, A. Khalina, A. S. Harmaen, I. A. Tawakkal, K. Zaman, M. Asim, M. Nurrazi, C. H. Lee, *Polymers* **2021**, *13*, 1436.

[247] A. Z. Naser, I. Deiab, B. M. Darras, *RSC Advances* **2021**, *11*, 17151–17196.

[248] G. Z. Papageorgiou, D. G. Papageorgiou, Z. Terzopoulou, D. N. Bikiaris, *European Polymer Journal* **2016**, *83*, 202–229.

[249] C. Tang, *Green Materials* **2013**, *1*, 62–63.

[250] K. J. Groh, T. Backhaus, B. Carney-Almroth, B. Geueke, P. A. Inostroza, A. Lennquist, H. A. Leslie, M. Maffini, D. Slunge, L. Trasande, A. M. Warhurst, J. Muncke, *Science of The Total Environment* **2019**, *651*, 3253–3268.

[251] S. Agarwal, R. K. Gupta in Applied plastics engineering handbook, Elsevier, **2017**, pp. 635–649.

[252] M. Eriksen, M. Thiel, L. Lebreton, *Hazardous chemicals associated with plastics in the marine environment* **2016**, 135–162.

[253] P. de Almeida, P. D. Silva, *Energy Policy* **2009**, *37*, 1267–1276.

[254] M. B. Comba, Y.-h. Tsai, A. M. Sarotti, M. I. Mangione, A. G. Suárez, R. A. Spanevello, *European Journal of Organic Chemistry* **2018**, *2018*, 590–604.

[255] X. Huang, T. Liu, J. Wang, F. Wei, J. Ran, S. Kudo, *Journal of the Energy Institute* **2020**, *93*, 2505–2510.

[256] A. M. Sarotti, R. A. Spanevello, A. G. Suárez, *Organic Letters* **2006**, *8*, 1487–1490.

[257] A. M. Sarotti, R. A. Spanevello, A. G. Suárez, *Tetrahedron* **2009**, *65*, 3502–3508.

[258] D. D. Ward, F. Shafizadeh, *Carbohydrate Research* **1981**, *95*, 155–176.

[259] N. Stamenković, N. P. Ulrih, J. Cerkovnik, *Physical Chemistry Chemical Physics* **2021**, *23*, 5051–5068.

[260] J. Kikuchi, M. Terada, *Chemistry – A European Journal* **2021**, *27*, 10215–10225.

[261] D. D. Ward, F. Shafizadeh, *Carbohydrate Research* **1981**, *95*, 155–176.

[262] T. A. Eggelte, H. de Koning, H. O. Huisman, *Tetrahedron* **1973**, *29*, 2491–2493.

[263] V. Froidevaux, M. Borne, E. Laborbe, R. Auvergne, A. Gandini, B. Boutevin, *RSC Advances* **2015**, *5*, 37742–37754.

[264] A. Gandini, *Progress in Polymer Science* **2013**, *38*, 1–29.

[265] C. K. McClure, K. B. Hansen, *Tetrahedron Letters* **1996**, *37*, 2149–2152.

[266] M. G. Banwell, X. Liu, L. A. Connal, M. G. Gardiner, *Macromolecules* **2020**, *53*, 5308–5314.

[267] S. Fadlallah, A. A. M. Peru, A. L. Flourat, F. Allais, *European Polymer Journal* **2020**, *138*, 109980.

[268] S. Fadlallah, A. A. M. Peru, L. Longé, F. Allais, *Polymer Chemistry* **2020**, *11*, 7471–7475.

[269] M. S. Mettler, D. G. Vlachos, P. J. Dauenhauer, *Energy & Environmental Science* **2012**, *5*, 7797–7809.

[270] A. Tuan Hoang, V. Viet Pham, *Renewable and Sustainable Energy Reviews* **2021**, *148*, 111265.

[271] C. Xu, W. Liu, B. Zhang, H. Liao, W. He, L. Wei, *Combustion and Flame* **2021**, *234*, 111631.

[272] J. P. Kutney, H. W. Hanssen, G. V. Nair, *Tetrahedron* **1971**, *27*, 3323–3330.

[273] B. T. Freure, J. R. Johnson, *Journal of the American Chemical Society* **1931**, *53*, 1142–1147.

[274] J. D. Prugh, A. C. Huitric, W. C. McCarthy, *The Journal of Organic Chemistry* **1964**, *29*, 1991–1994.

[275] Y. Fujiwara, R. Asano, I. Moritani, S. Teranishi, *The Journal of Organic Chemistry* **1976**, *41*, 1681–1683.

[276] A. Gandini, M. N. Belgacem, *Progress in Polymer Science* **1997**, *22*, 1203–1379.

[277] M. Muthukumar, D. Mohan, *Journal of Polymer Research* **2005**, *12*, 231–241.

[278] P. Sonar, T. R. B. Foong, S. P. Singh, Y. Li, A. Dodabalapur, *Chemical Communications* **2012**, *48*, 8383–8385.

[279] W. Ruelens, G. Koolen, B. Gricourt, A. Willem van Vuure, M. Smet, *Materials Letters* **2022**, *328*, 133025.

[280] P. Ares Elejoste, A. Allue, J. Ballestero, S. Neira, J. L. Gómez-Alonso, K. Gondra, *Polymers* **2022**, *14*, 1864.

[281] J. Surkau, K. Bläsing, J. Bresien, D. Michalik, A. Villinger, A. Schulz, *Chemistry – A European Journal*, *n/a*, DOI `https://doi.org/10.1002/chem.202201905`.

[282] H. Yamamoto, Y. Zhang, K. Shibatomi, *Synlett* **2005**, *n/a*, 2837–2842.

[283] A. M. Vos, R. A. Schoonheydt, F. De Proft, P. Geerlings, *Journal of Catalysis* **2003**, *220*, 333–346.

[284] K. A. Waibel, D. Barther, T. Malliaridou, D. Moatsou, M. A. R. Meier, *European Journal of Organic Chemistry* **2021**, *2021*, 4508–4516.

[285] V. Kottisch, Q. Michaudel, B. P. Fors, *Journal of the American Chemical Society* **2016**, *138*, 15535–15538.

[286] R. H. Lambeth, S. J. Pederson, M. Baranoski, A. M. Rawlett, *Journal of Polymer Science Part A: Polymer Chemistry* **2010**, *48*, 5752–5757.

A. Appendix

A.1. Abbreviation used

The following abbreviations are used in this manuscript:

LGO	Levoglucosenone
ROMP	Ring-Opening Metathesis Polymerisation
DCM	Dichloromethane
DMC	Dimethyl carbonate
THF	Tetrahydrofuran
DMT	Dimercaptotriazine
GII	Grubbs second generation catalyst
FOD	6,6,7,7,8,8,8-heptafluoro-2,2-dimethyl-3,5-octanedionato
AIBN	Azobisisobutyronitrile
NMR	Nuclear Magnetic resonance
SEC	Size exclusion chromatography
DHF	Dihydrofuran
DHT	Dihydrothiophene
ADMET	Acyclic diene metathesis polymerisation
RAFT	Reversible addition-fragmentation chain-transfer

A.2. List of pubblications

1. F. Ferrari, J. Braun, C. E. Anson, B. D. Wilts, D. Moatsou, C. Bizzarri, *Molecules* **2021**, *26*, 2567.